MODELING AND SIMULATION OF BIO-METHANOL FROM BIOGAS PRODUCTION PROCESS USING ASPEN PLUS SIMULATION SOFTWARE

By

MR. Rujiroj TAMNITRA

An Thesis Submitted in Partial Fulfillment of the Requirements

for Master of Engineering (CHEMICAL ENGINEERING)

Department of CHEMICAL ENGINEERING

Graduate School, Silpakorn University

Academic Year 2019

การสร้างแบบจำลองและการจำลองกระบวนการผลิตไบโอเมทานอลจากก๊าซชีวภาพด้วยโปรแกรมจำลองกระบวนการแอสเพนพลัส

โดย
นายรุจิโรจน์ ธรรมนิทรา

วิทยานิพนธ์นี้เป็นส่วนหนึ่งของการศึกษาตามหลักสูตรวิศวกรรมศาสตรมหาบัณฑิต
สาขาวิชาวิศวกรรมเคมี แผน ก แบบ ก 2 ระดับปริญญามหาบัณฑิต
ภาควิชาวิศวกรรมเคมี
บัณฑิตวิทยาลัย มหาวิทยาลัยศิลปากร
ปีการศึกษา 2562

MODELING AND SIMULATION OF BIO-METHANOL FROM BIOGAS PRODUCTION PROCESS USING ASPEN PLUS SIMULATION SOFTWARE

By

MR. Rujiroj TAMNITRA

An Thesis Submitted in Partial Fulfillment of the Requirements

for Master of Engineering (CHEMICAL ENGINEERING)

Department of CHEMICAL ENGINEERING

Graduate School, Silpakorn University

Academic Year 2019

Title	Modeling and simulation of bio-methanol from biogas production process using Aspen Plus simulation software
By	Rujiroj TAMNITRA
Field of Study	(CHEMICAL ENGINEERING)
Advisor	Assistant Professor Dr. Tarawipa Puangpetch , Ph.D.

Graduate School Silpakorn University in Partial Fulfillment of the Requirements for the Master of Engineering

.....Dean of graduate school

(Associate Professor Jurairat Nunthanid, Ph.D.)

Approved by

.....Chair person

(Assistant Professor Dr. Choowong Chaisuk , D.Eng.)

.....Advisor

(Assistant Professor Dr. Tarawipa Puangpetch , Ph.D.)

.....Co advisor

(Assistant Professor Dr. Weerawat Patthaveekongka , D.Eng.)

.....Co advisor

(Dr. Rujira Jitrwung , Ph.D.)

.....External Examiner

(Dr. Sophon Sirisattha , Ph.D.)

59404208 : Major (CHEMICAL ENGINEERING)
Keyword : process simulation, biomethanol production, kinetic modeling

MR. RUJIROJ TAMNITRA : MODELING AND SIMULATION OF BIO-METHANOL FROM BIOGAS PRODUCTION PROCESS USING ASPEN PLUS SIMULATION SOFTWARE
THESIS ADVISOR : ASSISTANT PROFESSOR DR. TARAWIPA PUANGPETCH, Ph.D.

The research aimed to simulate the industrial-scale, bio-methanol production form biogas process by using Aspen plus software. The simulated production rate was 15,000 kg of methanol per day. This bio-methanol production consisted of 2 reaction steps. The first step was reforming reaction and followed by the second step: methanol synthesis reaction. The kinetic models of both reactions were found out by using the data from the experimental designed by the full factorial design (FFD) method. The process model was created and simulated in three cases. Case I was the recycling residue gas as a raw material for methanol production. Case II was the recycling residue gas for substituting for renewable fuel in generator. Case III was recycling residue gas as a raw material for methanol production and added extra biogas for producing electricity. All cases of the process model were studied the economic feasibility and the sensitivity analysis to find out the most suitable model.

The experimental results gave the optimal conditions. For reforming reaction, the optimal condition was obtained as 700°C of temperature, 35% of CH_4/CO_2 volumetric ratio and 1.5 ml/min of water feed flow rate. For methanol synthesis reaction, the optimal condition was discovered as 5% CO_2 in feed, 2.8 H_2/CO ratio and 200°C of temperature. The achieve kinetic model provided the good simulated results for both reaction steps. For reforming reaction, the simulated results exhibited low value of mean absolute errors (MAE) of the CH_4 conversion, the CO_2 conversion and the H_2/CO ratio of 2.65 %, 2.91 % and 0.168, respectively. For methanol synthesis reaction, the simulated results also exhibited low value of MAE of the methanol yield, the CO Conversion and the H_2 conversion were 4.44, 6.16 % and 3.11 %, respectively. The results of process simulations showed that the Case III model was the most suitable model. This model exhibited the profitable yielded

19.3% of IRR and the good payback period of 4.72 years.

ACKNOWLEDGEMENTS

I would first like to thank my thesis advisor Assistant Professor Dr. Tarawipa Puangpetch and Assistant Professor Dr. Weerawat Patthaveekongka of Department of Chemical Engineering at Silpakorn University and Dr. Rujira Jitrwung of Expert Center of Innovative Clean Energy and Environment at Thailand Institute of Scientific and Technological Research (TISTR) who promptly supported help whenever I ran into a trouble spot or had a question about my research or writing. They steered me in the right direction whenever they thought I needed it.

I would also like to thank the experts who were involved in the validation survey for this research project: Assistant Professor Dr. Choowong Chaisuk and Dr. Sophon Sirisattha who have been the chair and committee of my thesis. Without their passionate participation and input, the validation survey could not have been successfully conducted.

I would also like to acknowledge Kamonrat Suksumrit, Kuntima Krekkeitsakul, Jiraporn chalongtham and Anantachai Wannajampa of the Expert Center of Innovative Clean Energy and Environment at Thailand Institute of Scientific and Technological Research (TISTR) as the second reader of this thesis, and I am gratefully indebted to them for very valuable comments on this thesis.

Finally, I must express my very profound gratitude to my parents, to my friends and to my girlfriend for providing me with unfailing support and continuous encouragement throughout my years of study and through the process of researching and writing this thesis. This accomplishment would not have been possible without them. Thank you.

Rujiroj TAMNITRA

TABLE OF CONTENTS

CHAPTER I
INTRODUCTION

1.1 Motivation

Energy consumption was realized influencing energy sustainability and environment, the more increasing energy consumption, the more rising of the energy crisis and greenhouse gas emission. Renewable energy was one solution for energy consumption because it had derived from natural processes and collected from renewable resources that are continuously replenished. So, renewable energy was interested in studying and suitable to be used for solving the energy crisis in the future[1].

Biogas is a renewable fuel that was interested as a substitute for fossil fuels such as coal and petroleum because it can be produced from manure, food, waste, tapioca starch, and sugarcane residue. Biogas contained mainly methane and carbon dioxide. In Thailand, industrial, the agricultural and food processing industries were more than 5,000 industrial plants. Large and medium sizes of plants spread throughout the country. The palm industry was one type of industry that built a biogas production system for producing electricity and sale to the provincial electricity authority (PEA). Currently, there were a number and capacities of completed factories that were shown in Appendix A-1. It was found that the highest biogas obtained from the tapioca starch wastewater then ethanol, liquor and beer, food, palm, rubber and paper, respectively (the department of industrial works, 2013). The most biogas was used for generating electricity to supply electrical energy for operating plant itself. The surplus biogas from the electricity process was left about 20,000 - 30,000 m^3/day. It was eliminated by combusting at a stack fair. As a result, the methane in biogas was burned, and it was transformed into carbon dioxide that impacted to the environment. However, the surplus biogas utilization had been studied changing to be bio-methanol for the purpose of raw material in the biodiesel process[2]. Bio-methanol obtained from renewable sources can be substituted commercial methanol. Five hundred million litres per year of commercial

methanol was imported in the year 2017 (data from the department of industrial works), and It was 100 per cent. As a result, the production of bio-methanol was interested not only in solving CO_2 problem form using biogas as renewable fuel but also alleviating the amount of methanol importing from aboard[3].

Methanol produced from biogas comprised of two main reactions: methane reforming and methanol synthesis. The methane reforming was a process in which carbon dioxide and methane were reacted to form synthesis gas (syngas) consisted of carbon monoxide and hydrogen[4]. For a practical process, water was added to the process. The methane reforming process consisted of three main reactions: dry reforming of methane reaction (1.1), steam reforming of methane (1.2), and water gas shift reaction (1.3). The methanol synthesis occurs via three reactions: hydrogenation of carbon monoxide (1.4), hydrogenation of carbon dioxide (1.5), and water gas shift reaction (1.6)[5].

Methane Reforming

$$CH_4 + CO_2 \rightarrow 2CO + 2H_2 \quad \Delta H = 274.7 \text{ kJ/mol} \quad (1.1)$$

$$CH_4 + H_2O \rightarrow CO + 3H_2 \quad \Delta H = 206.0 \text{ kJ/mol} \quad (1.2)$$

$$CO + H_2O \leftrightarrow CO_2 + 2H_2 \quad \Delta H = -41.12 \text{ kJ/mol} \quad (1.3)$$

Methanol Synthesis

$$CO + 2H_2 \rightarrow CH_3OH \quad \Delta H = -90.55 \text{ kJ/mol} \quad (1.4)$$

$$CO_2 + 3H_2 \rightarrow CH_3OH + H_2O \quad \Delta H = -49.43 \text{ kJ/mol} \quad (1.5)$$

$$CO + H_2O \leftrightarrow CO_2 + 2H_2 \quad \Delta H = -41.12 \text{ kJ/mol} \quad (1.6)$$

The bio-methanol composed of many reactions which can be modeled with kinetic rates. Kinetic modelling was a useful tool which gave a better understanding of mechanisms of reactions to calculate the size of a reactor. Simulation of the reactor must require kinetic modelling for material and energy balance at the

operating condition and combined simulation of other operating units to obtain process simulation.

In this thesis, the kinetic models were investigated for using in the reactor units of methane reforming and methanol synthesis reaction by using MATLAB software. Both reactors were assembled to create the bio-methanol processes by using ASPEN PLUS simulation software. The process simulation results were analyzed for economic feasibility.

1.2 Objective of Research

- To investigate the kinetic models for methane reforming reaction and methanol synthesis reaction

- To create a model of the bio-methanol production process from biogas by using ASPEN PLUS simulation software.

- To do the feasibility analysis of the designed bio-methanol production process.

1.3 Scope of Research

- The kinetic models of the methane reforming will be investigated under these reaction conditions: atmospheric pressure and reaction temperatures in the range of 600 – 700 °C.

- The kinetic models of the methanol synthesis will be investigated under these reaction conditions: reaction pressure in 40 bar and reaction temperature in the range of 170 - 230 °C.

- Both kinetic models will be investigated by using MATLAB software

- The model of a bio-methanol production process will be created by using ASPEN PLUS simulation software.

- The feasibility analysis of the designed bio-methanol production process will be studied by using ASPEN PLUS simulation software.

1.4 Definitions

Parameter	Definitions
r	reaction rate (mole g(cat)$^{-1}$ min^{-1})
p	partial pressure (bar)
k	reaction rate constant
K	equilibrium constant
R^2	correlation coefficient
y_i	Experimental data each species
$\overline{y}$	Mean of the experiment data set
f_i	Modelling data each species
ΔH	The heat of reaction (kJ/mol)
T	Temperature (°C)
P	Pressure (bar)
%CO_2	Volumetric per cent of CO_2 in feed
	Economic parameters
R_t	Net cash inflow-outflows during a single period t
i	Discount rate
t	Number of timer periods
C_t	Net cash inflow during the period t
C_0	Total initial investment cost
NPV	Net Present Value (THB)
IRR	Internal Rate of Return (%)
ROI	Return on Investment (%)
PB	Payback Period (years)
CAPEX	Capital Expenditures (THB)
COGS	Cost of Good Sold (THB)
GP	Gross Profit (THB)
OI	Operating Income (THB)
SG&A	General and Administrative Expenses
NOPAT	Net Operating Profit After Tax
LFAWO	Loss from asset write-off
VC	Variable Cost per unit (THB/kg MeOH)

CHAPTER II

LITERATURE REVIEWS

2.1 Overview

Methanol production was occurred in 1920 by BASF. It was applied in a wide variety of applications in industries [6]. Thailand's methanol consumption obtained 0.7 million metric tons in 2018, and it was predicted, reaching 1 million tons in 2020. In the present day, methanol was produced from fossil resources, but bio-methanol is in replacing. Various studies have been carried out in lab-scale or the semi-pilot plant. To enlarge for industrial size, the kinetic model and reaction mechanism are needed. These kinetic models studied were data using in the simulation to predict the optimal condition of the methanol process 1) Reforming reaction and 2) Methanol synthesis reaction. The kinetic results were compared with experimental results. Finally, the success of the industrial-scale was economic feasibility. It can confirm benefits to investors. The literature review analyzed the following appearances:

- Methane reforming reaction
- Methanol synthesis reaction
- Process simulation and economic feasibility reviews

2.2 Methane reforming reaction

Methane reforming reaction can be produced to syngas: hydrogen, carbon monoxide and carbon dioxide. The syngas is an intermediate component for methanol production. Most literature presented methane reforming reaction using a catalyst (usual nickel) under high temperature and pressure. The methane reforming reactions consist of steam reforming (2.1), dry reforming (2.2), and partial oxidation (2.3).

$$CH_4 + H_2O \rightarrow CO + 3H_2 \quad \Delta H = 206.0 \text{ kJ/mol} \quad (2.1)$$

$$CH_4 + CO_2 \rightarrow 2CO + 2H_2 \quad \Delta H = 274.7 \text{ kJ/mol} \quad (2.2)$$

$$CH_4 + \frac{1}{2}O_2 \rightarrow CO + 2H_2 \qquad \Delta H = -36 \text{ kJ/mol} \qquad (2.3)$$

The kind of catalysts and conditions for the reforming reaction were studied to obtain kinetic models by following a Langmuir-Hinshelwood rate expression. The results of previous works are reported in Table 1 [7-12].

Table 1 *Proposed Rate Expressions for Reforming of Methane with Carbon Dioxide*

Rate model	Catalyst	Conditions	Author(s)
$r_{ref}=\frac{k_{ref}P_{CH_4}(P_{CO_2}+P_{H_2O})}{(1+24(P_{CO_2}+P_{H_2O})+8P_{H_2})^2}$	Cu/SiO_2	T 630-890 ℃ P 1 atm	Lewis et al. (1949)[13]
$r_{ref}=\frac{k_{ref}P_{CH_4}}{1+a\frac{P_{H_2O}}{P_{H_2}}+bP_{CO}}$	Ni foil	T 600-750 ℃ P 1 atm	Bodrov et al. (1965) [14]
$r_{ref}=\frac{k_{ref}K_{CH_4}K_{CO_2}P_{CH_4}P_{CO_2}}{(1+K_{CH_4}P_{CH_4}+K_{CO_2}P_{CO_2})^2}$	Rh/Al_2O_3	T 600-800 ℃ P 1 atm	Richardson et al. (1990)[15]
$r_{ref}=\frac{k_{ref}K_{CH_4}K_{CO_2}P_{CH_4}P_{CO_2}}{(a+bP_{CO_2}^{\ 2}+cP_{CH_4})^2}$	Ni/Al_2O_3, $Ni/CaO\text{-}Al_2O_3$	T 650-750 ℃ P 1 atm	Zhang et al. (1994)[16]
$r_{ref}=\frac{k_{ref}(P_{CH_4}-\frac{P_{H_2}^{\ 2}P_{CO}^{\ 2}}{K_{ref}P_{CO_2}})}{1+\frac{P_{CO_2}^{\ 2}}{K_{R,C\text{-}z}P_{CO_2}}}$	Ir/Al_2O_3	T 550-850 ℃ P 1 atm	Mark et al (1996)[17]
$r_{ref}=\frac{k_{ref}K_{CH_4}(P_{CH_4}P_{CO_2}-\frac{P_{H_2}^{\ 2}P_{CO}^{\ 2}}{K_{ref}})}{1+K_{CH_4}P_{CH_4}}$	Ir/Al_2O_3	T 700-850 ℃ P 1 atm	Mark et al (1996)[17]
$r_{ref}=\frac{k_{ref}K_{CO_2}(P_{CH_4}P_{CO_2}-\frac{P_{H_2}^{\ 2}P_{CO}^{\ 2}}{K_{ref}})}{1+K_{CO_2}P_{CO_2}}$	Ir/Al_2O_3	T 700-850 ℃ P 1 atm	Mark et al (1996)[17]
$r_{ref}=\frac{k_{ref}K_{CH_4}K_{CO_2}(P_{CH_4}P_{CO_2}-\frac{P_{H_2}^{\ 2}P_{CO}^{\ 2}}{K_{ref}})}{(1+K_{CH_4}P_{CH_4}+K_{CO_2}P_{CO_2})^2}$	Ir/Al_2O_3	T 700-850 ℃ P 1 atm	Mark et al (1996)[17]
$r_{ref}=\frac{k_{ref}P_{CH_4}P_{CO_2}}{(1+K_1P_{CH_4}+K_2P_{CO})(1+K_3P_{CO_2})}$	$Ni/La/Al_2O_3$	T 700-900 ℃ P 1 atm	Olsbye et al. (1997)[18]

$r_{ref}=\frac{k_{ref}\sqrt{K_1K_2P_{CH_4}P_{CO_2}}}{(1+\sqrt{K_1P_{CH_4}}+\sqrt{K_2P_{CO_2}})^2}$	Ni/Al_2O_3, Ni/SiO_2, $Ni/CaO\text{-}Al_2O_3$	T 700-750 °C P 1 atm	Osaki et al. (2005)[19]
$r_{ref}=\frac{k_3K_1K_2P_{CH_4}P_{CO_2}P_{CO}P_{H_2}^2}{\left(P_{CO}P_{H_2}^2+K_1P_{CH_4}P_{CO}+K_2K_2P_{CO_2}P_{H_2}^2\right)^2}$	Ni/SiO_2	T 650-750 °C P 1 atm	Kroll et al. (1998) [20]
$r_{ref}=\frac{k_1P_{CH_4}P_{CO_2}}{\left(\frac{k_{-1}K}{k_7}\right)P_{CO}P_{H_2}^{(4-x)/2}+\left[1+\left(\frac{k_1}{k_7}\right)P_{CH_4}\right]P_{CO_2}}$	supported Pt and Ni	T 650-750 °C P 1 atm	Bradford et al. (1999)[21]
$r_{ref}=\frac{k_{ref}P_{CH_4}P_{CO_2}}{(1+K_{CH_4}P_{CH_4})(1+K_{CO_2}P_{CO_2})}$	Ni/Al_2O_3, $Ni/CeO_2\text{-}Al_2O_3$	-	Wang et al. (2000)[22]

2.3 Methanol synthesis reaction

Methanol synthesis reactions from syngas occur via three reactions, namely: hydrogenation on carbon monoxide (4), hydrogenation on carbon dioxide (5), and water-gas shift reaction (6). the reactions were researched on methanol synthesis mechanism based on Cu-based catalysts for a long time until the present day. There are two concepts regarding the reaction mechanism. The first concept, CO had received attention as the primary reactant to produce methanol. the mechanism of the reaction was studied in high feed ratio of CO / CO_2 by Leonov et al. and Natta et al.[23, 24] The second concept was CO_2 utilization because CO_2 had been the role of greenhouse gas. Thereby, it was primarily concerning about supporting CO_2 utilization in methanol production, CO_2 as a primary reactant to produce methanol was promoted by researchers such as Liu et al., and Chinchen et al. [25, 26].

$CO + 2H_2 \rightarrow CH_3OH \quad \Delta H = -90.55$ kJ/mol (2.4)

$CO_2 + 3H_2 \rightarrow CH_3OH + H_2O \quad \Delta H = -49.43$ kJ/mol (2.5)

$CO + H_2O \leftrightarrow CO_2 + 2H_2 \quad \Delta H = -41.12$ kJ/mol (2.6)

In this literature, it was presented that researchers regarded the mechanism of CO_2 hydrogenation as the main reaction. Chinchen et al. showed the evidence of CO_2 as the primary reactant in methanol production using 14C-labeled reactants[26].

The CO_2/CO ratio was studied to effect on methanol production by Takagawa and Ohsugi, in 1987. They determined the empirical rate equations for all three methanol synthesis reactions. They showed that methanol production rate increasing with rising in CO_2/CO ratio and the beginning of water in the reaction [27]. McNeil et al. showed that the experimental result of adding 2% by mole of CO_2 in feed exhibited a maximum yield on methanol production. Besides, they found that an adding CO_2 affect rising methanol formation at low temperature. These results opposed other research because they developed a reaction rate from including the effects of CO_2 and both as a methanol producer rate as well as a rate of the inhibitor[28].

Rozovskii et al. studied the methanol formation occurring through the hydrogenation of CO_2 by using Temperature Programmed Desorption (TPD) technique and C-14 labelling techniques. As a result, that was explained the unavailable hydrogenation on CO direct pathway to produce methanol [29]. In a study of methanol synthesis carried by Fujitani et al. [30]. They presented CO_2 hydrogenation reaction for methanol production at atmospheric pressure in a fixed flow reactor. it was found that CO_2 can be transforming on Cu and ZnO catalyst. The reaction rate of CO_2 hydrogenation was rapid than CO hydrogenation rate. The researcher reported that adding water and selecting catalysts species was mainly caused by a difference in the methanol production rate.

By the way, another research group supported the CO hydrogenation mechanism for methanol production. Natta et al.[24] presented the first kinetic for CO hydrogenation. They thought about only CO and H_2 as reactants and CO_2 as the only promoter under critical pressure without a catalyst. In 1982, Klier et al. reported that CO was the main reactant and it reacted with H_2 then transformed into methanol by adsorbing on the catalyst. But CO_2 served only as a promoter and not as the main reactant. In addition, they proposed maximum methanol yield at a CO_2/CO feed ratio equal to 2:28, which it was inhibited by strong adsorption of CO_2 [31]. Later, Liu et al. experimented to create an initial rate of methanol synthesis in a batch reactor and to determine feed ratio that affected to methanol production rate. These results showed that increasing CO_2 in feed influenced better methanol formation because it served to adjust balancing between H_2/CO in a reactor. A year

later, Liu et al. gave more detailed considering that the methanol was primarily produced from CO_2 at low temperature, low conversion and water generated. But the methanol was not primarily produced from CO at high temperature, low conversion and no water generated in producing methanol[32].

Recently, Lim et al. conducted a comprehensive study assuming CO and CO_2 to adsorb on Cu sites of a catalyst and water to adsorb on a ZnO site. They found that the CO hydrogenation rate was slower than the CO_2 hydrogenation rate, which decreased the methanol production rate and the water-gas-shift reaction rate. The researchers suggested that a kinetic mechanism relating only CO hydrogenation reactions because of the CO hydrogenation rate as a limiting step. In a more recent study by the same authors, they developed a kinetic model to evaluate the effect of carbon dioxide fraction on the methanol yield by including CO_2 adsorbing rate and ignoring CO_2 reaction on active site of the catalyst[33].

In this literature review, kinetic models were presented, and kinetic parameters were evaluated. The models had supported a different set of assumptions relating to the reaction mechanism and reaction conditions. Leonov et al. first presented a kinetic model for methanol synthesis over a $Cu/ZnO/Al_2O_3$ catalyst[23]. However, they did not examine the influence of CO_2 in the feed. Later, Klier et al. and Villa et al. proposed models that included the pCO_2 (partial pressure of CO_2) terms and they suggested that the CO_2 was the primary reactant[31, 34]. The models were proposed by Villa et al. and developed based on the scheme that methanol was produced from CO and CO_2 only. Adsorption term was included since CO2 adsorbs strongly at high concentrations. Ohsugi and Takagawa were researchers who derived empirical rate expressions for the three methanol synthesis reactions under a varying range of experimental conditions[27]. Skrzypek et al. had shown through their experiments that methanol synthesis prefered CO_2 despite CO as a carbon source [35]. The models were derived from a kinetic model considering both CO and CO_2 hydrogenation and the water gas shift reaction by Graaf et al. They derived 48 reaction schemes by assuming different elementary steps to be rate-limiting and then selected the best possible kinetic model using statistical discrimination [36]. McNeil et al. developed a CO_2 hydrogenation rate expression

based on the CO_2 reaction rate as well as methanol rate on an active surface by using empirical expressions method [28]. These were derived from their kinetic model based on Reactions (5) and (6).

Askgaard et al. presented a kinetic model and evaluated the kinetic parameters using gas-phase thermodynamics and surface science study. It was obtained that a good result of the calculated rates when extrapolated to actual conditions comparing with the measured rates [37]. Froment and Buschhe conducted experiments and developed a steady-state the same kinetic model based on a detailed reaction scheme assuming CO to be the primary carbon source of methanol. They still described the effects of temperature, pressure, and gas-phase composition on methanol production rates even beyond their experimental conditions [38]. Also, Kubota et al. studied kinetic equations for methanol synthesis and developed under assuming a condition of CO_2 hydrogenation rate that was faster than CO hydrogenation rate at low temperature and high pressure. The models were found that their equations reasonably accurate since the yield values obtained from the equations by comparing with their experimental conditions [39].

Rozovskii and Lin proposed building the theoretical kinetic models for two reaction schemes, which could fit the experimental data well. Two different gas phase compositions and one with pCO_2 term were developed and the additional with pCO term to apply of their models. It was found that both the schemes proved to be useful when dealing with a CO mixture, but the kinetic model did not match based on scheme one with the experimental data well when consuming a CO_2 mixture [29]. The model had been developed a comprehensive kinetic model consisting of 48 reaction rates based on different possible rate-determining steps by Lim et al. it was shown through parameter estimation that, among the 48 rates, the surface reaction of a methoxy intermediate was the rate-determining step for CO hydrogenation, hydrogenation of a C-H intermediate was the rate-determining step for CO_2 hydrogenation and formation of an H_3O^+ intermediate was the rate-determining step for the water-gas shift reaction by using a $Cu/ZnO/Al_2O_3/Zr_2O_3$ catalyst [33]. Grabow and Mavrikakis developed a comprehensive microkinetic model

using density functional theory calculations to solve with the uncertainties relating to the reaction mechanism and nature of active sites [40].

All of the above, they were a kinetic model of researchers to select a suitable model for methanol production in this thesis. Table 2 summarized the various kinetic models, proposed in literature along with the experimental reaction conditions.

Table 2 *Summary of Kinetic Models proposed in the literature for methanol synthesis.*

Rate model	Conditions	Author(s)
$r_{CH_3OH} = k\left(\frac{p_{CO}^{0.5}p_{H_2}}{p_{CH_3OH}^{0.66}} - \frac{p_{CH_3OH}^{0.34}}{p_{CO}^{0.5}p_{H_2}K_2^*}\right)$	498-523 K; 75 atm	Leonov et al., (1973) [23]
$r_{CH_3OH} = \text{const}\frac{K_{redox}^3(p_{CO_2}/p_{CO})^3(p_{CO}p_{H_2}^2 - p_{CH_3OH}/K_2^*)}{[1+K_{redox}(p_{CO_2}/p_{CO})]^3(F+K_{CO_2}p_{CO_2})^n}$ $+k'(p_{CO_2} - (1/K_1^*)(p_{CH_3OH}p_{H_2O}/p_{H_2}^3)).$	498-523 K; 75 atm	Klier et al., (1982) [31]
$r_{CH_3OH} = \frac{f_{CO}f_{H_2}^2 - f_{CH_3OH}/K_2^*}{(A+Bf_{CO}+Cf_{H_2}+Gf_{CO_2})^3}$ $r_{RWGS} = \frac{f_{CO_2}f_{H_2} - f_{CO}f_{H_2O}K_3^*}{M^2},$	N/A	Villa et al., (1985) [34]
$r_{CH_3OH} = \frac{k_1K_{CO}\left(c_{CO}c_{H_2}^{3/2} - c_{CH_3OH}/c_{H_2}^{1/2}K_1^{eq}\right)}{\left(1+K_{CO}c_{CO}+K_{CO_2}c_{CO_2}\right)\left(c_{H_2}^{1/2}+\left(K_{H_2O}/K_{H_2}^{1/2}\right)c_{H_2O}\right)}$ $r_{H_2O} = \frac{k_2K_{CO_2}\left(c_{CO_2}c_{H_2} - c_{H_2O}c_{CO}/K_2^{eq}\right)}{\left(1+K_{CO}c_{CO}+K_{CO_2}c_{CO_2}\right)\left(c_{H_2}^{1/2}+\left(K_{H_2O}/K_{H_2}^{1/2}\right)c_{H_2O}\right)}$ $r_{CH_3OH}^* = \frac{k_3K_{CO_2}\left(c_{CO_2}c_{H_2}^{3/2} - c_{CH_3OH}c_{H_2O}/c_{H_2}^{3/2}K_3^{eq}\right)}{\left(1+K_{CO}c_{CO}+K_{CO_2}c_{CO_2}\right)\left(c_{H_2}^{1/2}+\left(K_{H_2O}/K_{H_2}^{1/2}\right)c_{H_2O}\right)}$	483-518 K; 15-50 bar	Graaf et al., (1988) [36]
$r = \frac{k_f'K_{CH}K_{H_2}^2K_H^2K_{CO}(p_{CO}p_{H_2}^2 - p_{CH_3OH}/K_{eq})}{K_{CH}K_{H_2}^{3/2}K_H^{3/2}K_{CO}p_{CO}p_{H_2}^{3/2} + K_{CO_2}p_{CO_2} + K_{H_2}'p_{H_2}}$ $+\frac{k_f''K_{H_2}K_HK_{CO_2}K_{CHO_2}[p_{CO_2}p_{H_2} - p_{CH_3OH}p_{H_2O}/(K_{eq}''p_{H_2}^2)]}{K_{H_2}^{1/2}K_H^{1/2}K_{CO_2}K_{CHO_2}p_{CO_2}p_{H_2}^{1/2} + K_{CO_2}''p_{CO_2}^2 + K_{H_2O}p_{H_2O}^3}$	483-513 K; 2.89-4.38 MPa	McNeil et al., (1989) [28]
$r_+ = k_{-11}K_5^{-3/2}K_8^{-1}K_9K_{10}K_{11}\left(\frac{p_{H_2}}{p_o}\right)^{3/2}\left(\frac{p_{CO_2}}{p_o}\right)\theta_*^2$ $r_- = k_{-11}K_5^{-3/2}K_8^{-1}K_9K_{10}K_{11}\frac{1}{K_G}\frac{p_{CH_3OH}p_{H_2O}}{p_{H_2}^{3/2}p_o^{1/2}}\theta_*^2.$	483-563 K; 1-4 bar	Askgaard et al., (1995) [37]

$r_{MeOH} = \frac{k'_{5a}K'_2K_3K_4K_{H_2}p_{CO_2}p_{H_2}[1-(1/K^*)(p_{H_2O}p_{CH_3OH}/p^3_{H_2}p_{CO_2})]}{(1+(K_{H_2O}/K_8K_9K_{H_2})(p_{H_2O}/p_{H_2})+\sqrt{K_{H_2}p_{H_2}}+K_{H_2O}p_{H_2O})^3}$ $r_{RWGS} = \frac{k'_1p_{CO_2}[1-K^*_3(p_{H_2O}p_{CO}/p_{CO_2}p_{H_2})]}{(1+(K_{H_2O}/K_8K_9K_{H_2})(p_{H_2O}/p_{H_2})+\sqrt{K_{H_2}p_{H_2}}+K_{H_2O}p_{H_2O})}$,	453-553 K; 15-51 bar	Froment and Bussche (1996) [38]
$R_M = \frac{k_M\{P(CO_2)P(H_2)-P(CH_3OH)P(H_2O)/[K_MP^2(H_2)]\}}{[1+K_{CO_2}\times P(CO_2)+K_{H_2O}\times P(H_2O)]^2}$ $R_R = \frac{k_R\{P(CO_2)-P(CO)P(H_2O)/[K_R\cdot P(H_2)]\}}{1+K_{CO_2}P(CO_2)+K_{H_2O}P(H_2O)}$	473-548K; 4.9 MPa	Kubota et al., (2001) [39]
$r_{Me} = A_{Me}e^{\left(-\frac{E_{Me}}{RT}\right)}\frac{c_{CO_2}\left(c_{H_2}-c_{H_{2,eq}}\right)}{\left(1+A_We^{\left(\frac{E_W}{RT}\right)}c_{H_2O}\right)^2}$ $r_{H_2O} = A_{H_2O}e^{\left(-\frac{E_{H_2O}}{RT}\right)}\frac{c_{CO_2}-c_{CO_{2,eq}}}{\left(1+A_We^{\left(\frac{E_W}{RT}\right)}c_{H_2O}\right)}$	473-513 K; 34-41 bar	Šetinc and Levec, (2001) [41]
$r = \frac{k_3p_{H_2}(1-\frac{p_{wg}p_{H_2O}}{K_{p(wg)}p^2_{H_2}p_{CO_2}})}{1+K_{-2}p_{H_2O}+K_{-2}p_{H_2O}/(K_1p_{CO_2})}$	513 K; 5.2 MPa	Rozovskii and Lin,(2003) [29]
$r_A = \frac{k_AK_{CO}K_{H_2}{}^2K_{CH,CO}(P_{CO}P_{H_2}{}^2-P_{CH_3OH}/K_{PA})}{(1+K_{CO}P_{CO})(1+K_{H_2}{}^{0.5}P_{H_2}{}^{0.5}+K_{H_2O}P_{H_2O})}$ $r_B = \frac{k_BK_{CO_2}K_{H_2}{}^{0.5}(P_{CO_2}P_{H_2}-P_{CO}P_{H_2O}/K_{PB})/P_{H_2}{}^{0.5}}{(1+K_{CO}P_{CO})(1+K_{H_2}{}^{0.5}P_{H_2}{}^{0.5}+K_{H_2O}P_{H_2O})(1+K_{CO_2}P_{CO_2})}$ $r_C = \frac{k_CK_{CO_2}K_{H_2}K_{CH,CO_2}(P_{CO_2}P_{H_2}{}^3-P_{CH_3OH}P_{H_2O}/K_{PC})/P_{H_2}{}^2}{(1+K_{H_2}{}^{0.5}P_{H_2}{}^{0.5}+K_{H_2O}P_{H_2O})(1+K_{CO_2}P_{CO_2})}$	523-553 K; 5 MPa	Lim et al., 2009 [33]

2.4 Process simulation and economic feasibility reviews

Few researchers reported about process simulation of methanol production from biogas. In this topic, it was presented by similar research to be a guideline assuming simulation and economic parameters. Liu et al. presented an analysis applied to Carbon Capture, Utilization, and Storage (CCUS) by integrating the enhanced recovery gas (ERG) with methanol production. The natural gas (NG) mixture (Mostly CH_4) from the NG production was sent to the methanol plant. The gas mixture was reacted with the captured CO_2 in the reformer (based on bi-reforming reaction) to produce a syngas mixture which it was suitable for methanol synthesis. Simulations were carried out in Aspen Plus. As results, it was shown that the proposed process had the highest CO_2 reduction intensity (45.5%) among another comparable with investigated scenarios[32].

CO_2 can be reacted by H_2 obtained from the electrolysis of water to produce methanol. The process was operated at a constant temperature under 533 K and 80 bars using $CuO/ZnO/Al_2O_3$ catalyst. A number of reaction kinetic models had been proposed so far based on the commercial catalysts such as Cu/Zn/Al catalyst[30, 42-44]. In the other technology for methanol production, CO_2 and H_2O can be co-electrolyzed to produce methanol at only high temperature. An economic study showed that the hydrogenation for methanol production was economically unfeasible with an accurate analysis of the high cost of H_2 production. For this reason, the research activity for the high temperature of CO_2 electrolysis had difficulty in minimizing the investment cost[45]. It is still needed much knowledge for studying on regarding the new electrocatalysts, reaction mechanism, catalyst degradation, cell design, and system design for commercial-scale [8, 46, 47].

The entire Gas to Methanol (GTM) process was analyzed by Zhang et al. [9, 10]. The researchers considered energy efficiency and carbon dioxide emissions. They suggested two innovative CO_2-utilization GTM processes (CGTM) for methanol synthesis, and then they experimented with converting CO_2 through reforming and hydrogenation. Later, Zhang et al.[9] developed two options of carbon-dioxide-utilization in the gas-to-methanol process (CGTM) with a fresh CO_2 feeding method as

the main configuration difference. The first option, the fresh CO_2 was first fed to the reforming unit for producing CO, which was sent to the methanol synthesis unit to produce methanol. While, the last option, the fresh CO_2 was supplied to the methanol synthesis unit as direct methanol production. Process simulations were performed in Aspen Plus, and the Langmuir-Hinshelwood-Hougen-Watson (LHHW) kinetic was applied in the Plug model reactor by using previous experimental results [33]. The feasibility parameters such as NPV, IRR, and BP for both options were in the range of 483.41–858.80 MUSD$, 17.15–22.65%, and 6.23–9.52 years, respectively. In addition, the results suggested that the methanol price and the natural gas price were a major influence on economic feasibility.

Laquaniello et al. [48] analyzed a process in methanol production by gasification of municipal solid wastes (MSW) which were a main source of carbon. The methanol plant was composed of three gasifiers at high temperature in order to guarantee the plant maintenance while maintaining continuity of the production. Then it was simulated using PRO-II software. Economic analysis results were carried out the plant produced methanol at 110 €/ton treating 300 ton/d of wastes. The ROI was equal to 29%. The waste to methanol (WTM) plant could produce methanol with 40% of the waste and 30–35% reduction in Greenhouse Gas (GHG) emissions by comparing with methanol production from fossil fuel and bio-resources. Besides, the comparison between waste to energy (WTE) process and the waste to methanol (WTM). The advantages of methanol product were easy storage and distribution even on a long-distance, whereas the electrical energy was depended on the capacity of grid line for the power production, these considerations suggested that the WTM was a valuable solution from an economic, strategic and environment.

In addition, the methanol production process from gasification of biomass was analyzed by Specht et al. [49] that explored the only possibility to achieve high carbon conversion for methanol synthesis from biomass feedstocks. Hydrogen was added to the gasified syngas. The conversion of biomass to methanol by addition of external hydrogen required high investment cost from an electrolysis unit; however, the adding hydrogen resulted in high methanol production rates. Conventional

gasification process without hydrogen addition was showed that the investment cost of CO_2 removal was lower than the gasification process with hydrogen addition, but carbon conversion of the conventional process was limited due to the stochiometric adjustment and the high purge gas rate.

Martin and Grossmann [50] developed a process to produce methanol from switchgrass (Panicum virgatum). The process consists of two sections were the methanol production from syngas which was generated by biomass processing (biomass to methanol process) and the electrolytic section where hydrogen was produced to react with CO_2 that had been captured during syngas cleaning. A 25% KOH solution, the wind energy and operating at 101 kPa 353 K were used in the electrolyzer. The switchgrass is gasified to produce bio-syngas, and then the bio-syngas was purified by a membrane/PSA system. A flow of 1,700 tons/day of biomass was processed, producing 207 million gallons/year of methanol. The high investment was around 1000 million €, but the variable cost of methanol was in a range of 0.25–0.35 €/kg with a high production capacity. While Shamsul et al.[51] simulated the production of methanol from renewable sources. Biomass feedstocks vary from agricultural waste, forestry waste, livestock and poultry waste, fishery waste, and sewage sludge. The researcher reported the result that a carbon/hydrogen ratio of feedstock was a significant impacting on the variable cost of methanol.

In this thesis, the study is focusing on syngas to methanol process. It significantly advantages, because the conversion of syngas to methanol is more than the conversion of CO2 to methanol. Additionally, it leads to a low amount of by-products. In a feasibility study, It will find the optimal capacity of methanol production. In this case, the capacities on previous works were referenced some pilot plants for examples a capacity of 100 ton/year, built by Mitsui Chemicals (Japan), 4000 ton/year, constructed by Carbon Recycling International and operating since 2011 (Iceland) and 100 ton/year using renewable hydrogen (Osaka) [52]. Table 3 showed studied results of the advantages and disadvantages of various technologies.

Table 3 *The results of the advantages and disadvantages of various technologies.*

Technology	Advantages	Disadvantages
The natural gas mixture to methanol process	- First technology - Low variable cost - Low investment cost	- Conventional source - Low CO_2 Conversion - Adding methanol purification
Biomass/Biogas to methanol process	- Renewable source - Low variable cost - High CO_2 Conversion	- Two-steps to methanol
Waste to Methanol (WTM) Process	- Recycle waste - Waste management	- Complicated process - Expensive variable cost - Expensive investment cost
Co-electrolyzed to methanol process	- New technology - High performance - One step to methanol	- Expensive variable cost - Expensive investment cost

CHAPTER III

THEORY

This chapter explained all the necessary theoretical aspects behind the whole process to transform biogas to methanol. The related theories were used for the methanol process simulation such as biogas to methanol reactions, Langmuir-Hinshelwood-Hougen-Watson (LHHW), nonlinear regression method to evaluate kinetic parameters, and the definition of economic variables.

3.1 Biogas to methanol reactions

3.1.1 Reforming Reaction

Methane reforming reactions comprised of steam reforming, autothermal reforming, partial oxidation and dry reforming reaction for producing hydrogen and carbon monoxide using a catalyst. The most common reactions in the industry were autothermal reforming (ATR) and steam methane reforming (SMR). The most nickel-based catalyst was used at high temperature[53].

SMR required an external heating source to supply the packed catalyst that converted steam and methane feedstock into hydrogen and carbon monoxide as a component of syngas because thermodynamics of this reaction was strongly endothermic. In the past, SMR was used for transforming natural gas to commercial hydrogen about 95% of the world hydrogen production. Currently, the catalyst of SMR was developed for syngas production by a metal-based catalyst[54]. The reaction of steam methane reforming was presented in equation 3.1.

Steam methane reforming (SMR)

$$CH_4 + H_2O \rightarrow CO + 3H_2 \qquad \Delta H = 206.0 \text{ kJ/mol} \qquad (3.1)$$

Autothermal reforming (ATR), methane was reacted with oxygen, carbon dioxide, and steam. The ATR produced an H_2/CO ratio equal to 1 with adding carbon dioxide while adding steam in the reaction produced H_2/CO ratio equal to 2.5. The ATR was divided into two sub-reactions by different reactants as carbon dioxide and steam for adjusting an H_2/CO in gas products. The ATR using carbon dioxide generated H_2/CO ratio equal to 1 following equation 3.2, while steam was used to produce more H_2/CO ratio following equation 3.3. Both reactions were exothermic

because the methane was oxidized with oxygen. SMR was different form ATR by no requiring oxygen [55].

Autothermal reforming (ATR) using CO_2:

$$2CH_4 + O_2 + CO_2 \longrightarrow 3H_2 + 3CO + H_2O \qquad (3.2)$$

Autothermal reforming (ATR) using steam:

$$4CH_4 + O_2 + 2H_2O \longrightarrow 10H_2 + 4CO \qquad (3.3)$$

Partial oxidation (POX) required the limited oxygen for partial combustion in a reactor to obtain rich hydrogen. The POX was exothermic and was not required an external heating source. This reaction was operated without using a catalyst, but it was needed to control the desired temperature by cooling for safety. Nevertheless, to obtain high yield production, it was required a catalyst. The reaction was presented in the following equation 3.4[56].

Partial oxidation (POX) reaction:

$$CH_4 + 1/2O_2 \longrightarrow 2H_2 + CO \qquad \Delta H = -36 \text{ kJ/mol} \qquad (3.4)$$

Dry reforming reaction (DRM) was most studied for the utilization of carbon dioxide. The reaction was performed at a high temperature because it was highly endothermic. DRM was less suitable than SMR for pure H_2 production, but the DRM reaction was mainly used for a process that required a higher CO ratio. The advantages of DRM were the high conversion of methane and the rapid reaction rate. The thermodynamics of DRM was similar to SMR under the same condition. However, the main difference between DRM and SMR was a number of cokes forming which inhibited the activity of reaction leading to catalyst deactivation. The retarded coke activation of catalysts such as Ni, Rh and Ru catalysts[4]. In SMR, the addition of water or steam can eliminate coke in a reactor. As a result, the catalyst was more stable. In addition, the dry reforming reaction (Eq. 3.5) was usually caused of several side reactions, for example, the CH4 cracking (Eq. 3.6), Boudouard reaction (Eq. 3.7) and reverse water gas shift reaction (RWGS) (Eq. 3.8). The RWGS was less than dry and steam reforming reaction. The temperature was required higher than 700°C for completely converting CH_4 and CO_2 to syngas[4].

Dry reforming reaction:

$$CH_4 + CO_2 \longrightarrow 2H_2 + 2CO \quad \Delta H = 274.7 \text{ kJ/mol} \quad (3.5)$$

Methane cracking:

$$CH_4 \longrightarrow C + 2H_2 \quad \Delta H = 74.9 \text{ kJ/mol} \quad (3.6)$$

Boudouard reaction:

$$2CO \longrightarrow C + CO_2 \quad \Delta H = -172.4 \text{ kJ/mol} \quad (3.7)$$

Reverse Water–Gas shift:

$$CO_2 + H_2 \longrightarrow CO + H_2O \quad \Delta H = 49.43 \text{ kJ/mol} \quad (3.8)$$

The reactions in this work were combining steam and dry reforming reaction for the purposes of high H2/CO ratio in syngas and stability of a catalyst. By the way, the side reaction of the process was studied by reverse water gas shift reaction.

3.1.2 Methanol Synthesis

The most technologies for syngas to methanol (STM) was operated under pressure and low temperature. The commercial catalyst based on Copper/Zinc catalyst with supporters such as aluminium oxide or Chromium (III) Oxide. The reactions of methanol synthesis were hydrogenation on CO or CO_2 showed in equations 3.9 and 3.10, respectively. A little water was a product of side reaction which came from a reverse water gas shift reaction. These three reactions were mild exothermic. It was shown that the rising yield of methanol by decreasing temperature and increasing pressure[57].

CO hydrogenation reaction:

$$CO + H_2 \longrightarrow CH_3OH \quad \Delta H = -90.55 \text{ kJ/mol} \quad (3.9)$$

CO_2 hydrogenation reaction:

$$CO_2 + H_2 \longrightarrow CH_3OH + H_2O \quad \Delta H = -49.43 \text{ kJ/mol} \quad (3.10)$$

These reaction theories were previously mentioned; they were carried in kinetic models regarding the Langmuir-Hinshelwood-Hougen-Watson (LHHW) model. The LHHW kinetic was theoretically presented in the next topic.

3.2 Langmuir-Hinshelwood-Hougen-Watson (LHHW) kinetic

The LHHW model had commonly simplified the approximation of modelling heterogeneous catalytic reactor. It was first developed by Hinshelwood, and therefore, it sometimes called Langmuir-Hinshelwood kinetics. This model was modified by Hougen and Watson in 1943. The developed model was assumed that all active sites were uniform, beginning adsorbed species did not interact with already adsorbed species, active sites were similar kinetic and thermodynamic characteristics, the entropy and enthalpy of adsorption were constant and not depending on the adsorbed amount, the species adsorbed on the mono-layer of coverage in a porous catalyst and the rate of adsorption related to the concentration of the active sites which not occupied (an empty) and the partial pressure of a component in the gas phase[58]. Therefore, the kinetic rate expression was called Langmuir-Hinshelwood-Hougen-Watson (LHHW) kinetic. It was written in equation 3.10.

$$rate = \frac{(Kinetic\ term)\bullet(Potential\ term)}{(Adsorption\ term)^{n}} \qquad (3.10)$$

The constant parameters of the rate expression were fitted with experimental data by using the nonlinear regression method.

3.3 Full Factorial Design (FFD)

a full factorial design is a method that investigated the effect of all the factors and the interaction of two/three factors. All input factors are set at two/three levels, and each These levels are termed the high (centre for three factors) and low or + 1, (0), and - 1 respectively. The total number of experiments was calculated via 2^k, 3^k for two and three levels respectively, by k is the amount of all factors. **Figure 1** was the 2^3 design as a cube that full factorial design for three inputs, each at two-level. The number of experiments was calculated as eight runs of experiments.

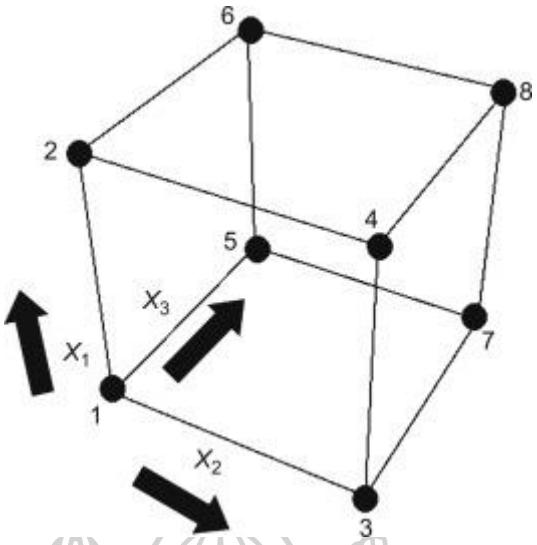

Figure 1 *Representation of a 2^3 design as a cube*

3.4 MATLAB and Aspen plus software

MATLAB is a programming platform designed specifically. It is used for analyzed data, developed algorithms, create models and application. In the kinetic study, the using MATLAB was challenged task due to computational modelling methods of the mathematics complexity properties (Li and Huang, 2017)[59].

Aspen plus was a most widely used software in the simulation of the chemical process for modelling, equipment design and process optimization. The software-based on unit operation platforms such as mixer, heater, distillation column and reactor. Also, it included libraries of chemicals and physical properties that simplify the design process.

3.5 Nonlinear Regression Method

Nonlinear regression was a method of regression analysis for evaluating model parameters. The experimental data were modelled by a function that combined the model parameters depending on one or more independent variables. Appropriate nonlinear repression was the least-squares method which was a standard approach in regression analysis to approximate kinetic parameters of overdetermined models (sets of data in the model had over number than unknown kinetic parameters)[60]

by minimizing the variability of the data set which can be restrained. It was used for three sums of squares formulas:

The total sum of squares:

$$SS_{tot} = \sum_i (y_i - \bar{y})^2 \qquad (3.11)$$

The regression sum of squares:

$$SS_{reg} = \sum_i (f_i - \bar{y})^2 \qquad (3.12)$$

The sum of squares of residuals:

$$SS_{res} = \sum_i (y_i - f_i)^2 \qquad (3.13)$$

The formulas of the coefficient of determination was general defined by:

$$R^2 = 1 - \frac{SS_{reg}}{SS_{tot}} \qquad (3.14)$$

where y_i Experimental data each species

$\bar{y}$ Mean of the experiment data set

f_i Modelling data each species

All references of reactions, kinetic and nonlinear regression method theories were used for creating the kinetic models. The obtained kinetic models were used in reactor models which were assembled with other unit operations by using ASPEN PLUS software to build the process simulation of methanol production. The results of process simulation were mass balance, energy balance and preliminary data for sizing equipment to calculate economic variables.

3.4 Economic variables

The economic feasibility was evaluated by financial variables such as the Net Present Value (NPV), Internal Rate of Return (IRR), Return on Investment (ROI) and Payback Period (PB)[61].

Net present value (NPV) was the difference between the present value of the net cash outflows and the present value of net cash inflows. The NPV was used for

feasibility analysis. If the Present Value (PV) of the net cash inflow is greater than the PV of the net cash inflow then the NPV was more than zero and, on the other hand, the NPV had a negative value. In theory, investors should choose to invest in projects with the highest NPV value among the available options.

The NPV was calculated by the formula:

$$NPV = \sum_{t=1}^{n} \frac{R_t}{(1+i)^t} \qquad (3.15)$$

where:

R_t Net cash inflow and outflows during period t

i Discount rate

t Number of timer periods

The internal rate of return (IRR) was an index used in capital budgeting to estimate the profitability of investments.

The internal rate of return (IRR) was a financial indicator that was widely used for the decision to invest in available projects. It was used in conjunction with another equally widely used measure known as Net Present Value (NPV). The IRR meant the discount rate that causes the present value of all cash flows equal to zero. The IRR was calculated that was the same formula in the NPV equation, as shown in equation 3.16.

$$0 = NPV = \sum_{t=1}^{T} \frac{C_t}{(1+IRR)^t} - C_0 \qquad (3.16)$$

where:

C_t Net cash inflow during the period t

C_0 Total initial investment cost

IRR The internal rate of return

t The number of time periods

Return on Investment (ROI) was an indicator that exhibited the return on investment. It was commonly used for comparing various investments in marketing investment analysis. The high ROI showed a lot of profits comparing with the capital invested. The ROI was calculated by the profits of an investment dividing by the investment cost as follows:

$$ROI = \frac{Current\,Value\,of\ Investment - Cost\,of\ Investment}{Cost\,of\ Investment} \qquad (3.16)$$

Payback Period (PB) meant the investment period that the net cash inflows were equal to the net cash outflows. It was an indicator for evaluating the feasibility of investments. The payback period was calculated as following by:

$$Payback\ Period = \frac{Initial\ Investment}{Net\ Cash\ Flow\ per\ Period} \qquad (3.17)$$

All these economic variables were used to indicate the feasibility of each designing process. In this thesis, the economic variables were used to compare the cases studied in the methanol production processes.

CHAPTER IV

RESEARCH METHODOLOGY

The purposes of this work were to estimate the constant parameters of the kinetic model referenced in the literature, to simulate the methanol production process and to compare the designing processes based on economic feasibility. The methodology for achieving the aims was divided into four main sections. The first section was the experimental procedure to identify fitting kinetic parameters. The second section was kinetic modelling of the system by using MATLAB software. The third section was the process simulation by using Aspen Plus software to obtain input/output results. The last section was the preliminary economic analysis to compare the viability of each study case.

4.1 Experimental section

4.1.1 Materials

The details of the materials used in this work are shown in **Table 4**

Table 4 *Materials used in the semi-pilot plant of the methanol production process*

Materials	Grade	Company
Raw materials		
Methane (CBG)	99.99%	Cryotech Asia Co., Ltd.
Carbon dioxide	99.99%	Thai Special Gas Co., Ltd.
Syngas	CO_2 5%, CO 47%, H_2 48%	Thai Special Gas Co., Ltd.
Hydrogen	99.99%	Thai Special Gas Co., Ltd.
Deionized Water		TISTR
Catalyst activation gas	10% H_2 in N_2 balance	Thai Special Gas Co., Ltd.
Catalysts		
Ni/Al_2O_3	Commercial	TISTR
$Cu/Zno/Al_2O_3$	Commercial	TISTR

4.1.2 Equipment

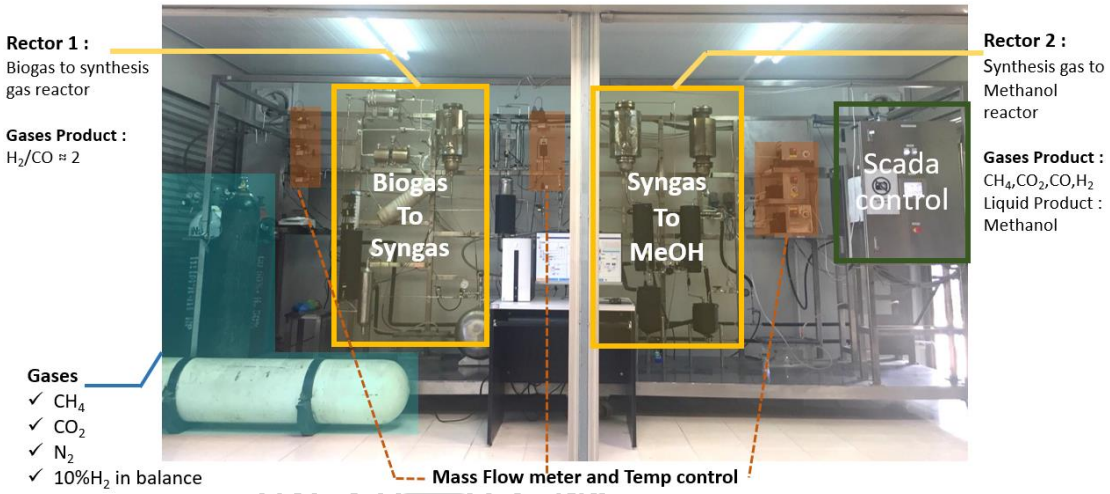

Figure 2 *the semi-pilot plant of the methanol production process*

A semi-pilot plant with a capacity of one litre per day of methanol synthesis, which was used for this research located at the Thailand Institute of Scientific and Technological Research (TISTR). Details of unit operation for methanol synthesis are shown in **Figure 2**, and the flow diagram, as shown in **Figure 3**. The semi-pilot plant comprises of unit operations as follows:

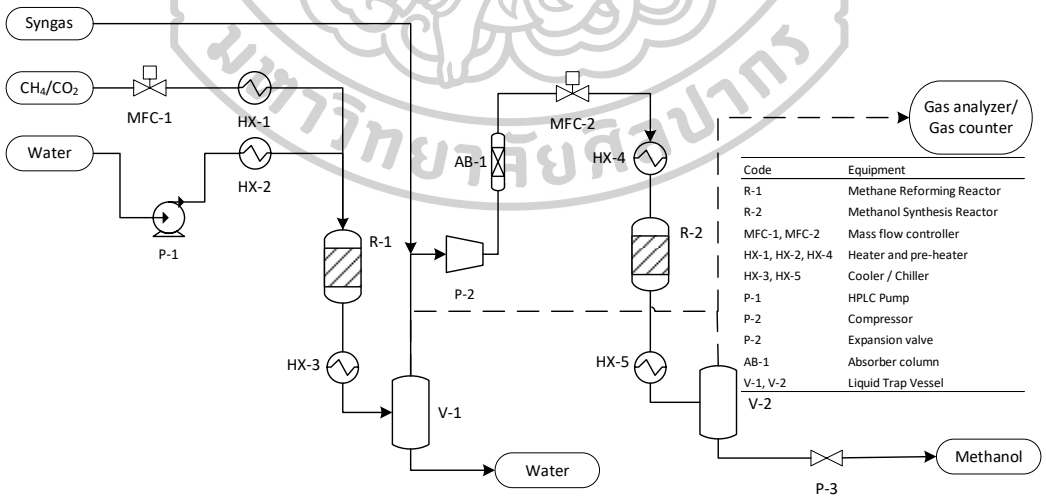

Figure 3 *Block flow diagram of methanol synthesis from biogas*

4.1.1.1 Methane Reforming Reactor (R-1)

The primary equipment of the unit operation for the methanol process was the methane reforming reactor (R-1) that was a fixed-bed continuous flow reactor. It was made with 304 stainless steel, 30 cm of length, 15 cm of inside diameter and 17 cm of the outside diameter. The reforming reactor was packed with 0.7 kg of Ni/Al_2O_3 catalyst supplied by TISTR.

4.1.1.2 Methanol Synthesis Reactor (R-2)

Methanol Synthesis Reactor (R-2) had dimensions similar to the R-1 reactor. It was packed with 1 kg of $Cu/ZnO/Al_2O_3$ catalyst supplied by TISTR.

4.1.1.3 Mass flow controller (MFC-1, MFC-2)

All gas flows were controlled by 0 – 10 litre/min mass flow controllers supplied by (Bronkhorst Instruments).

4.1.1.4 Heater and pre-heater (HX-1, HX-2, HX-4)

Heaters and pre-heaters were heated by electrical heaters with PID controllers to maintain temperatures in the range of operating conditions.

4.1.1.5 Fittings and valves

Fittings and valves were made of 304 stainless steel by Swagelok Instruments

4.1.1.6 Cooler / Chiller by AMPLECOOL (HX-3, HX-5)

The cool water was supplied by a cooler produced by AMPLECOOL company.

4.1.1.7 Gas counter

The gas counter had dimensions of 18 x 30 x 16 cm of width × length x height, respectively. It was used air replacing water to count gas volume.

4.1.1.8 Compressor (P-2)

A reciprocating compressor was used for increasing pressure of syngas by 380/220V rated voltage with the explosion-proof magnetic starter (BQC-10A type)

4.1.1.9 HPLC pump (P-1)

Water inlet was maintained with a high-pressure pump (HPLC pump) by RS-232 SSI Scientific Series II. The HPLC pump provided flow rates from 0.01 to 12.0 ml/min

4.1.1.10 Absorber column (AB-1)

A 304 stainless steel absorber column was cylinder-shaped with 30 x 50 cm of diameter x length, respectively. It was packed with silica gel adsorbent for resisting 50 bar pressure.

4.1.1.11 Water and Methanol Trap Vessel (V-1, V-2)

Trap vessels were used for liquid gas separation in the product stream. It was made by 304 stainless steel insulated with polyethylene sheet.

4.1.1.12 Gas Analyzer

Compositions of gas products were analyzed by using portable VARIOluxx gas analyzer (MRU Instruments) which it measured gases comprised of methane, carbon dioxide, carbon monoxide, hydrogen, oxygen and nitrogen.

4.1.1.13 Controller system

Controller system was set up on a SCADA controller.

4.1.3 Experimental Design

The experiments were designed using the Full Factorial Designs (FFD) method in 3-levels (low, medium, high), which yielded the main effect and interactions of all factors. Maximum, centre and minimum levels for each factor were selected based on previously reported data by Rujira et al. [62, 63]. The experiments were contained with two parts as Methane reforming (MR) and Syngas to Methanol (STM).

4.1.2.1 Methane Reforming experiment

Methane Reforming experiment was performed to investigate three outputs: CH_4 conversion, CO_2 conversion, and H_2/CO ratio, which were calculated by using the equations 4.1, 4.2 and 4.3, respectively. The input parameters of this experiment were the methane/carbon dioxide feed ratio, the water feed flow rate, and the temperature. These input parameters were organized by Full Factorial Design (FFD) as shown in **Table 5** and detailed for 27 runs, as shown in **Table 6**.

CH_4 conversion:

$$X_{CH_4} = \frac{mole\,of\ CH_4\ reacted}{mole\,of\ CH_4\ fed} \quad (4.1)$$

CO_2 conversion:

$$X_{CO_2} = \frac{mole\,of\ CO_2\ reacted}{mole\,of\ CO_2\ fed} \quad (4.2)$$

H_2/CO ratio:

$$H_2/CO\ ratio = \frac{H_2\ Outlet\ flow\,rate}{CO\,Outlet\ flow\,rate} \quad (4.3)$$

Table 5 *Factors and values of three levels chosen in Methane Reforming*

Factor	Level		
	(-1)	**(0)**	**(+1)**
Temperatures (°C)	600	650	700
CH_4-to-CO_2 volumetric ratio (%)	15	35	55
H_2O feed flow (ml/min)	0.7	1.1	1.5

Table 6 *Experimental design and factors of Reforming reaction*

RUN #	Temperature (°C)	CH_4-to-CO_2 volumetric ratio (%)	H_2O feed flow (ml/min)
1	-1	-1	-1
2	0	-1	-1
3	+1	-1	-1
4	-1	0	-1
5	0	0	-1
6	+1	0	-1
7	-1	+1	-1
8	0	+1	-1
9	+1	+1	-1
10	-1	-1	0
11	0	-1	0
12	+1	-1	0
13	-1	0	0
14	0	0	0
15	+1	0	0
16	-1	+1	0
17	0	+1	0
18	+1	+1	0
19	-1	-1	+1
20	0	-1	+1
21	+1	-1	+1
22	-1	0	+1
23	0	0	+1
24	+1	0	+1
25	-1	+1	+1
26	0	+1	+1
27	+1	+1	+1

4.1.2.2 Methanol Synthesis experiment

The Methanol Synthesis experiments were studied to investigate three outputs: CO conversion, H_2 conversion, and methanol yield, which were calculated via equations 4.4, 4.5 and 4.6 respectively.

CO conversion:

$$X_{CO} = \frac{mole\,of\ CO\,reacted}{mole\,of\ CO\ fed} \quad (4.4)$$

H_2 conversion:

$$X_{H_2} = \frac{mole\,of\ H_2\,reacted}{mole\,of\ H_2\ fed} \quad (4.5)$$

Methanol yield:

$$Methanol\ yield = \frac{MeOH\,producted}{CO\,reacted} \quad (4.6)$$

Three inputs contained temperatures, H_2/CO ratios, and %CO_2 (by volume) in feed were studied by using Full Factorial Design (FFD) as shown in ***Table 7*** *and organized in 27 runs as shown in*

Table 8*.*

Table 7 *Factors and values of three levels chosen in Methanol synthesis*

Factor	Level		
	(-1)	(0)	(+1)
Temperatures (°C)	170	200	230
H_2/CO (Ratio)	1.2	2	2.8

CO_2 Feed (%)	5	25	45

Table 8 *Experimental design and factors of Methanol synthesis*

RUN #	Temperature (°C)	H_2/CO (Ratio)	$\%CO_2$ in feed (%)
1	-1	-1	-1
2	0	-1	-1
3	+1	-1	-1
4	-1	0	-1
5	0	0	-1
6	+1	0	-1
7	-1	+1	-1
8	0	+1	-1
9	+1	+1	-1
10	-1	+1	0
11	0	+1	0
12	+1	+1	0
13	-1	0	0
14	0	0	0
15	+1	0	0
16	-1	-1	0
17	0	-1	0
18	+1	-1	0

19	-1	-1	+1
20	0	-1	+1
21	+1	-1	+1
22	-1	0	+1
23	0	0	+1
24	+1	0	+1
25	-1	+1	+1
26	0	+1	+1
27	+1	+1	+1

The results of all experiments were analyzed the main effect and the interaction effect between two inputs via Analysis of Variance (ANOVA) by using the software Minitab 17. The analyzed results were divided into two parts: reforming reaction and methanol synthesis and were discussed in the form of the main effects and the interaction effects. The main effects were the effect of each input on each output, and the interaction effect was the simultaneous effect of two inputs on each output.

4.2 Kinetic modelling

The procedures of kinetic modelling were divided into three steps.

4.2.1 Selection of kinetic models.

4.2.2 Output evaluation by using ordinary differential equations.

4.2.3 Estimation of parameter values by using a nonlinear regression method.

4.2.1 Selection of kinetic models

The kinetic models were selected and modified based on the suitability of the reaction condition and the type of catalyst. The kinetic rate expression was derived by assuming an obvious rate-limiting step in the reaction mechanism. It was exhibited consisting of 3 terms as the kinetic term, potential term and adsorption term. The reaction rate equations were derived using a Langmuir–Hinshelwood rate expression as shown in equation 4.7

$$Reaction\,rate = \frac{\left(Kinetic\ \ term\right)\bullet\left(Potential\ \ term\right)}{\left(Adsorption\ \ term\right)^{n}} \qquad (4.7)$$

For the methane reforming reactions, the three main kinetic models were selected for dry reforming, steam reforming and reverse water gas shift reactions. Richardson and Paripatyadar studied kinetic models for dry reforming and reverse water gas shift reactions based on temperature about 450 – 500 °C at ambient pressure and Ni-based catalyst where the rate equations of models included a term that the effect of external and internal diffusion, the internal effectiveness factors were about 0.3 or more referenced by Introduction to Chemical Engineering Kinetics and Reactor Design book [64]. The rate equations of dry reforming and reverse water gas shift reactions were written in equation 4.8 and 4.9, respectively [15]. Additionally, the model considered in the steam reforming that reaction of steam was reacted under reforming condition. The model was used for the steam reforming reaction by proposing of Abbas et al. [65]. The model based on the effect of operating parameters as shown in equation 4.10.

Dry reforming of methane reaction (DRM)

$$r_{DRM} = \frac{k_1 p_{CH_4} p_{CO_2}}{\left(1+K_{CO_2,1}p_{CO_2}+K_{CH_4,1}p_{CH_4}\right)^2}\left(1-\frac{\left(p_{CO}p_{H_2}\right)^2}{K_{p_1}\left(p_{CH_4}p_{CO_2}\right)}\right) \qquad (4.8)$$

Reverse water-gas shift reaction (RWGS)

$$r_{RWGS} = \frac{k_3 p_{CO_2} p_{H_2}}{\left(1+K_{CO_2,3}p_{CO_2}+K_{H_2,3}p_{H_2}\right)^2}\left(1-\frac{p_{CO}p_{H_2}}{K_{p_3}\left(p_{CO_2}p_{H_2}\right)}\right) \qquad (4.9)$$

Steam reforming of methane reaction (SRM)

$$r_{SRM} = \frac{k_2(p_{CH_4}p_{H_2O}/p_{H_2})}{(1+K_{CO,2}p_{CO}+K_{CO_2,2}p_{CO_2}+K_{H_2,2}p_{H_2}^{0.5}+K_{H_2O,2}(p_{H_2O}/p_{H_2})+K_{CH_4,2}(p_{CH_4}/p_{H_2}))}\left(1-\frac{p_{CO}p_{H_2}^3}{K_{p_2}(p_{CH_4}p_{H_2O})}\right)$$

(4.10)

For the methanol synthesis reaction, reaction rate models were proposed by Bussche and Graaf [38, 66], which developed factor independent kinetic equations of CO hydrogenation and CO_2 hydrogenation. The CO hydrogenation was considerably the main reaction (equation 4.11), and the CO_2 hydrogenation was side reaction (equation 4.12). Additionally, CO_2 can be converted to CO via the reverse water-gas shift reaction for which the model was referred from Rozovskii et al. [29] as shown in equation 4.13.

CO hydrogenation reaction

$$r_{MeOH} = k_{MeOH,1} \frac{\left(p_{CO} p_{H_2}^{3/2} - p_{CH_3OH} / \left(p_{H_2}^{1/2} K_{p_4} \right) \right)}{\left(1 + K_{a,1} p_{CO} + K_{b,1} p_{CO_2} p_{H_2}^{1/2} + K_{c,1} p_{H_2O} \right)} \quad (4.11)$$

CO_2 hydrogenation reaction

$$r_{MeOH} = k_{MeOH,2} \frac{(p_{CO_2} p_{H_2}) - (1/K_{p_5})(p_{CH_3OH} p_{H_2O} / p_{H_2}^2)}{(1 + K_{a,2}(p_{H_2O}/p_{H_2}) + K_{b,2}\sqrt{p_{H_2}} + K_{c,2} p_{H_2O})^3} \quad (4.12)$$

Reverse water-gas shift reaction (RWGS)

$$r_{RWGS} = k_{RWGS,3} \frac{p_{CO_2} - (1/K_{p_6})(p_{CO} p_{H_2O} / p_{H_2})}{(1 + K_{a,3}(p_{H_2O}/p_{H_2}) + K_{b,3}\sqrt{p_{H_2}} + K_{c,3} p_{H_2O})} \quad (4.13)$$

In this present work, constant values of each model were modified for ASPEN simulator and applied to fit the laboratory result.

4.2.2 Output Evaluation

This model provided the value of outputs for each set of input (experimental data) via the reactor mode. A reactor model was based on a one-dimensional distributed model. The model was applied by Froment et al. [67] in the differential form of the mole balance.

$$\frac{dF_i}{dW} = \sum r_i \qquad (4.14)$$

When F_i Mole flow rate of specie i

W Catalyst weight

r_i The reaction rate of specie i

Equation 4.14 was reactor models and used for fixed bed reactors simulation. The equations were ordinary differential equations (ODEs) containing functions of mole flow rate and catalyst weight as independent variables. The ODEs were solved using MATLAB software via the ODE45 function obtaining flow rate profiles of each species. The flow rate profiles were used for calculating response variables such as methane conversion, H_2/CO ratio, and methanol yield to estimate kinetic parameters. The reactor models were written coded in MATLAB function by using kinetic constants and the proposed factors in the section 4.1.2 as inputs function and response variables as outputs function. The MATLAB function was written for simulation is given in Appendix C-1.

4.2.3 Estimation of parameters

The parameter estimation was performed by using the nonlinear regression method in the MATLAB software. The least-squares sense (lsqcurvefit) function was applied via a MATLAB library via the Levenberg–Marquardt algorithm (Seber and Wild, 1989 [68]) to minimize the least square error following section 3.3. In addition, the fitted kinetic parameters were estimated based on the response variables given by the MATLAB function in Appendix C-2. The “lsqcurvefit” function returned the fitted kinetic parameters.

4.3 Process Simulation in Aspen Plus

ASPEN Plus software was used for methanol process simulations that support by Silpakorn University. Methanol operating units and utilities were simulated, which consisted of 7 units operation. Methodologies of ASPEN simulator were explained in the following content.

4.3.1 Setting the environment properties and operation units

In process simulation, environment and properties setting were the first steps of simulation. All the components of involved chemicals had to be specified or declared, as shown in **Figure 4**. The properties were based on NRTL-RK method which was a combination of NRTL and Redlich-Kwong where The NRTL activity coefficient model was used for the liquid phase while The Redlich-Kwong equation of state was used for the vapour phase. The specification of the property method was selected in the simulation, as shown in **Figure 5**.

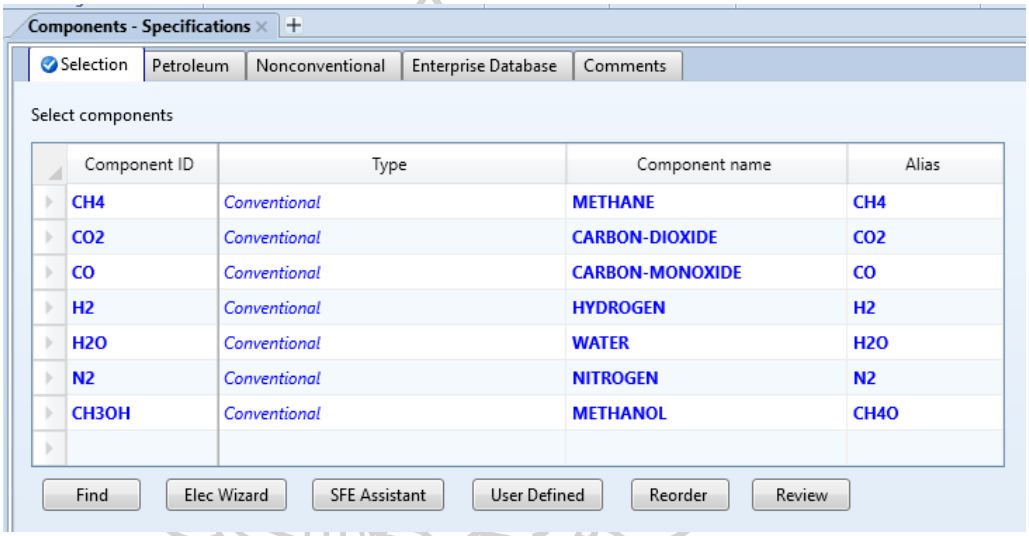

Figure 4 *the component of chemical involved in Methanol Process*

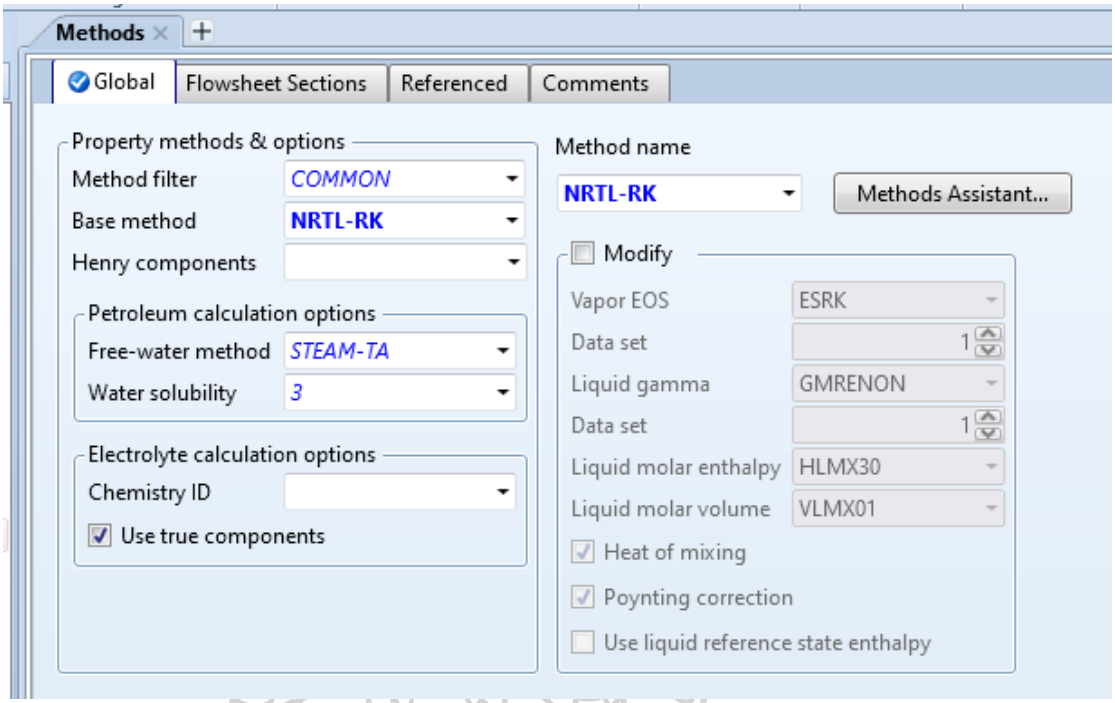

Figure 5 *The specification of the property method*

4.3.1.1 Process Streams

Process streams were used for inlet stream setting that the parameters of streams were determined by flow rate, composition, pressure and temperature, as shown in **Figure 6**.

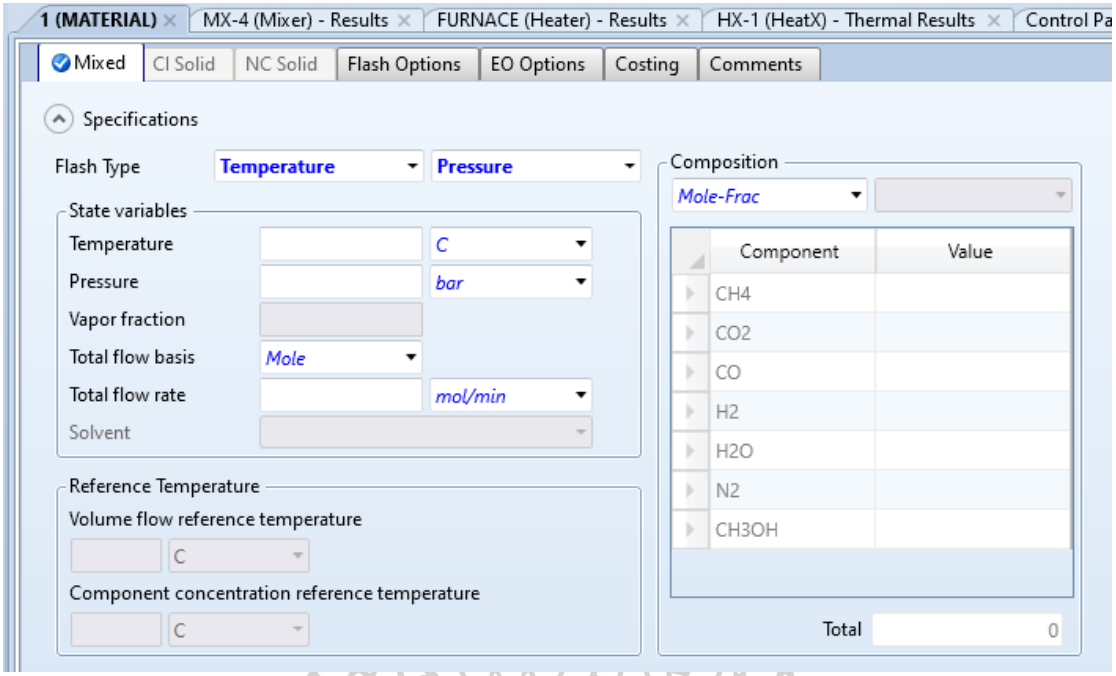

Figure 6 *Specification of the process streams*

4.3.1.2 Reactors

The reactor unit was chosen to the plug model in the simulator because the reactor in this work was fixed bed reactor and reaction rates depending on the weight of the catalyst. The plug model assumed that perfect mixing occurred in the radial direction, and no mixing occurred in the axial direction. It can be used for model two-phase reactors with thermal fluid streams (counter-current), and it required the generalized Langmuir-Hinshelwood-Hougen-Watson (LHHW) kinetic model for reactor models showed in **Figure 7**. The specific kinetic data were used to set up a built-in LHHW expression for calculating the rate of reaction.

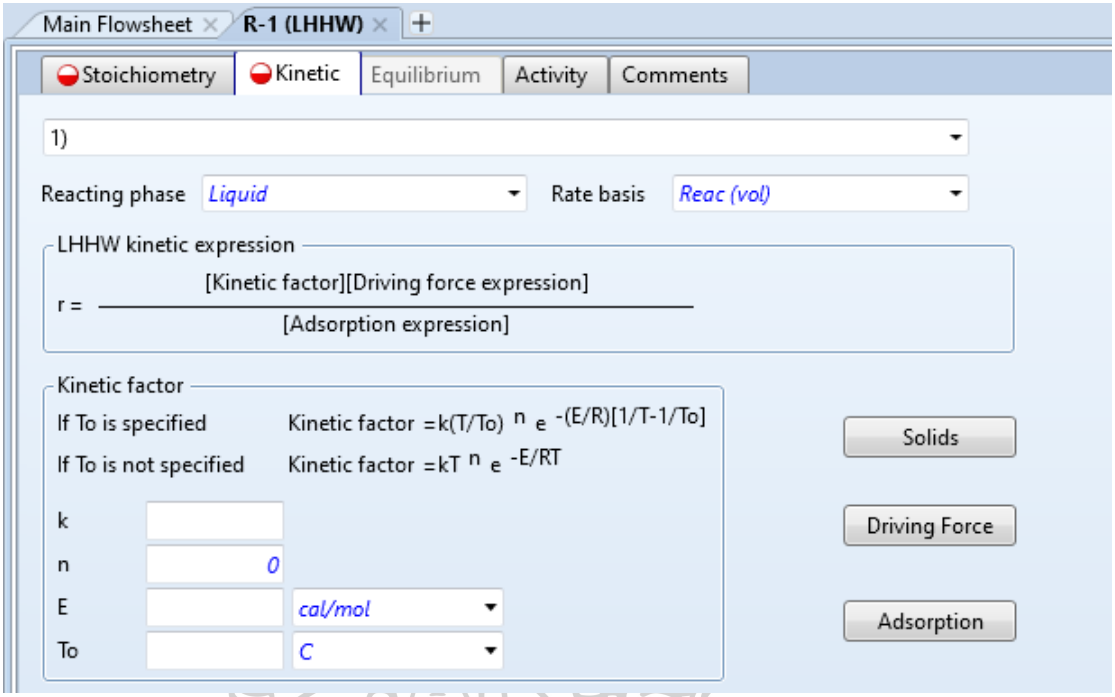

Figure 7 *The specification of LHHW rate reaction*

The rate was calculated in kmol/s-(basis) where the basis was kg catalyst for Rate Basis Cat (wt). The (LHHW) kinetic models were obtained in section 4.2 (kinetic modelling), and then they were formatted to the general LHHW expression and were applied in the reactor model.

The general LHHW expression was:

$$r = \frac{(kinetic\ \ factor)(driving\ force\ expression)}{(adsorption\ trem)}$$

Where:

Kinetic factor: $k(T/T_0)^n e^{-(E/R)[1/T-1/T_0]}$

Driving force expression: $k_1\prod_{i=1}^{N}p_i^{\alpha_i} - k_2\prod_{j=1}^{N}p_j^{\beta_j}$

Adsorption term: $\left[\sum_{i=1}^{M}K_i(\prod_{j=1}^{N}p_j^{\nu_j})\right]^m$

4.3.1.3 Mixer and splitter

The mixer was used to combine inlet streams into one stream. The pressure was set to 0 due to the assumption of no pressure drop during mixing assumption. Valid phases inputs were set to Vapor and Liquid that were shown in **Figure 8**.

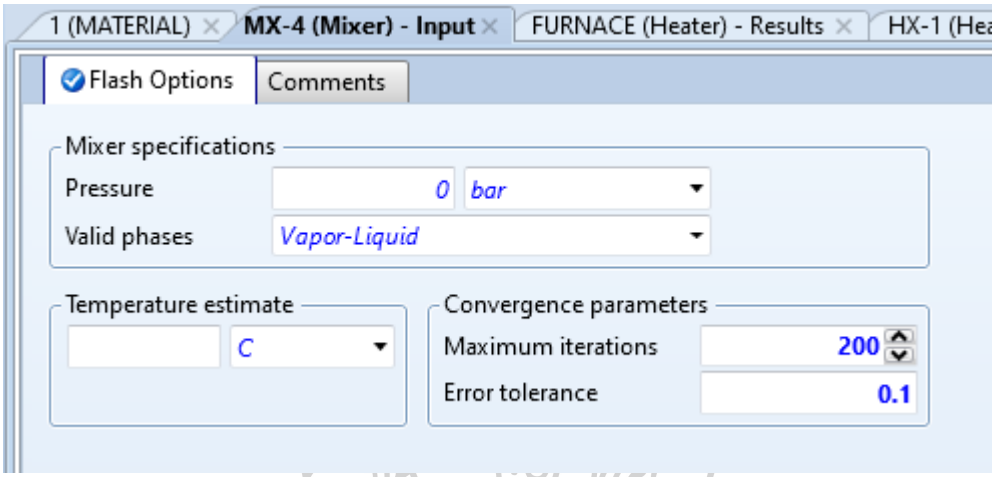

Figure 8 *The specification of Mixer*

Splitter was a tool divided feed based on splits specified for the outlet streams (FSplit model) which can divide the resulting stream into two or more streams of the same phases. The condition and composition of outlet streams were similar to the mixed inlet. The splitter model was used for a recycling system where the off-gas stream was sent to the inlet process for increasing productivity, and another stream was a purge for inhibiting component accumulation. The specification of a splitter, as shown in **Figure 9**. In this work, the recycling system was used 100%.

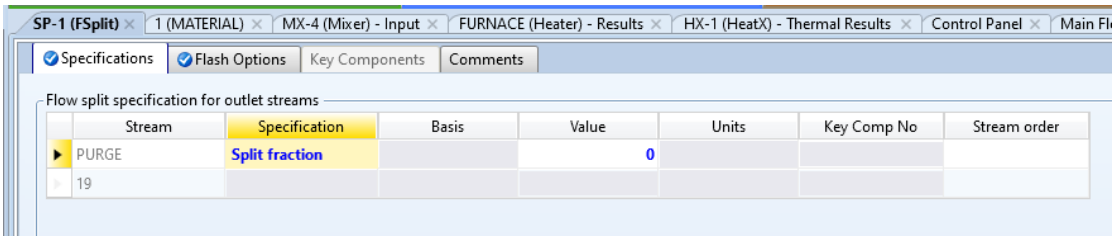

Figure 9 *The specification of Splitter*

4.3.1.4 Coolers and Heaters

Coolers/Heaters were used to decrease or increase the temperature of process streams base on heat exchanger calculation (HeatX model). The specification of HeatX was selected as shortcut model for determining stream outlet temperature. The model was set that the flow direction was countercurrent through the heater. The results of shortcut model were used for calculating shell and tube heat exchanger by changing model fidelity to shell and tube heat exchanger for sizing, as shown in **Figure 10**.

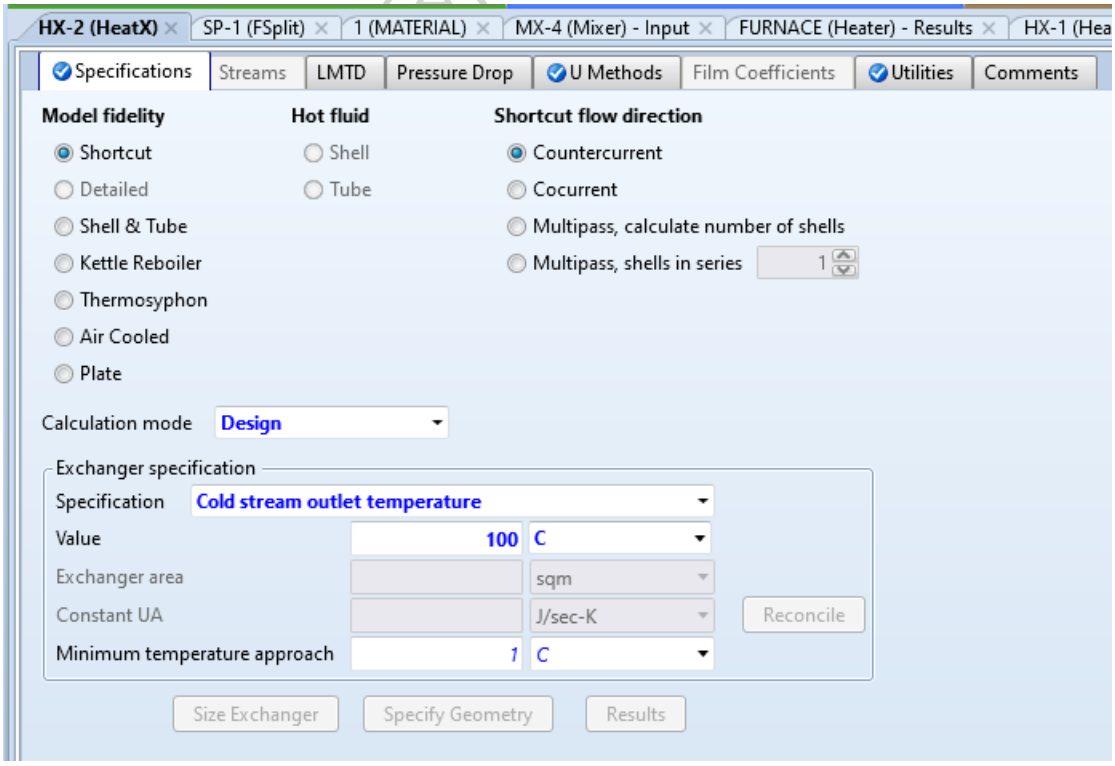

Figure 10 *The specification of Cooler and Heaters*

4.3.1.5 Flash

Flash was the equipment for separating two states between the gas phase and the liquid phase, which were at the same temperature and pressure according to the theory of the phase equilibrium. The flash was mostly insulated to maintain temperature conditions, so heat duty of flash could be set to zero. The specification of the flash is shown in **Figure 11**.

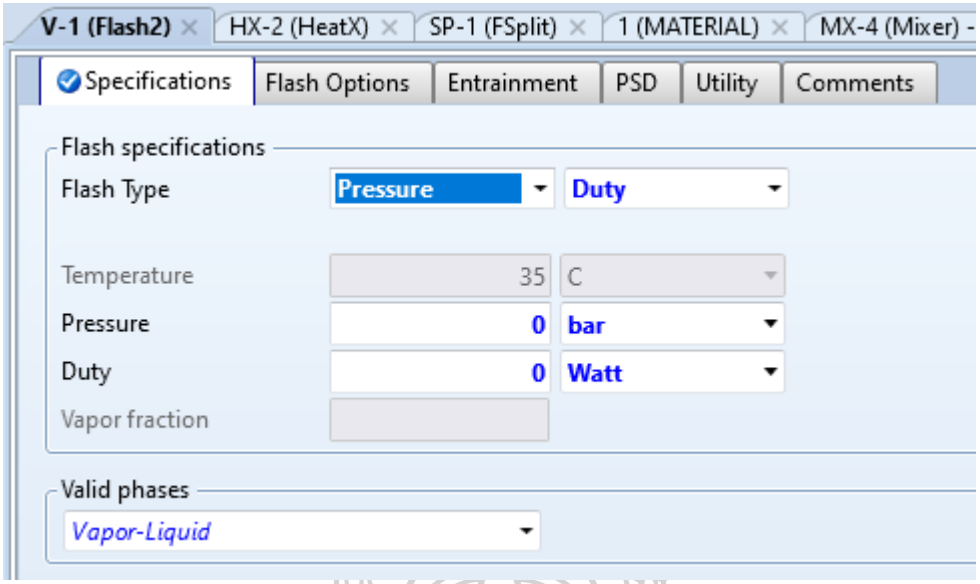

Figure 11 *The specification of Flash*

4.3.1.6 Compressors

A compressor was equipment to increase the pressure of process streams. The compressor was selected to work only with the gas phase. A higher increase of pressure required cooling due to the effect of higher temperature at the compressor output. In this work, the produced syngas had required pressure of about 45 bar for suitability to the methanol synthesis, and therefore the compressor used was the multi-stage type with three stages, the compressor model was used for isentropic and cooling was produced by cooling water. The parameter specification of compressors was presented in **Figure 12**.

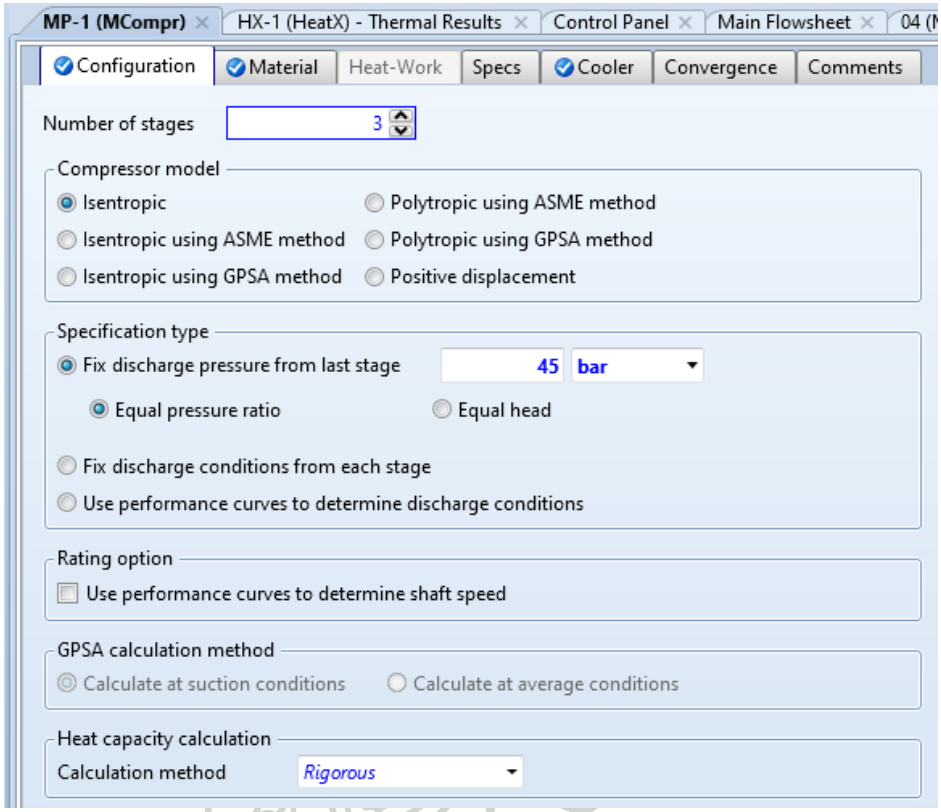

Figure 12 *The specification of Compressors*

4.3.2 Process simulation

All the mentioned operating units were connected and simulated for the methanol production process. The process in **Figure 13** explained that biogas was preheated by low-pressure steam (HX-1), mixed (MX-2) with preheated water about 100 °C (HX-2) and then the mix-gases was heated up in furnace to raise to a high temperature to meet up the desired temperature in the reactor (R-1). After the reforming reaction, the fluid was cooled down in the heat exchanger (HX-3) and trapped in a flash vessel (V-1). The fluid was separated into two phases. The liquid was fed back with water by the pump (P-1), mixing with fresh water in the mixer (MX-1). Vapour or syngas was compressed and was fed to an absorption unit removing water before passing the syngas to the next step. The methanol reaction occurred in the reactor (R-2) at the operating temperature range of 170-230 °C. The methanol product and residue gas were cooled down to 40 °C by water-cooled heat exchanger (HX-4). The fluid was containing two phases: vapour and a liquid stream. Methanol

mix was firstly trapped in the vessel (V-2), and liquefied component was depressurized to atmospheric pressure by a relief valve (P-2) then liquid methanol was secondly collected to the vessel (V-3) and finally produced purified methanol. The upper steam of V-2 was to send residue gas to mix with the vapour stream at the mixer (MX-4). This recycle gas was partially purged and fed back to the biogas stream for producing methanol.

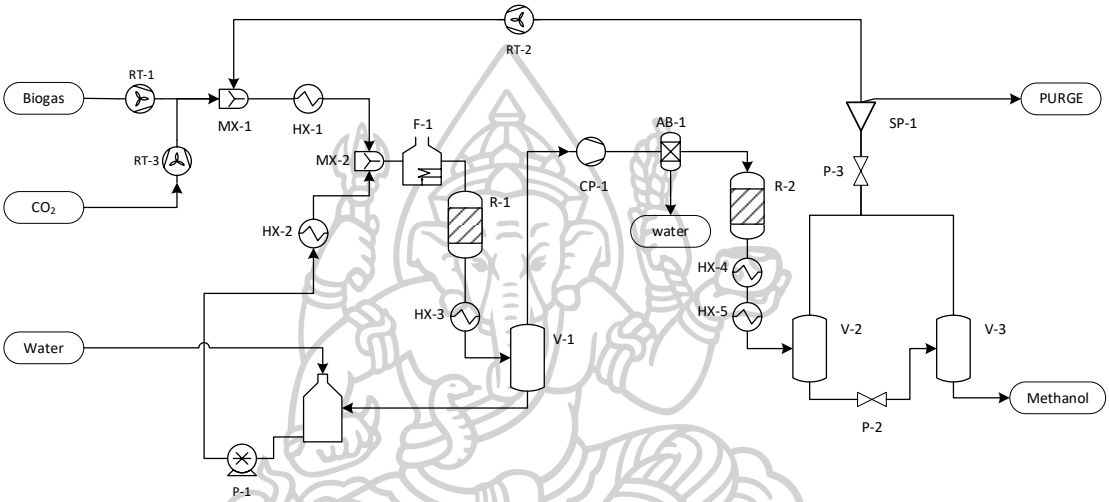

Figure 13 *The process diagram of methanol production.*

The different process simulations were studied in three cases to compare the preliminary economic feasibility. The first case was consulted with recycling residue gases to reduce raw material costs. The case I: recycle system shown in ***Figure 14***. The second case was to study the residue gases containing CO and H_2, which were the energy source for a generator, so it can reduce electricity cost and assure stable electricity supply to the operating process. Case II: Residue gases to generator shown in ***Figure 15***. The last case was combined with the recycling system and generating electrical energy by itself. The residue gases were sent to gases inlet, and it can increase the productivity of bio-methanol while the extra biogas being fed to the generator for electricity generation for the process. The case III: Recycle system and Extra biogas to generator shown in ***Figure 16***.

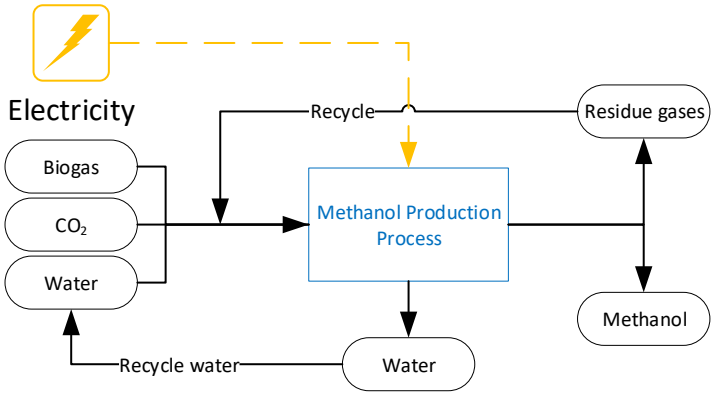

Figure 14 *Case I: Recycle system*

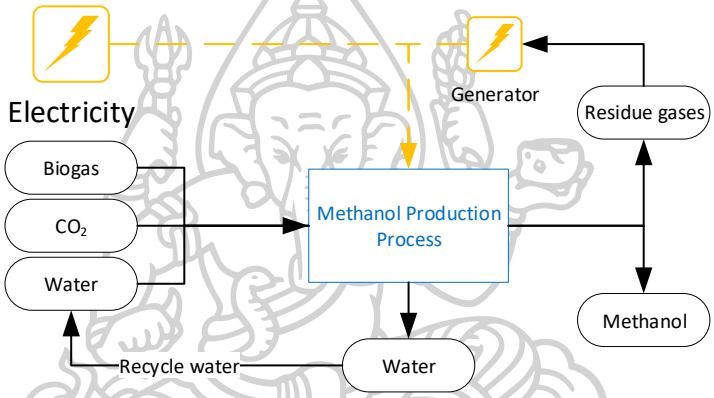

Figure 15 *Case II: Residue gases to the generator*

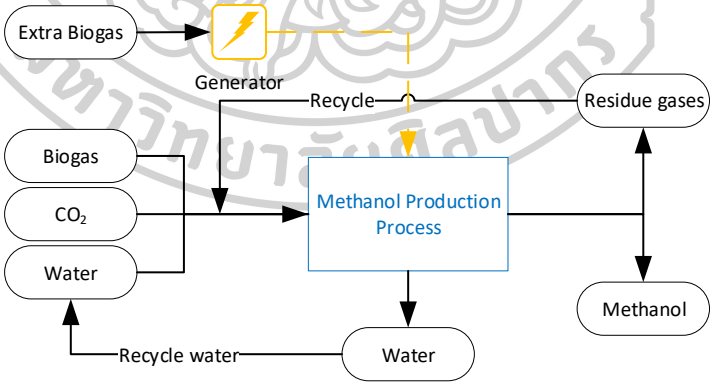

Figure 16 *Case III: Recycle system and Extra biogas to the generator*

All case studies were based on 15,000 kg/day of methanol production rate that was suitable for a biogas production source. After that, preliminary designs were developed in this work for sizing of proposed processes. The design was based on 1

litre/day bio-methanol production on the semi-pilot plant by TISTR and approximate process method. The preliminary material balance was obtained by the results of the Aspen plus simulator, and then it was used for equipment design which involved determining the size of equipment in terms of the volume, flow rate, surface area, and Reynolds number.

4.4 Economic Feasibility Analysis

In economics, variable costs and fixed costs were the two main components for calculating economics variables. Variable costs depended on the production volume of the process, whereas the fixed costs remained constant regardless of the production volumes of the operation.

4.4.1 Variable Cost

Variable costs were the cost per unit calculated by costs depending on plant operating costs and raw material costs. The costs consisted of raw material, energy cost (electrical and thermal), catalysts and direct Labour (i.e. labour hours) which were calculated based on THB/kg of methanol unit reported in table type.

4.4.2 Fixed Cost

The fixed costs were the initial cost of investment and did not change with an increase/decrease in production rate. These costs were divided as equipment costs, piping, valve, land, office, and control system. The costs were estimated from the published purchased cost data or real data from industries.

Fixed and variable components of cost were used for preparing a cash flow statement which was a financial statement that summarized the amount of cash inflow and cash outflow. The financial statement was used for comparing the proposed case studies of methanol process. The case with best financial viability was evaluated by changing economic parameters such as methanol prices, raw material prices and production rates by using the sensitivity analysis.

CHAPTER V

RESULT AND DISCUSSION

5.1 Experimental results.

The raw experimental data (Shown in Appendix B) were analyzed the main effect and the interaction effect between two inputs. The analyzed results were divided into two parts: reforming reaction and methanol synthesis and were discussed in the form of the main effects and the interaction effects. The main effects were the effect of each input on each output, and the interaction effect was the simultaneous effect of two inputs on each output.

5.1.1 Reforming reaction analyzed results

The main effects of inputs (temperature, CH_4-to-CO_2 volumetric ratio, and H_2O) to outputs (%CH_4 conversion, %CO_2 conversion, and H_2/CO ratio) shown in **Figure 17**, **Figure 18**, and **Figure 19** respectively. The interaction effects of the two inputs to the individual outputs were shown in **Figure 20**, **Figure 21**, and **Figure 22**.

5.1.1.1 The Main Effect of the Reforming Reactor

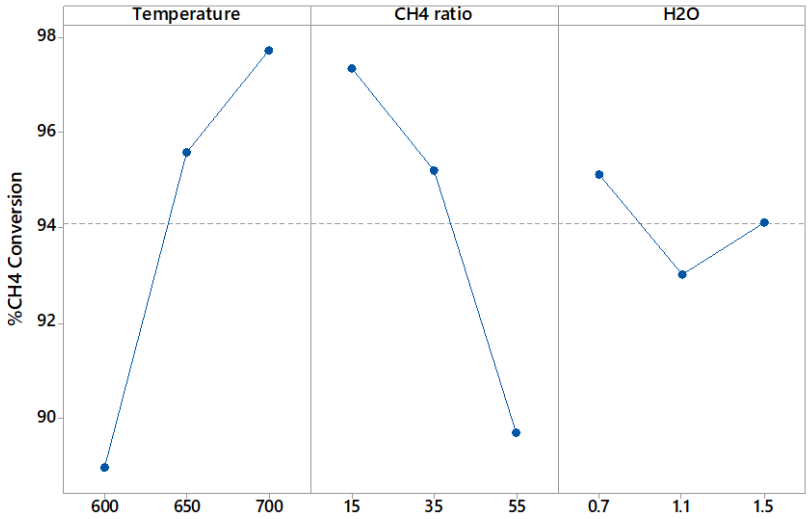

Figure 17 *The main effects of Temperature, CH_4-to-CO_2 volumetric ratio, H_2O Feed flow rate on CH_4 Conversion*

The three main effects of input variables (Temperature (°C), CH_4-to-CO_2 volumetric ratio (%), Water feed flow rate (ml/min)) on CH_4 conversion were grouped and presented in **Figure 17**. The average of CH_4 conversion was 94 % from all

experiments shown by the dashed line. The results showed that the major influences were the temperature and CH_4-to-CO_2 volumetric ratio. The increased in both temperatures led to the increased in CH_4 conversions but the increased in CH_4-to-CO_2 volumetric ratio led to the decreased in CH_4 conversions. The water feed flow rate did not influence to the CH_4 conversion. The temperature results were similar to those phenomena reported that increasing temperature had a positive effect on methane conversion by (Abd Ghani et al. 2018).

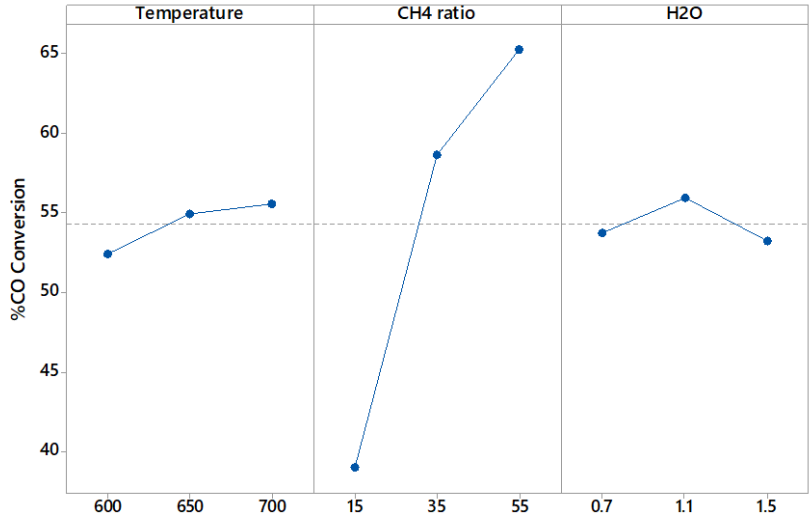

Figure 18 *the main effects of Temperature, CH_4-to-CO_2 volumetric ratio, H_2O Feed flow rate on CO_2 Conversion*

Figure 18 showed the main effect of the input variables on CO_2 conversion. The average of CO_2 conversion was 54% represented from all experiments that showed with a dashed line. CH_4-to-CO_2 volumetric ratio strongly affected on CO_2 conversion, and the temperature slightly affected on CO_2 conversion. The water feed flow rate did not affect on CO_2 conversion. However, the adding water significantly affected catalyst durability because it could inhibit catalyst deactivation and adjust the balancing of H_2 as reported by previous experiment and Abd Ghani et al. [69].

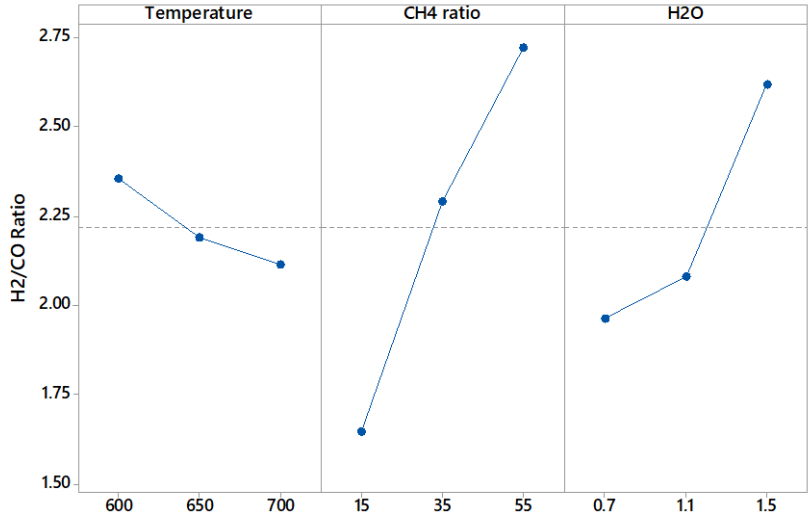

Figure 19 *The main effects of Temperature, CH_4-to-CO2 volumetric ratio, H_2O Feed flow rate on H_2/CO ratio*

Figure 19 showed the main effect of the input variables on the H_2/CO ratio. The average of H_2/CO was 2.24 represented from all experiments that were shown by a dashed line. The case of temperature effect, the results showed that the increased in temperature led to the decreased in H_2/CO ratio. The CH_4-to-CO_2 volumetric ratio and H_2O feed flow rate exhibited the same effects on the H_2/CO ratio. The H_2/CO ratio was increased when the CH_4-to-CO_2 volumetric ratio and H_2O feed flow rate increased.

5.1.1.2 The Interaction of Input Variables in Reforming Reactor

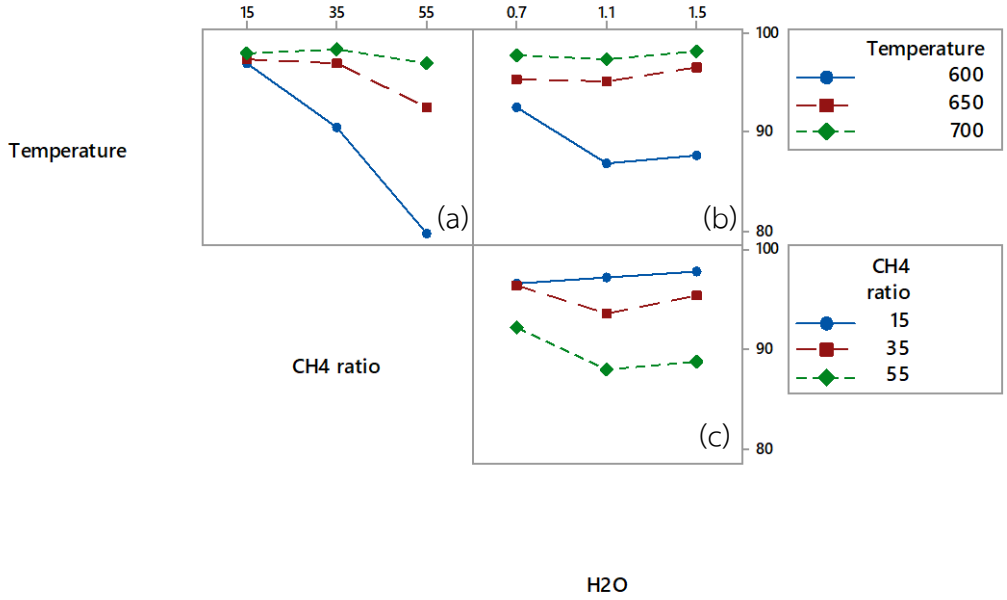

Figure 20 *The interactions of temperature, CH_4-to-CO_2 volumetric ratio, water feed flow rate effected to CH_4 Conversion in the reforming reactor.*

Figure 20 showed the variation of % CH_4 conversion by the combined effects of two inputs: (a) temperature and CH_4-to-CO_2 volumetric ratio, (b) temperature and water feed, and (c) CH_4-to-CO_2 volumetric ratio and water feed. At low CH_4-to-CO_2 volumetric ratio (15%), the temperature did not affect the CH_4 conversion and obtained over 97% conversion but at higher CH_4-to-CO_2 volumetric ratio (35-55%), the increased in temperature led to the decreased dramatically in CH_4 conversion as shown in **Figure 20** (a). This reforming reaction did not have the interaction effects between the water feed flow rate/the temperature and water feed flow rate/the CH_4-to-CO_2 volumetric ratio as shown in **Figure 20** (b) and (c). This was because the water feed rate did not affect the CH_4 conversion (from the previous results). To obtain the highest yield of CH_4 conversion, Figure 20 can be summarized that the temperature, CH_4-to-CO_2 volumetric ratio and water feed flow rate were maximum (700°C), minimum (15%) and maximum (1.5 ml/min) level respectively.

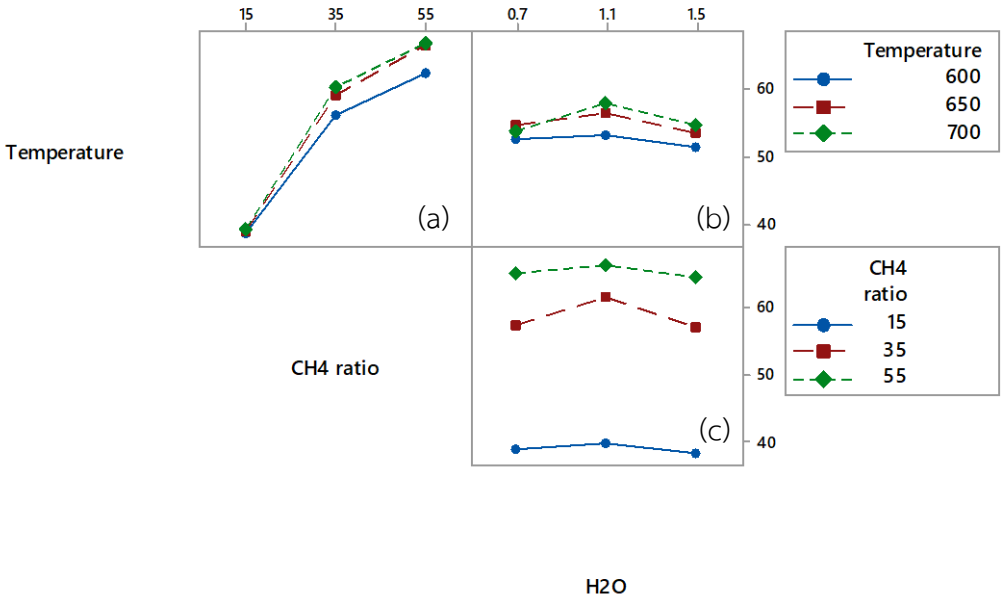

Figure 21 *The interaction of temperature CH_4-to-CO_2 volumetric ratio, water feed flow rate effect to CO_2 Conversion in the reforming reactor.*

The result in **Figure 21** (a) showed that there was slightly interaction between the temperature and the CH_4-to-CO_2 volumetric ratio because at the minimum level of the CH4-to-CO2 volumetric ratio, the temperatures did not affect the CO_2 conversion while at the maximum level of the CH_4-to-CO_2 volumetric ratio, centre level of temperature (600°C) was CO_2 conversion lower than the minimum (600°C) and maximum (700°C) level of temperatures. The interaction between the temperature and the water feed flow rate, the CH_4-to-CO_2 volumetric ratio and the water feed flow were not a significant influence on the CO_2 conversion as shown in **Figure 21** (b) and (c). Also, the results of CO_2 conversion indicated that the centre level of water feed flow rate (1.1 ml/min) accorded highest CO_2 conversion. The optimal condition of CO_2 conversion can summarize that the temperature, CH_4-to-CO_2 volumetric ratio and water feed flow rate were maximum (700°C), maximum (55%) and centre (1.1 ml/min) level respectively.

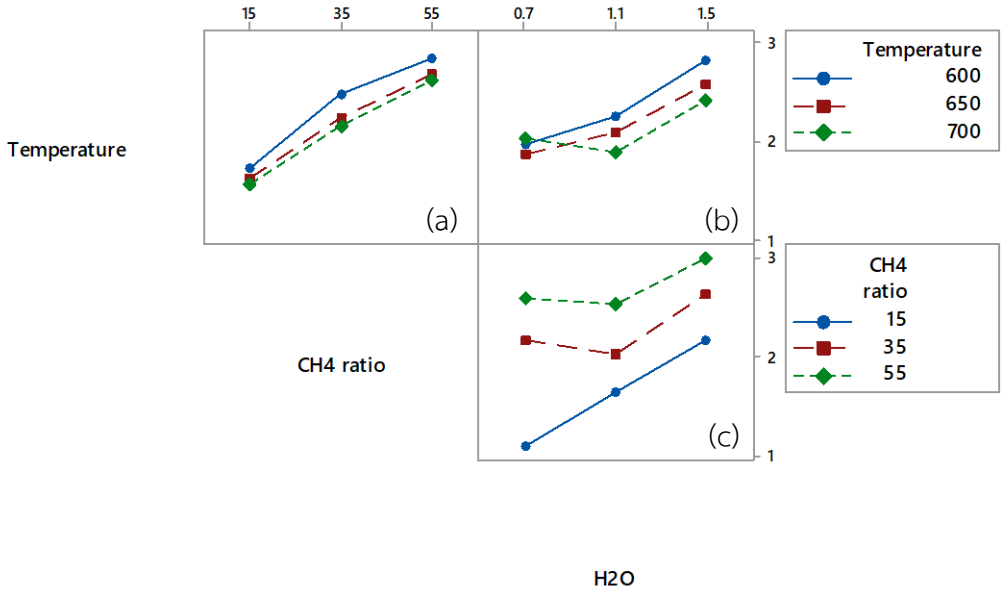

Figure 22 *The interaction of temperature, CH_4-to-CO_2 volumetric ratio, water feed flow rate effect to H_2/CO in the reforming reactor.*

The result in **Figure 22**(a) was found that there was no interaction between the temperature and the CH_4-to-CO_2 volumetric ratio. The temperature and the water feed flow rate showed the interaction effect on H_2/CO ratio. At the lowest water feed flow rate (0.7 ml/min), the temperature did not affect the H_2/CO ratio. While at high water feed flow rate (1.1, 1.5 ml/min), the increasing in temperature led to the decreasing in the H_2/CO ratio, as shown in **Figure 22** (b). The CH_4-to-CO_2 volumetric ratio and the water feed flows rate showed the interaction effect on the H_2/CO ratio. At lowest CH_4-to-CO_2 volumetric ratio (15%), the increasing in the water feed flow rate led to the increasing in the H_2/CO ratio. At high CH_4-to-CO_2 volumetric ratio (35, 55%), when increased the water feed flow rate from 0.7 to 1.1 ml/min, the H_2/CO ratio did not change. But the increasing in the water feed flow rate from 1.1 to 1.5 ml/min resulted in the increasing in H_2/CO ratio, as shown in **Figure 22**(c). To obtain the highest yield of H_2/CO ratio, it can summarize that the temperature, the CH_4-to-CO_2 volumetric ratio and the water feed flow rates were centre (600°C), maximum (55%) and maximum (1.5 ml/min) levels respectively.

The optimum condition for the reforming reaction was at

1) the maximum level of temperature due to the highest CH_4 conversion and CO_2 conversion,
2) the centre level of CH_4-to-CO_2 volumetric ratio because it provided the H_2/CO ratio higher than the stoichiometric ratio of CO hydrogenation,
3) The maximum level of water feed flow rate due to highest H_2/CO ratio.

5.1.2 Methanol synthesis reaction analyzed results

The main effects of inputs (%CO_2 in feed, H_2/CO ratio, and temperature) to outputs (% methanol produced, %CO conversion, and %H_2 conversion) shown in Figure 23, Figure 24, and Figure 25 respectively. The interaction effects of the two inputs to the individual outputs were shown in Figure 26, Figure 27, and Figure 28.

5.1.2.1 The main effect of the methanol synthesis reactor

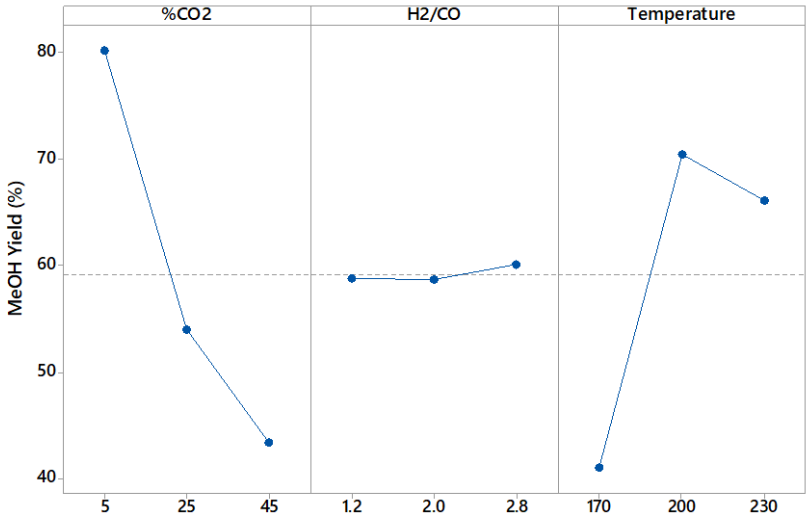

Figure 23 *the main effects of %CO_2 in feed, H_2/CO, Temperature on Methanol yield*
The 58% of average was represented

The 58% of average on the methanol yield was shown by a dashed line in **Figure 23**. The results showed that the increasing %CO_2 feed ratio dramatically affected in the decreasing methanol yield. At the center and maximum level of

%CO_2 feed, the ratio resulted that methanol yield was lower than 60%. The H_2/CO feed ratio did not major factor on methanol yield. The effect of temperature provided the optimum point of methanol yield at the center level of temperature (200°C). The highest methanol yield can be summarized in minimum, any centre level of %CO_2 feed, H_2/CO feed ratio and temperature respectively.

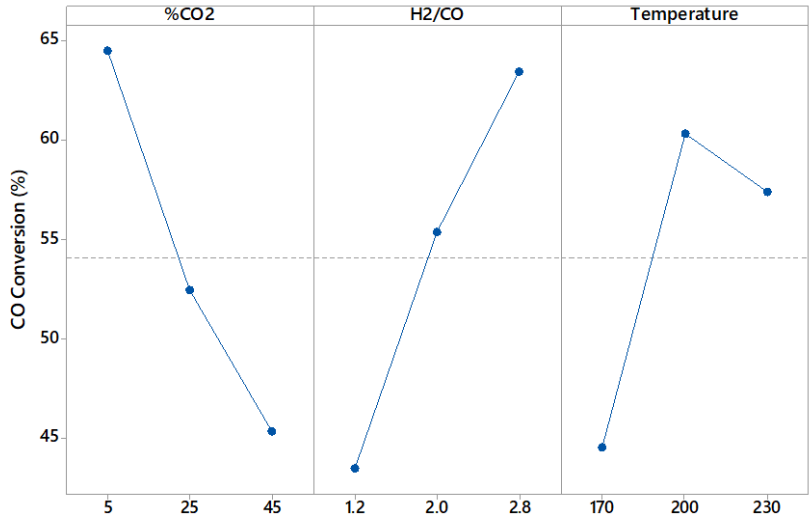

Figure 24 *The main effects of %CO_2 in feed, H_2/CO, Temperature on CO conversion*

Figure 24 showed the main effect of the input variables on CO conversion. The average of CO conversion was 53% represented in a dashed line. The results showed that increasing % CO_2 feed ratio was the most significant in decreasing CO conversion. While the increasing H_2/CO feed ratio affected in the increasing CO conversion. The CO conversion increased dramatically from 45% to about 60% between minimum to centre level of temperatures (170 - 200°C), but the temperature was more than centre level (>200 °C) affected in decreasing CO conversion. The highest CO conversion can conclude that the %CO_2 feed, the H_2/CO ratio and the temperature were minimum (5%), maximum (2.8%) and centre (200°C) level respectively.

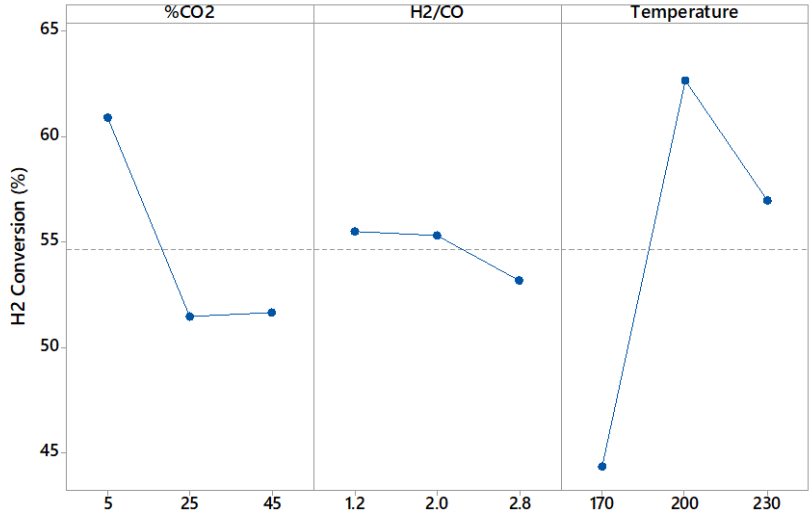

Figure 25 *The main effects of %CO_2 in feed, H_2/CO, Temperature on H_2 conversion*

The three main effects of input variables (Temperature (°C), CH_4-to-CO_2 volumetric ratio (%), Water feed flow rate (ml/min)) on CH_4 conversion were grouped and presented in **Figure 25**. The average of CH_4 conversion was 53% from all experiments shown by the dashed line. The results showed that increasing % CO_2 feed from minimum to centre level (170 - 200°C) affected in sharply decreasing on H_2 conversion while increasing % CO_2 feed was more than 25% that was not significant in the H_2 conversion. The increasing H_2/CO ratio affected in slightly decreased on H_2 conversion. The effect of H_2 conversion varying temperatures was similar to the effect of CO conversion. The optimal of H_2 conversion varying temperatures can find that the temperature was 200 °C. The highest H_2 conversion can conclude that the %CO_2 feed, the H_2/CO ratio and the temperature were minimum (5%), minimum (1.2%) and centre (200°C) level respectively.

5.1.2.2 The interaction of input variables in the methanol synthesis reactor

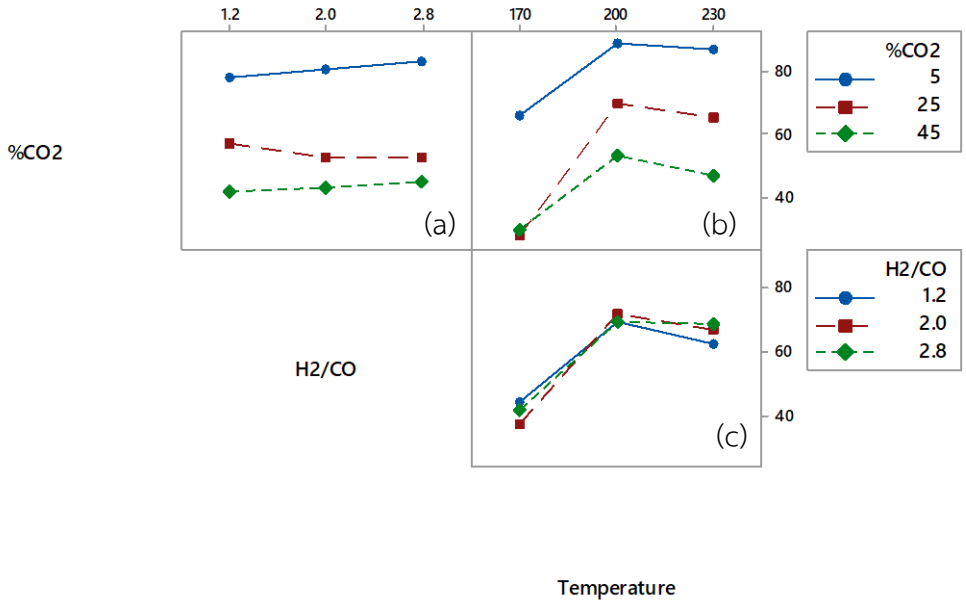

Figure 26 *The interaction between %CO_2 in feed, H_2/CO ratio and temperature effect to Methanol yield in the reforming reactor*

Figure 26 showed that the percentage of CO_2 feed ratio was no interaction with H_2/CO feed on methanol yield, but having small interaction between the center (25%) to maximum (45%) levels of %CO_2 in the feed as shown in **Figure 26** (a). The percentage of CO_2 feed ratio and the temperatures were no interaction excepting the 25% CO_2 feed ratio with temperature from 170 to 200 °C as shown in **Figure 26** (b). The interaction between the H_2/CO ratio and the temperature in **Figure 26** (c) did not clear. The result provided the highest methanol yield at the temperature as 200°C with any H_2/CO ratio. To obtain the optimal condition on methanol yield, these results summarized that the minimum and centre levels of the %CO_2 in feed and temperature with any H_2/CO ratio provided highest methanol yield.

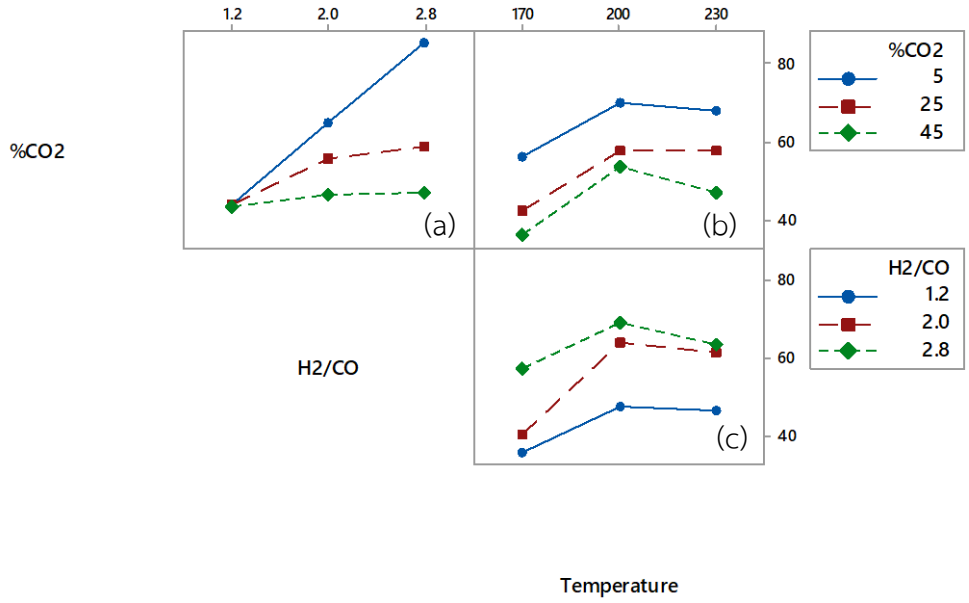

Figure 27 *the interaction between %CO_2 in feed, H_2/CO ratio and temperature effect to CO conversion in the reforming reactor*

The result in **Figure 27**(a) was found that there was most interaction between the %CO_2 in feed and H_2/CO ratio. At the minimum level of H_2/CO ratio (1.2), the CO conversion did not change when the %CO_2 in feed was increased, but at the maximum level of H_2/CO ratio (2.8), the CO conversion sharply decreased by the increasing %CO_2 in the feed. The interaction between the %CO_2 in feed and the temperature was lightly interaction, as shown in **Figure 27** (b). Also, the peak of CO conversion was obtained with the center level of temperature (200 °C) as in **Figure 27** (b) and (c). The %CO_2 in feed and the temperatures were no interaction excepting at the 25% CO_2 feed ratio with temperature from 170 to 200 °C as shown in **Figure 27** (c). To obtain the highest yield of CO conversion, it can summarize that the %CO_2 in feed, H_2/CO ratio and temperature were minimum (5%), maximum (2.2) and centre (200°C) levels respectively.

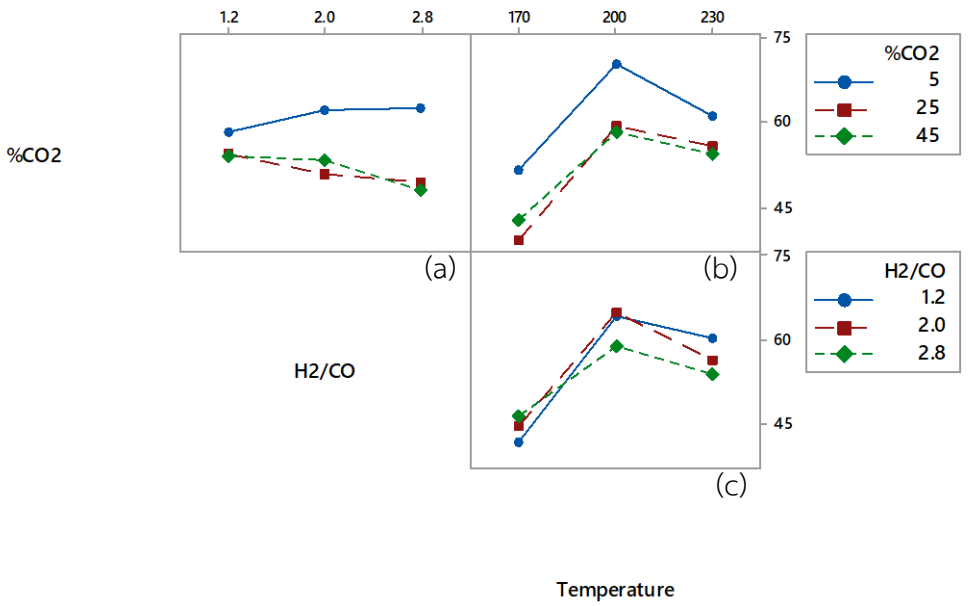

Figure 28 *The interaction between %CO_2 in feed, H_2/CO ratio and temperature effect to H_2 conversion in the reforming reactor*

Figure 28(a) showed that there was a small interaction between the %CO_2 in feed and H_2/CO ratio. The increased H_2/CO ratio with centre (25%) and maximum (45%) level of %CO_2 in feed affected in decreasing CO conversion but the increased H_2/CO ratio with minimum (5%) level of %CO_2 in feed affected in slightly increasing CO conversion. **Figure 28** (b) showed that there was no interaction between the %CO_2 in feed and temperature. The interaction between the H_2/CO ratio and the temperature in Figure 27 (c) did not clear. In addition, the result provided the highest H_2 conversion at centre level (200°C) of temperature with any H_2/CO ratio and any %CO_2 in the feed. To obtain a high yield of H_2 conversion, it can summarize that the %CO_2 in feed and temperature was minimum (5%) and centre (200°C) levels respectively.

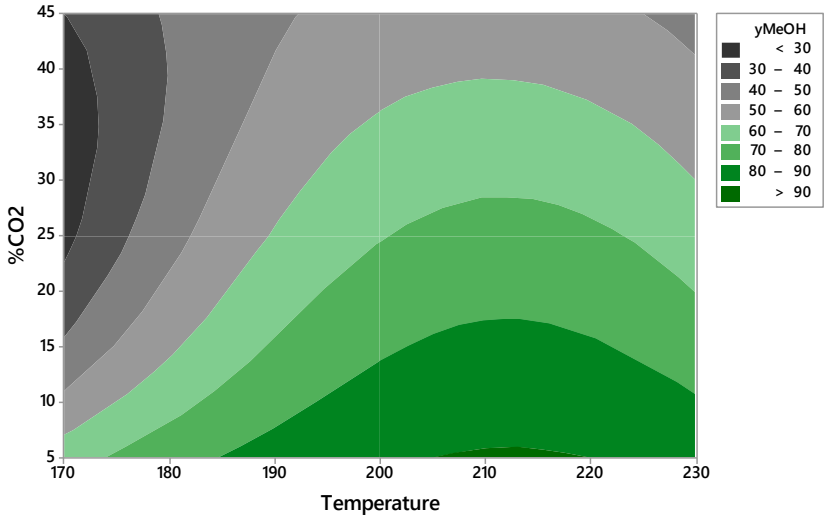

Figure 29 *Contour Plot of Methanol yield (yMeOH) vs Temperature, %CO_2 in feed*

The optimal condition for the methanol synthesis reaction was chosen for the maximum yield of methanol. The results found that any H_2/CO feed ratio was not affected on methanol yield, and the result of reforming reaction was obtained more 2 of H_2/CO ratio. Thus, the optimal condition was chosen by inputs of temperature and %CO_2 feed. Contour Plot of Methanol yield vs Temperature, CO_2 feed ratio in **Figure 29** was shown that the optimal condition was centre and the minimum point of temperature and %CO_2 feed ratio, respectively.

In conclusion, the optimal condition for methanol synthesis as the major output was the minimum, centre, and centre points for %CO_2 feed, H_2/CO ratio, and temperature, respectively.

5.2 Kinetic model and parameters estimation

The estimation of the parameters was based on minimizing the objective function (F_{obj}) and squared errors. The kinetic parameters were calculated and evaluated using experimental data and physical properties and nonlinear data-fitting with the ordinary differential equation of the reactor model. The approximation was created by using the MATLAB (MathWorks, Inc.) "lsqcurvefit" subroutine. The functions were written as per the designed algorithm in **Figure 30**.

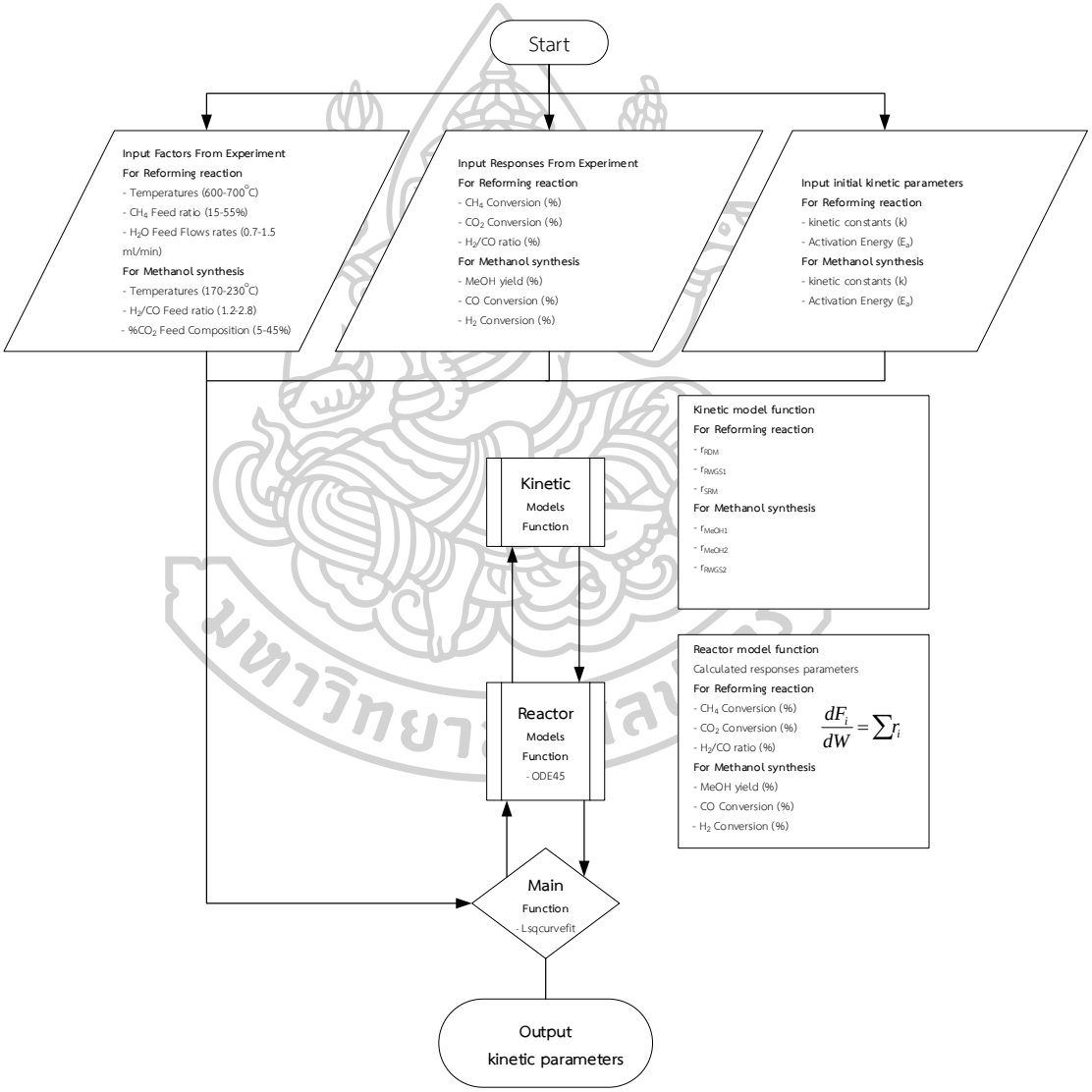

Figure 30 *Flowchart of kinetic modelling for evaluating kinetic parameters*

Figure 30 explained the step of programming that the first step, cases of experiments (27 runs of the experiment) for reforming reaction were imported in the main function of MATLAB. There were classified inputs and outputs as parameters. The inputs parameters composed of the temperatures (600-700°C), the CH_4-to-CO_2 volumetric ratio (15-55%) and H_2O feed flows rates (0.7-1.5 ml/min). The outputs parameters composed of CH_4 conversion (%), CO_2 conversion (%) and H_2/CO ratio. Next step, the kinetic constants (ki) and activation energy (Ea) were initially defined value to zero for the initialized guess parameters. Finally, the lsqcurvefit was performed that the reactor models were used for calculating the outputs via the mole balance equations. The reaction rates of the reactor models were determined by the kinetic models function which was obtained the kinetic models for dry reforming, reverse water gas shift and steam reforming reactions. The kinetic constants (ki) and activation energy (Ea) were fitted by minimizing the sum of the squares of the errors between the experimental data and the resulted models via the Levenberg-Marquardt algorithm.

For methanol synthesis, the step of programming was similar to the step of programming for reforming reaction. The inputs and outputs were represented that the inputs parameters composed of the temperatures (170-230°C), the H_2/CO ratio (1.2-2.8) and the $\%CO_2$ in the feed (5-45%). The outputs parameters composed of methanol yield (%), CO conversion (%) and H_2 conversion.

The results of kinetic modelling of both reactors were shown in **Table 9** and **Table 10** for the reforming reactor and the methanol synthesis reactor, respectively. Therefore, the kinetic parameters were used for calculating the response variables via reactor models and the results of reactor models were presented in sections 5.2.1 and 5.2.2.

Table 9 *Kinetic parameters estimated and reported review value in the reforming reactor.*

Parameters	Value	Parameters	Value
k_1	$2.23\cdot 10^{6}\exp(\frac{-109,345}{RT})$	$K_{H_2O,2}$	$3.12\cdot 10^{-7}\exp(\frac{97,550}{RT})$
k_2	$8.66\cdot 10^{6}\exp(\frac{-79,698}{RT})$	$K_{CH_4,2}$	$2.23\cdot 10^{-1}\exp(\frac{0}{RT})$
k_3	$6.25\cdot 10^{6}\exp(\frac{-59,998}{RT})$	$K_{CO_2,3}$	$2.87\cdot 10^{8}\exp(\frac{104,086}{RT})$
$K_{CO_2,1}$	$2.61\cdot 10^{15}\exp(\frac{16,360}{RT})$	$K_{H_2,3}$	$6.77\cdot 10^{14}\exp(\frac{-36,650}{RT})$
$K_{CH_4,1}$	$2.77\cdot 10^{8}\exp(\frac{54,630}{RT})$	K_{p_1}	$3.39\cdot 10^{14}\exp(\frac{-342,574}{RT})$
$K_{CO,2}$	$1.578\cdot 10^{6}\exp(\frac{-1,395}{RT})$	K_{p_2}	$2.21\cdot 10^{2}\exp(\frac{-23,547}{RT})$
$K_{CO_2,2}$	$5.67\cdot 10^{-3}\exp(\frac{-556}{RT})$	K_{p_3}	$1.95\cdot 10^{9}\exp(\frac{-186,607}{RT})$
$K_{H_2,2}$	$2.43\cdot 10^{-2}\exp(\frac{486}{RT})$		

Table 10 *Kinetic parameters estimated and reported review value in the methanol synthesis reactor.*

Parameters	Value	Parameters	Value
$k_{MeOH,1}$	$1.23\cdot 10^{5}\exp(\frac{-53,125}{RT})$	$K_{c,2}$	$4.56\cdot 10^{-6}\exp(\frac{87,980}{RT})$
$k_{MeOH,2}$	$7.99\cdot 10^{3}\exp(\frac{-25,787}{RT})$	$K_{a,3}$	$8.36\cdot 10^{-6}\exp(\frac{665}{RT})$
$k_{RWGS,3}$	$5.44\cdot 10^{3}\exp(\frac{-58,477}{RT})$	$K_{b,3}$	$2.67\cdot 10^{7}\exp(\frac{112,089}{RT})$
$K_{a,1}$	$2.91\cdot 10^{7}\exp(\frac{589}{RT})$	$K_{c,3}$	$6.54\cdot 10^{14}\exp(\frac{-74,488}{RT})$
$K_{b,1}$	$3.34\cdot 10^{8}\exp(\frac{69,789}{RT})$	K_{p_4}	$5.54\cdot 10^{10}\exp(\frac{-541,551}{RT})$
$K_{c,1}$	$8.25\cdot 10^{9}\exp(\frac{-695}{RT})$	K_{p_5}	$2.24\cdot 10^{5}\exp(\frac{-5,848}{RT})$
$K_{a,2}$	$5.66\cdot 10^{-5}\exp(\frac{-5,655}{RT})$	K_{p_6}	$1.69\cdot 10^{6}\exp(\frac{-18,445}{RT})$
$K_{b,2}$	$9.61\cdot 10^{-2}\exp(\frac{6,988}{RT})$		

5.2.1 The model validation for the reforming reactor.

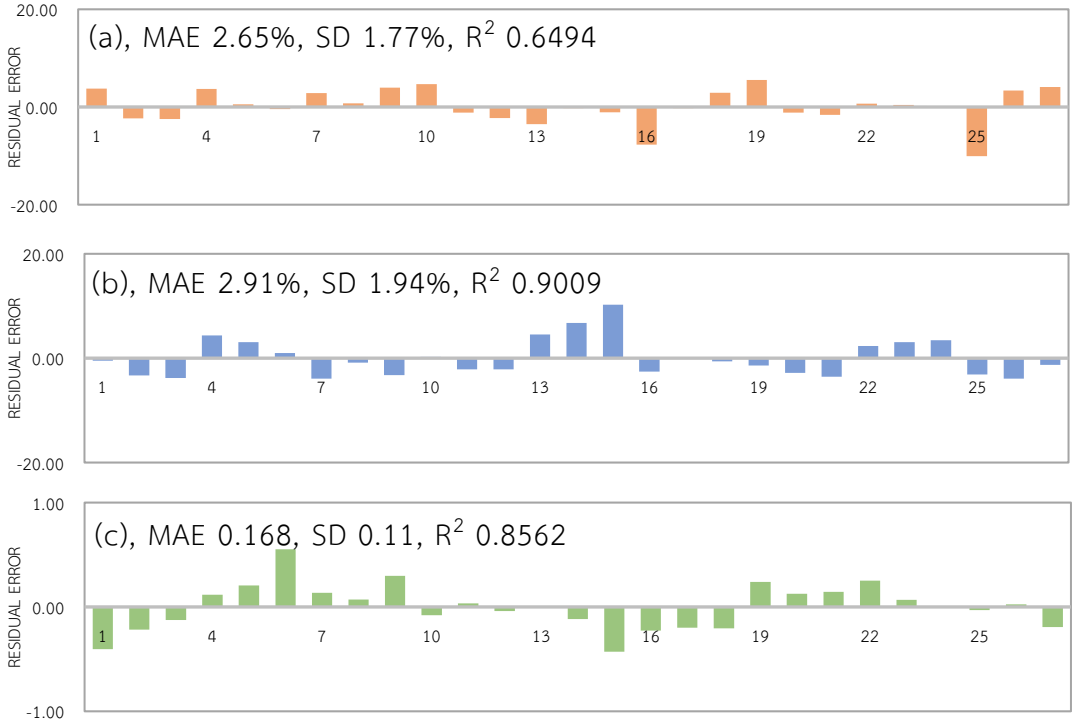

Figure 31 *Residual Errors between Experiment results and Simulation results on (a) CH_4 Conversion, (b) CO_2 Conversion, (c) H_2/CO Ratio*

The kinetic parameters form **Table 9** were put to reactor simulator. A simulation of the reforming reaction was performed under operating conditions given in **Table 6** (see Section 4.1.2.1). **Figure 31** showed residual error between experiment and simulation on outputs: (a) CH_4 Conversion, (b) CO_2 Conversion, (c) H_2/CO Ratio. The horizontal axis was run the number of conditions (#Run 1-27). Results showed that the highest value of residual errors of CH_4 conversion, CO_2 conversion and H_2/CO ratio was -10.03 (#Run 25), 10.27 (#Run 18) and 0.55 (#Run 6) as shown in **Figure 31** (a), **Figure 31** (b) and **Figure 31** (c). The mean absolute errors (MAE) of the CH_4 conversion, the CO_2 conversion and the H_2/CO ratio were 2.65, 2.91 and 0.168, respectively. The standard deviation (SD) was obtained in 1.77 for the CH_4 conversion, 1.94 for the CO_2 conversion and 0.11 for the H_2/CO ratio. R^2 values were obtained 0.6494, 0.9009 and 0.8562 of CH_4 conversion, CO_2 Conversion

and H_2/CO Ratio, respectively. The model was agreed between experiment and simulation for the preliminary design process that was also confirmed by values of R^2

5.2.1 The model validation for the methanol synthesis reactor.

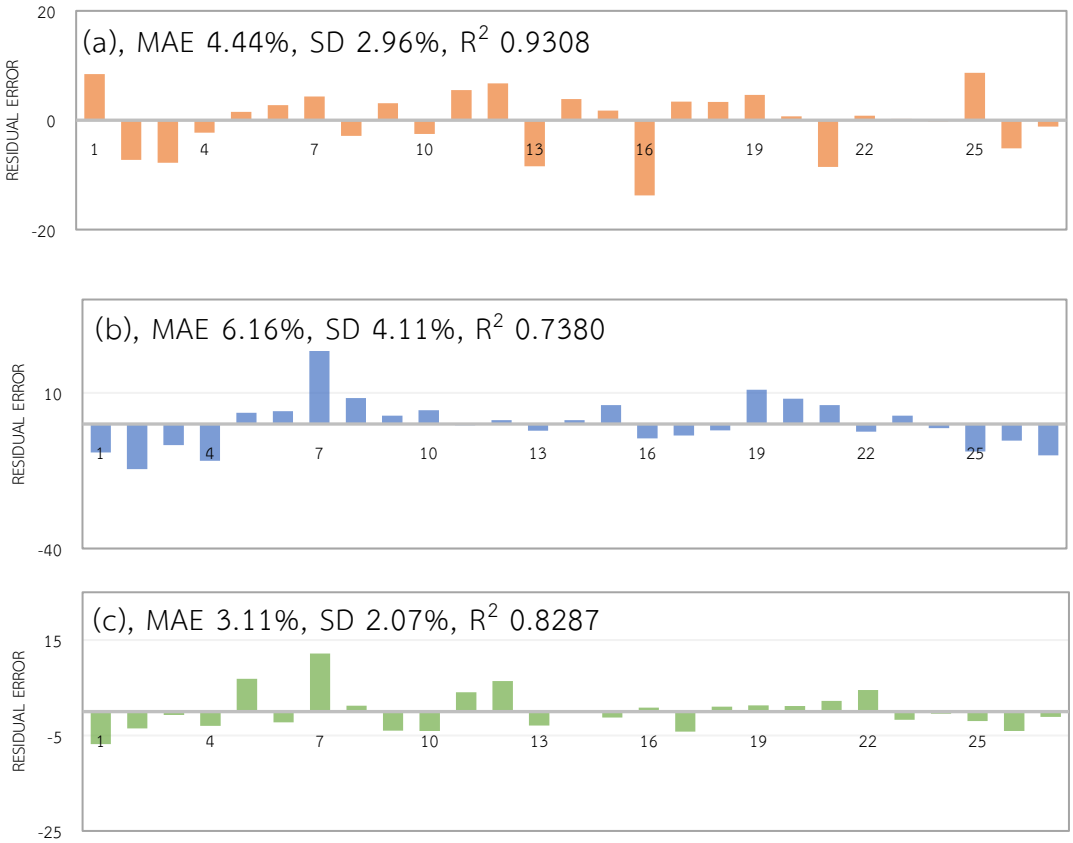

Figure 32 *Residual Errors between Experiment results and Simulation results on (a) MeOH yield, (b) CO Conversion, (c) H_2 Conversion of the methanol synthesis reactor*

The kinetic parameters form ***Table 10*** *were putter to reactor simulator. A simulation of the methanol synthesis reactor was investigated under operating conditions given in*

Table 8 *(see Section 4.1.2.2).* ***Figure 32*** *presented residual error between experiment and simulation on outputs: (a) Methanol yield, (b) CO Conversion, (c) H_2 Conversion. The highest value errors of Methanol yield, CO Conversion, H_2 Conversion were -13.37 (#Run 16), 14.46% (#Run 2) and 12.14% (#Run 7) as shown in* ***Figure 32****(a),* ***Figure 32****(b),* ***Figure 32****(c).). The mean absolute errors (MAE) of the Methanol yield, the CO Conversion and the H_2 Conversion were 4.44, 6.15 and 3.11, respectively. The standard deviation (SD) was obtained in 2.96 for the Methanol yield, 4.11 for the CO Conversion and 2.07 for the H_2 Conversion. R^2 values indicated 0.9308, 0.7380 and 0.8287 of Methanol yield, CO Conversion and H_2 Conversion, respectively, which were acceptable for process simulation.*

5.3 Process simulation results

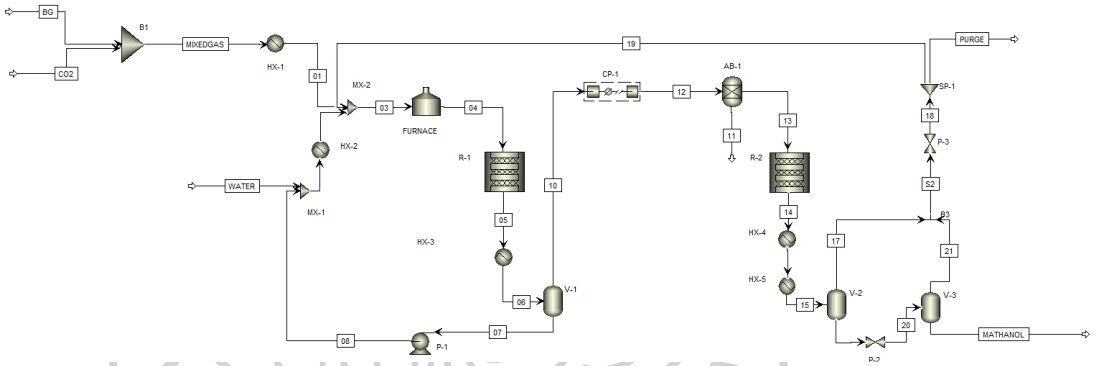

Figure 33 *Methanol Production Process in Aspen Plus V10*

The optimization conditions of both reforming process and methanol synthesis received from item 5.1 and 5.2 were scaled and simulated for under three cases of 15,000 kg/day bio methanol production produced from biogas. The Aspen plus software was used for the bio-methanol process, as shown in **Figure 33**. The Configurations of the reforming process simulation were set under biogas feedstock contained 30 % methane balanced with carbon dioxide, ratio water over biogas feed flow rate 0.7ml/min /1,100 ml/min, and controlled temp at 650 ^{o}C. Because of the composition of outlet gases (residue gases) from a methanol separation unit composed of carbon dioxide, carbon monoxide and hydrogen which could be utilized for increasing profit such as returning to

reforming reactor for increasing the amount of methanol production or substituting fuel for heat or electricity supply. Therefore, it can conclude three cases methanol process simulation as follows:

- The case I Recycling residue gas as a raw material for methanol production shown in Figure 14
- Case II Recycling residue gas for substituting for renewable fuel in the generator shown in Figure 15
- Case III Recycling residue gas as a raw material for methanol production and added extra biogas for producing electricity shown in Figure 16

The simulation results of each case were reported in terms of material balance and energy consumption shown in **Table 11**. Biogas was used as the main raw material in this process. There was no difference of biogas using as thermal energy for all three cases. However, it can see that case I consumed only 11,012 m^3/day of biogas for only methanol production, case II used extra 2,842 m^3/day of biogas for electricity generation, and case III spent 5,116 m^3/day of biogas for electricity generation. Case II experienced, so no residue recycle gas for methanol process that no compensate for raw material substitution, and this extra biogas used for electricity compensation reduced electricity paid as described in Item 5.4. By the way, CO_2 was used for balancing the reactions. There was a difference in CO_2 consumption for each case. The case I and III consumed the close amount of CO_2 around 3,082 and 3,890 m^3/day, respectively, and case II spent the most amount CO_2 till 825 m^3/day. It could be classified in % CO_2 consumption for the case I, II, III as 34.7%, 18.8%, and 6.7% respectively.

Table 11 *Material balance, carbon dioxide utilization, energy usage for -1,000 kg per days of methanol production*

Cases study	**Case I**	**Case II**	**Case III**
Methanol production (kg/day)	15,000	15,000	15,000
Biogas (m^3/day)			
- For Reaction	11,012	14,757	11,012
- For Heater	6,367	6,529	6,367
Extra Biogas (m^3/day)	**0**	**2,842**	**5,116**
Total Biogas (m^3/day)	**17,379**	**24,128**	**22,495**
CO_2 For Reaction (m^3/day)	1,060	9,838	1,060
CO_2 Consumptions (m^3/day)	3,082	3,890	825
CO_2 Consumptions (%)	**34.7%**	**18.8%**	**6.7%**
Water (m^3/day)	11.7	15.7	11.7
Electrical usage (kwh/hr)	639	639	639
Thermal usage (kcal/hr)	1,326,447	1,360,270	1,326,447

The material and energy balance were obtained by the results of the Aspen plus simulator. They were used for equipment design which involved determining the size of equipment base on basic principles of scale-up via scale-up factors such as Reynolds number, residence time and retention time [70] as shown in Appendix D-1 (Table C-1.1).

5.4 Economic Feasibility Results

5.4.1 Variable Cost Calculation results

Economic feasibility of commercial production of bio methanol was evaluated in terms of fixed cost and variable costs. Variable costs of three cases showed in **Table 12**. Variable costs were divided into four items:

1) Raw materials comprised biogas, CO_2, and H_2O cost

2) Catalyst had two types for Ni/Al_2O_3 and $Cu/ZnO/Al_2O_3$

3) Electrical cost

4) Heating cost.

All three cases did not have any effect from CO_2 and H_2O cost, but biogas. The most biogas consumption appeared in Case II, and then it resulted to the highest variable cost of raw material as 4.02, 3.75, and 2.90 THB/kg MeOH for case II, III, and I respectively. Case II was also consumed more catalyst cost, but it slightly around 1.19 THB/kg MeOH increased by 38% comparing with 0.89 THB/kg MeOH of Case I and III. Electrical costs were reduced when recycling gases compensated to the system for using as renewable fuel case II and used extra biogas as fuel for electricity. So, Electrical costs showed 3.58, 1.99, and 0.85 THB/kg MeOH for the case I, II, and III respectively. The last observation was heating cost; it was almost no change in all cases. To summary, variable costs were classified from high to low as 9.45, 8.90, and 7.05 THB/kg MeOH for case II, I, and III, respectively. As a result, case III yielded the lowest variable cost.

Table 12 *Variable cost of each case study for methanol production processes*

Cases study	Case I	Case II	Case III
1. Raw material			
1.1 Biogas (2.5 THB/m^3)	2.90	4.02	3.75
1.2 CO_2 (1 THB/m^3)	0.07	0.66	0.07
1.3 H_2O (15 THB/m^3)	0.01	0.02	0.01
2. Catalyst			
2.1 Ni/Al_2O_3 (600 THB/kg)	0.89	1.19	0.89
2.2 $Cu/ZnO/Al_2O_3$ (547 THB/kg)	0.39	0.52	0.39
3. Electrical Cost - Extra Biogas (2.5 THB/m^3) - Electricity (3.5 THB/kwh)	**3.58**	**1.99**	**0.85**
4. Heating Cost (0.0005 THB/kcal)	1.06	1.06	1.09
Total Variable cost (THB/kg MeOH)	**8.90**	**9.45**	**7.05**

5.4.2 Fixed Cost Estimation results

The equipment costs were evaluated from the local vendor, and real industries cost based on basic design showed price in Bath (THB) per unit in Appendix D-2 (Table D-2.1). All three cases of 15,000 kg MeOH per day bio-methanol process simulation can be operated under minimum unit operations and obtained unit pricing from sources (Table C-2.1) as shown in **Table 13**. The costs of equipment were estimated by evaluating prices from local vendors via the basic design of equipment. The case I represented the normal case without the electric generator, the fixed cost price was 54.11 MTHB. The case II and III would need the extra electric generator, the processes were added 2 of 700 KW generators which yielded fixed cost 74.11 MTHB.

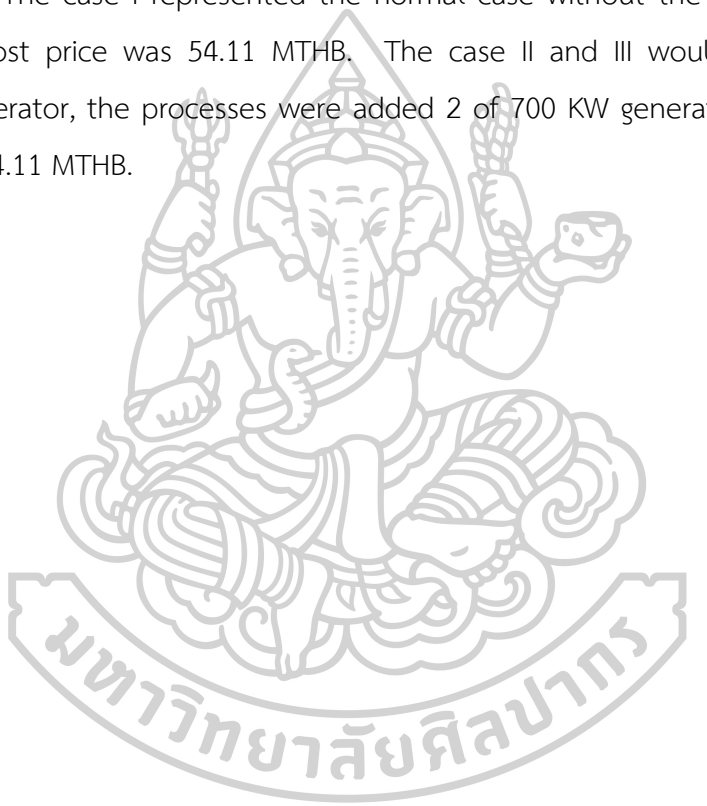

Table 13 *Cost Estimation*

Code	Equipment	unit	Price (THB/unit)	Price (THB)
RT-1,2	Biogas, Syngas root blower	2	175,000	350,000
RT-3	CO_2 root blower	1	175,000	175,000
MX-1,2	Biogas Mixer 1,2	2	200,000	400,000
HX-1	Biogas preheater	2	1,000,000	2,000,000
HX-2	Water preheater	2	1,000,000	2,000,000
HX-3	Syngas cooler	2	1,000,000	2,000,000
HX-4	Methanol cooler by CW	2	1,000,000	2,000,000
HX-5	Methanol cooler by CH	2	1,000,000	2,000,000
CP-1	Syngas compressor	2	1,256,250	2,512,500
V-1	Water trap vessel	1	500,000	500,000
V-2,3	Methanol trap vessel	2	500,000	1,000,000
R-1	Reforming reactor	1	3,000,000	3,000,000
R-2	Methanol synthesis reactor	1	2,000,000	2,000,000
AB-1	Water absorber	1	1,000,000	1,000,000
P-1	Water tank pump	2	19,000	38,000
F-1	Furnace	1	5,000,000	5,000,000
CW	Cooling tower	1	1,050,000	1,050,000
CH	Chiller	1	1,575,000	1,575,000
	Electric generator (700kW) (For case II, III)			20,000,000
	Piping & valve			2,000,000
	Land (3,200 m^2) & Office (180 m^2)			7,000,000
	Laboratory			5,000,000
	Safety & control			8,000,000
	Commissioning			3,600,000
			Total Fixed Cost (THB)	74,113,000

Therefore, it can summarize the comparison of the case I, case II, and case III in terms of total biogas and CO_2 usage, the variable cost, and fixed cost in **Table 14**.

The case I showed the highest percentage CO_2 consumption and lowest biogas consumption out of the three options. Also, the process was simple compared to the other two options, and therefore investment cost was lower. Since case I did not include electricity generation, it can be affected most by the electricity price increase. It also depended on grid electricity affected the reliable operation of the plant.

Case II had the option to generate electricity within the plant. It used recycled gases for power generation. Therefore, electricity price did not give much influence as the case I and also operating reliability was higher. CO_2 consumption was better compared to case III. This option required the highest biogas feed to operate. The investment cost was higher mainly due to the cost of the generator. Operating cost was also higher, which makes this option less favorable.

Case III also had the option to generate electricity, and therefore the operation was reliable and also the operating cost was at the lowest. CO_2 consumption, in this case, is lowest of all cases. This option required the highest biogas input and also required the highest investment.

These data were used for calculation of economic feasibility parameters such as NPV, ROI, IRR, and PBB.

Table 14 *Variables summary for the study of the feasibility of 15,000 kg MeOH per day*

Cases study	**Case I**	**Case II**	**Case III**
Total Biogas (m^3/day)	17,379	24,128	22,495
CO_2 (THB/ day)	1,060	9,838	1,060
CO_2 Consumptions (%)	34.7%	18.8%	6.7%
Total Variable cost (THB/kg)	8.90	9.45	7.05
Fixed Cost (MTHB)	54.29	74.29	74.29

5.4.3 Cash flow statements

Financial factors affecting the economic viability of bio methanol production were shown in **Table 15**. Depreciation of 10 years was assumed as the expected

lifetime of the plant. Most of the costs other than the investment were susceptible to price inflation. Demand and input cost increase rates were estimated based on existing statistical data. Cash conversion cycle (working capital cycle) was estimated based on the buyer's payment cycles.

Table 15 *Economic assumption*

Assumption	**Amount**	**unit**
Depreciation	10	Year
Demand growth rate	1.0	%
MeOH Price growth rate	2.0	%
Incremental fixed costs	1.0 M	THB
SG&A growth rate	1.0	%
WACC (or interest rate)	7.0	%
Tax Rate	20	%
Cash conversion cycle (CCC)	50	Day
Employees cost growth rate	5.3	%
Annual maintenance cost	2.0	%

Cash flow forecasts were prepared based on the assumption of financial data and plant configurations of cases 1, 2 & 3. Cash flows were calculated by removing non-cash from the Net Operating Profit After Tax (NOPAT). The prediction was prepared for ten years of operation including estimated price growth and demand expansion. The calculations of economic feasibility parameters were reported in terms of NPV, ROI, IRR, and PBB in ***Table 16****,* ***Table 17****, and*

Table 18 *for the case I, II, and III, respectively. Then all three cases of economic feasibility parameters were compared in* ***Table 19****.*

Table 16 Cash flow statements of Case I

INCOME STATEMENT	UNIT	Year 0	Year 1	Year 2	Year 3	Year 4	Year 5	Year 6	Year 7	Year 8	Year 9	Year 10
Demand MeOH	kg		4.9 M	5. M	5. M	5.1 M	5.2 M	5.2 M	5.3 M	5.3 M	5.4 M	5.4 M
MeOH Price	THB		12	12	12	13	13	13	14	14	14	14
Net Sales	THB		59.4 M	61.2 M	63.0 M	64.9 M	66.9 M	68.9 M	71.0 M	73.2 M	75.4 M	77.6 M
Cost of Good Sold (COGS)	THB		45.2 M	45.6 M	46.1 M	46.5 M	47.0 M	47.4 M	47.9 M	48.4 M	48.8 M	49.3 M
Depreciation of Investment	THB		5.4 M	5.4 M	5.4 M	5.4 M	5.4 M	5.4 M	5.4 M	5.4 M	5.4 M	5.4 M
Gross Profit (GP)	THB		8.8 M	10.2 M	11.6 M	13.0 M	14.5 M	16.1 M	17.7 M	19.4 M	21.1 M	22.9 M
SG&A	THB		1.1 M	1.1 M	1.1 M	1.1 M	1.1 M	1.1 M	1.2 M	1.2 M	1.2 M	1.2 M
Loss from asset write-off	THB		.7 M	.7 M								
Employees cost	THB		2.9 M	3.0 M	3.2 M	3.4 M	3.5 M	3.7 M	3.9 M	4.1 M	4.4 M	4.6 M
Annual maintenance cost	THB		1.1 M	1.1 M	1.1 M	1.1 M	1.1 M	1.1 M	1.1 M	1.1 M	1.1 M	1.1 M
Operating Income (OI)	THB		3.0 M	4.2 M	6.2 M	7.4 M	8.8 M	10.1 M	11.5 M	13.0 M	14.5 M	16.0 M
Tax	THB		.6 M	.8 M	1.2 M	1.5 M	1.8 M	2.0 M	2.3 M	2.6 M	2.9 M	3.2 M
Net Operating Profit After Tax (NOPAT)	THB		**2.4 M**	**3.4 M**	**4.9 M**	**6.0 M**	**7.0 M**	**8.1 M**	**9.2 M**	**10.4 M**	**11.6 M**	**12.8 M**
Investment (Capital Expenditure)	THB	54.3 M	0	0								
Cash Conversion Cycle	Day		50	50	50	50	50	50	50	50	50	50
Working Capital	THB		8.2 M	8.5 M	8.8 M	9.0 M	9.3 M	9.6 M	9.9 M	10.2 M	10.5 M	10.8 M
Working Capital Changed	THB		8.2 M	.2 M	.3 M	.3 M	.3 M	.3 M	.3 M	.3 M	.3 M	.3 M
Free Cash Flow	THB	**-54.3 M**	**.3 M**	**9.3 M**	**10.1 M**	**11.1 M**	**12.2 M**	**13.2 M**	**14.4 M**	**15.5 M**	**16.7 M**	**18.0 M**
Cumulative Free Cash Flow	THB	**-54.3 M**	**-54.0 M**	**-44.7 M**	**-34.6 M**	**-23.5 M**	**-11.3 M**	**1.9 M**	**16.3 M**	**31.8 M**	**48.5 M**	**66.5 M**

NPV	22,935 k
IRR	14.0%
ROI	4.1%
PAYBACK PERIOD	5.85 y

Table 17 Cash flow statements of Case II

INCOME STATEMENT	UNIT	Year 0	Year 1	Year 2	Year 3	Year 4	Year 5	Year 6	Year 7	Year 8	Year 9	Year 10
Demand MeOH	kg		4.9 M	5. M	5. M	5.1 M	5.2 M	5.2 M	5.3 M	5.3 M	5.4 M	5.4 M
MeOH Price	THB		12	12	12	13	13	13	14	14	14	14
Net Sales	THB		59.4 M	61.2 M	63.0 M	64.9 M	66.9 M	68.9 M	71.0 M	73.2 M	75.4 M	77.6 M
Cost of Good Sold (COGS)	THB		47.8 M	48.3 M	48.7 M	49.2 M	49.7 M	50.2 M	50.7 M	51.2 M	51.7 M	52.2 M
Depreciation of Investment	THB		7.4 M	7.4 M	7.4 M	7.4 M	7.4 M	7.4 M	7.4 M	7.4 M	7.4 M	7.4 M
Gross Profit (GP)	THB		4.2 M	5.5 M	6.9 M	8.3 M	9.8 M	11.3 M	12.9 M	14.6 M	16.3 M	18.0 M
SG&A	THB		1.5 M	1.5 M	1.5 M	1.5 M	1.5 M	1.6 M	1.6 M	1.6 M	1.6 M	1.6 M
Loss from asset write-off	THB		1.0 M	1.0 M								
Employees cost	THB		2.9 M	3.0 M	3.2 M	3.4 M	3.5 M	3.7 M	3.9 M	4.1 M	4.4 M	4.6 M
Annual maintenance cost	THB		1.5 M	1.5 M	1.5 M	1.5 M	1.5 M	1.5 M	1.5 M	1.5 M	1.5 M	1.5 M
Operating Income (OI)	THB		-2.6 M	-1.5 M	.7 M	1.9 M	3.2 M	4.6 M	5.9 M	7.4 M	8.8 M	10.3 M
Tax	THB		-.5 M	-.3 M	.1 M	.4 M	.6 M	.9 M	1.2 M	1.5 M	1.8 M	2.1 M
Net Operating Profit After Tax (NOPAT)	THB		**-2.1 M**	**-1.2 M**	**.6 M**	**1.5 M**	**2.6 M**	**3.6 M**	**4.7 M**	**5.9 M**	**7.1 M**	**8.3 M**
Investment (Capital Expenditure)	THB	74.3 M	0	0								
Cash Conversion Cycle	Day		50	50	50	50	50	50	50	50	50	50
Working Capital	THB		8.2 M	8.5 M	8.8 M	9.0 M	9.3 M	9.6 M	9.9 M	10.2 M	10.5 M	10.8 M
Working Capital Changed	THB		8.2 M	.2 M	.3 M	.3 M	.3 M	.3 M	.3 M	.3 M	.3 M	.3 M
Free Cash Flow	THB	**-74.3 M**	**-2.0 M**	**7.0 M**	**7.7 M**	**8.7 M**	**9.7 M**	**10.8 M**	**11.9 M**	**13.0 M**	**14.2 M**	**15.4 M**
Cumulative Free Cash Flow	THB	**-74.3 M**	**-76.2 M**	**-69.3 M**	**-61.6 M**	**-52.8 M**	**-43.1 M**	**-32.3 M**	**-20.4 M**	**-7.4 M**	**6.8 M**	**22.2 M**

NPV	-11,620 k
IRR	4.0%
ROI	-1.9%
PAYBACK PERIOD	8.52 y

Table 18 *Cash flow statements of Case III*

INCOME STATEMENT	UNIT	Year 0	Year 1	Year 2	Year 3	Year 4	Year 5	Year 6	Year 7	Year 8	Year 9	Year 10
Demand MeOH	kg		4.9 M	5. M	5. M	5.1 M	5.2 M	5.2 M	5.3 M	5.3 M	5.4 M	5.4 M
MeOH Price	THB		12	12	12	13	13	13	14	14	14	14
Net Sales	THB		59.4 M	61.2 M	63.0 M	64.9 M	66.9 M	68.9 M	71.0 M	73.2 M	75.4 M	77.6 M
Cost of Good Sold (COGS)	THB		35.9 M	36.2 M	36.6 M	36.9 M	37.3 M	37.7 M	38.0 M	38.4 M	38.8 M	39.2 M
Depreciation of Investment	THB		7.4 M	7.4 M	7.4 M	7.4 M	7.4 M	7.4 M	7.4 M	7.4 M	7.4 M	7.4 M
Gross Profit (GP)	THB		16.1 M	17.5 M	19.0 M	20.6 M	22.2 M	23.8 M	25.6 M	27.3 M	29.2 M	31.1 M
SG&A	THB		1.5 M	1.5 M	1.5 M	1.5 M	1.5 M	1.6 M	1.6 M	1.6 M	1.6 M	1.6 M
Loss from asset write-off	THB		1.0 M	1.0 M								
Employees cost	THB		2.9 M	3.0 M	3.2 M	3.4 M	3.5 M	3.7 M	3.9 M	4.1 M	4.4 M	4.6 M
Annual maintenance cost	THB		1.5 M	1.5 M	1.5 M	1.5 M	1.5 M	1.5 M	1.5 M	1.5 M	1.5 M	1.5 M
Operating Income (OI)	THB		9.3 M	10.5 M	12.8 M	14.2 M	15.6 M	17.1 M	18.6 M	20.1 M	21.7 M	23.4 M
Tax	THB		1.9 M	2.1 M	2.6 M	2.8 M	3.1 M	3.4 M	3.7 M	4.0 M	4.3 M	4.7 M
Net Operating Profit After Tax (NOPAT)	THB		**7.4 M**	**8.4 M**	**10.3 M**	**11.4 M**	**12.5 M**	**13.6 M**	**14.9 M**	**16.1 M**	**17.4 M**	**18.7 M**
Investment (Capital Expenditure)	THB	74.3 M	0	0								
Cash Conversion Cycle	Day		50	50	50	50	50	50	50	50	50	50
Working Capital	THB		8.2 M	8.5 M	8.8 M	9.0 M	9.3 M	9.6 M	9.9 M	10.2 M	10.5 M	10.8 M
Working Capital Changed	THB		8.2 M	.2 M	.3 M	.3 M	.3 M	.3 M	.3 M	.3 M	.3 M	.3 M
Free Cash Flow	THB	**-74.3 M**	**7.6 M**	**16.6 M**	**17.4 M**	**18.5 M**	**19.6 M**	**20.8 M**	**22.0 M**	**23.2 M**	**24.5 M**	**25.8 M**
Cumulative Free Cash Flow	THB	**-74.3 M**	**-66.7 M**	**-50.1 M**	**-32.7 M**	**-14.2 M**	**5.5 M**	**26.3 M**	**48.2 M**	**71.5 M**	**96.0 M**	**121.8 M**

NPV	53,404 k
IRR	19.3%
ROI	10.7%
PAYBACK PERIOD	4.72 y

Table 19 *Comparison of the feasibility of all three cases*

Cases study	Case I	Case II	Case III
NPV (THB)	22.93 M	-11.62M	53.40M
IRR (%)	14.0%	4.0%	19.3%
ROI (%)	4.1%	-1.9%	10.7%
PAYBACK PERIOD (years)	5.85	8.25	4.72

Comparing all three cases, it was found that Case II was not acceptable for running the business, because NPV was negative value (-11.62 MTHB) and negative ROI (-1.9%), then effecting to the lowest IRR (4.0%) and the longest payback period (8.25 years). The reason for case II was that only used residue gases for a generation. The heating value of residue gases was three times lower than that of biogas. Therefore, it was not a viable option for electricity generation. The case I and III were reasonable for business operation, because both cases yielded positive NPV 22.93 and 53.40, IRR 14.0% and 19.3%, and ROI 4.1% and 10.7% and resulting in good payback period 5.85 and 4.72 years respectively. Both cases reflected the acceptable

primary economic feasibility. However, these two cases would be tested with sensitivity analysis.

5.4.4 Sensitivity Analysis

This section studied the sensitivity of the financial indicators to the changes in input costs and selling prices. This study was essential because the actual costs in the future may change from the previous expectation. In this section the sensitivity analysis was tested by changing methanol price from 10 to 14 THB/kg, biogas price ranging 2.00 to 4.00 THB/m^3, and spending 1 to 5 THB for kwh electricity, then they were reported in **Table 20**, **Table 21**, and **Table 22** respectively.

Table 20 *Methanol Price Sensitivity Analysis of each case*

NPV			IRR		
MeOH PRICE	CASE I	CASE III	**MeOH PRICE**	CASE I	CASE III
10	-34,275 k	-3,806 k	10	-6.2%	6.0%
11	-5,670 k	24,799 k	11	5.1%	13.0%
12	22,935 k	53,404 k	12	14.0%	19.3%
13	51,540 k	82,009 k	13	21.9%	25.1%
14	80,145 k	110,614 k	14	29.1%	30.5%
ROI			**PAYBACK PERIOD**		
MeOH PRICE	CASE I	CASE III	**MeOH PRICE**	CASE I	CASE III
10	-6.4%	-0.8%	10	-	7.80 y
11	-1.0%	5.1%	11	8.22 y	5.91 y
12	4.1%	10.7%	12	5.85 y	4.72 y
13	9.1%	16.1%	13	4.46 y	3.93 y
14	13.8%	21.3%	14	3.59 y	3.36 y

The result in **Table 20** showed the methanol price effecting to NPV, IRR, ROI, and Payback Period. Methanol price was lower than 12 THB, which effected to negative NPV for the case I and if it was lower than 11 THB, which caused negative NPV for case III. So, case III can absorb for much changing of the methanol selling price. In this sensitivity the methanol price should be not lower than 12 THB/kg to cover both cases, it resulted for the case I and III on NPV 22,935k to 80,145k and 53,404k to 110,614k, on IRR 14.0% to 19.1% and 19.3% to 30.5%, on ROI 4.1% to

13.8% and 10.7% to 21.3%, and on Payback period 5.85 year to 3.59 year and 4.72 years to 3.36 year.

Table 21 *Biogas Price Sensitivity Analysis of each case*

NPV			IRR		
Biogas Price	CASE I	CASE III	**Biogas Price**	CASE I	CASE III
2.00	44,489 k	84,181 k	2.00	20.2%	25.7%
2.50	22,935 k	53,404 k	2.50	14.0%	19.3%
3.00	1,381 k	22,626 k	3.00	7.4%	12.4%
3.50	-20,172 k	-8,152 k	3.50	0.1%	4.9%
4.00	-41,726 k	-38,930 k	4.00	-8.7%	-3.9%
ROI			**PAYBACK PERIOD**		
Biogas Price	CASE I	CASE III	**Biogas Price**	CASE I	CASE III
2.00	8.5%	18.7%	2.00	4.69 y	3.82 y
2.50	4.1%	10.7%	2.50	5.85 y	4.72 y
3.00	0.2%	4.2%	3.00	7.53 y	6.09 y
3.50	-3.2%	-1.4%	3.50	9.96 y	8.22 y
4.00	-6.4%	-6.1%	4.00	-	-

The result in ***Table 21*** showed the biogas price effecting to NPV, IRR, ROI, and Payback Period. Biogas price was higher than 3.00 THB/$m^{3,}$ which effected to negative NPV for both cases I. So, both cases can absorb for much changing of the biogas buying price. In this sensitivity the biogas price should be not higher than 3.00 THB/m^3, it resulted for biogas price from 2.00 to 3.00 THB/m^3 resulting on the case I and III on NPV 44,489k to 1,381k and 84,181k to 22,626k, on IRR 20.2% to 7.4% and 25.7% to 12.4%, on ROI 8.5% to 0.2% and 18.7% to 4.2%, and on Payback period 4.69 year to 7.53 year and 3.82 years to 6.09 year.

Table 22 *Electricity Price Sensitivity Analysis of each case*

NPV			IRR		
Electricity Price	CASE I	CASE III	**Electricity Price**	CASE I	CASE III
1.00	92,116 k	53,404 k	1.00	32.9%	19.3%
2.00	64,443 k	53,404 k	2.00	25.6%	19.3%
3.00	36,771 k	53,404 k	3.00	18.0%	19.3%
4.00	9,099 k	53,404 k	4.00	9.9%	19.3%
5.00	-18,574 k	53,404 k	5.00	0.7%	19.3%
ROI			**PAYBACK PERIOD**		
Electricity Price	CASE I	CASE III	**Electricity Price**	CASE I	CASE III
1.00	20.4%	10.7%	1.00	3.18 y	4.72 y
2.00	13.1%	10.7%	2.00	3.93 y	4.72 y
3.00	6.9%	10.7%	3.00	5.06 y	4.72 y
4.00	1.6%	10.7%	4.00	6.86 y	4.72 y
5.00	-3.0%	10.7%	5.00	9.74 y	4.72 y

The result in ***Table 22*** showed the electricity price effecting to NPV, IRR, ROI, and Payback Period. Electricity price was higher than 4 THB/kWh which effected to negative NPV for the case I but all the economical parameters of case III did not change following the electricity price because it can operate by self-generated electrical. So, both cases can absorb for much changing of electricity paying price. In this sensitivity the electricity price should be not higher than 4.00 THB/kWh for the case I, it resulted for electricity price from 1.00 to 4.00 THB/kWh resulting on the case I on NPV 92,116k to 9,099k, on IRR 32.9 to 9.9%, on ROI 20.4% to 1.6% and on Payback period 3.18 year to 6.86 year. However, the profitability of the Case I was better than the Case III when the electricity price was lower than 2.00 THB/kwh. The IRR of the Case I was obtained 25.6%, which was more than the Case I resulting 19.3% of IRR.

When all economic parameters were compared between case I and III, it found that case III can absorb more gap change in methanol selling price, biogas price, and electricity paying the price. Therefore, the variation of methanol capacity

was plotted in graphical against NPV, IRR, ROI, and Payback period, as shown in Figure 34, Figure 35, Figure 36, and Figure 37, respectively.

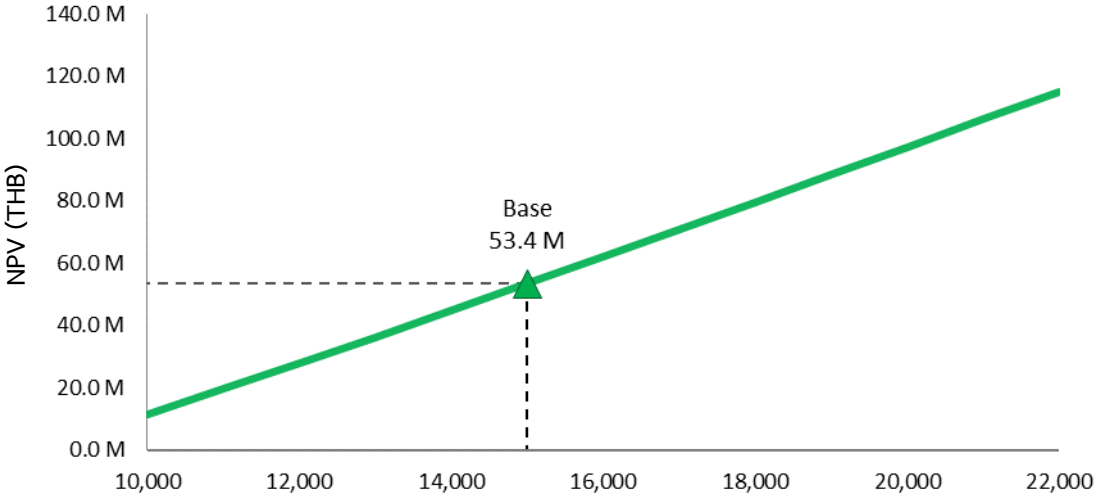

Figure 34 *Methanol production rate sensitivity of NPV*

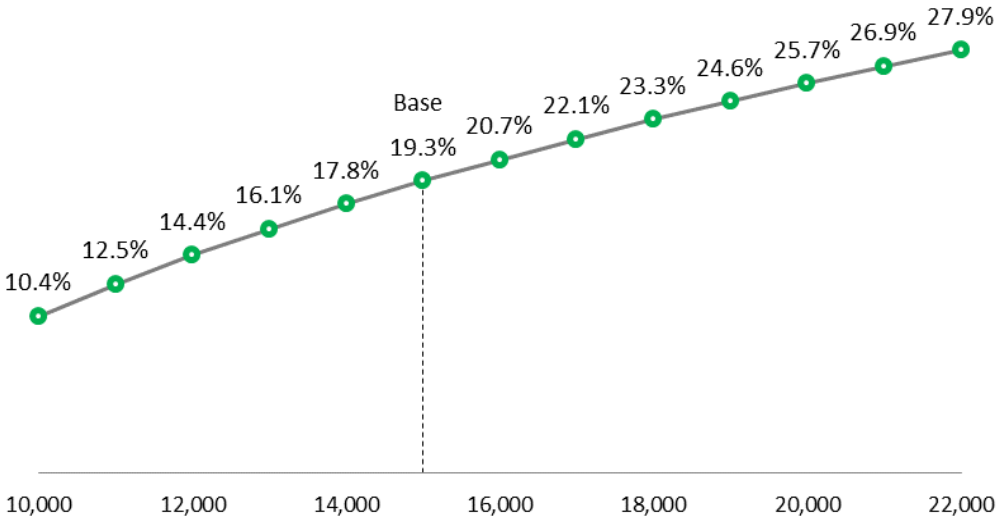

Figure 35 *Methanol production rate sensitivity of IRR*

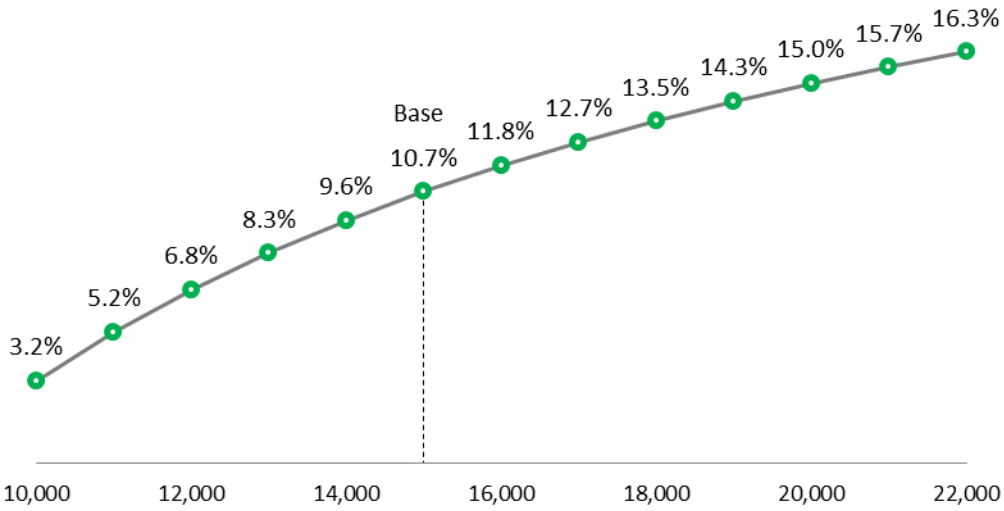

Figure 36 *Methanol production rate sensitivity of ROI*

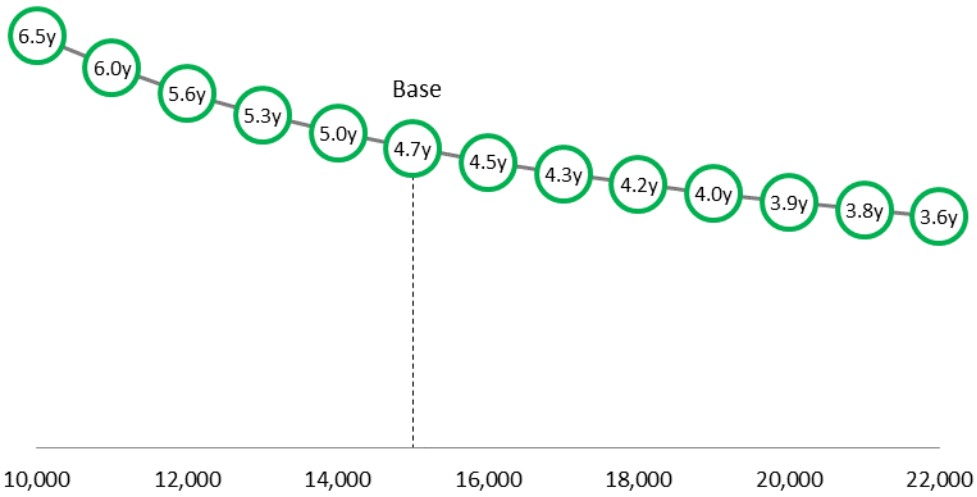

Figure 37 *Methanol production rate sensitivity of Payback Period*

The production rate of the plant or the production capacity of the plant was also a contributing factor to the profitability of the investment. Most of the existing biogas production plants had capacity in the range of 10,000 – 20,000 kg/day. The analysis was based on that range in this study. **Figure 34** showed the sensitivity of methanol production rate to the NPV of the investment. It showed that the increase in production capacity increased the NPV. NPV was linearly increasing with the production capacity. An investor was interested in economies of scale to select the

optimum capacity of the plant to an investor. The production capacity decision also depended on other factors such as demand, availability of raw materials and cost of investment. The sensitivity of production rate to IRR was shown in **Figure 35**. IRR was not linearly increasing with the increased of production rate. The capacity selected for the study represented an IRR of 19.3%. ROI of the investment's sensitivity to the production capacity was shown in **Figure 36**, which had an increasing trend in the range of analysis. **Figure 37** showed the impact of plant capacity over the payback period. It also showed the influencing of scale on the profitability of the investment. In summary, economies of scale applied when the production capacity was higher. But the expandability of production was limited due to several factors. In practice, limitations in raw materials, environmental impact, the elasticity of demand and prices were also taken into consideration when investment decisions were taken.

CHAPTER VI

CONCLUSION AND RECOMMENDATIONS

Methanol is an important chemical for downstream chemicals. The process simulation of methanol produced from biogas was analyzed by ASPEN PLUS using the developed kinetic data. The study had shown that the conversion of CH_4, CO_2 and H_2/CO ratio was optimum in ranges of high temperature in both reactors. The accuracy of kinetic models was obtained in each condition. The best case of feasibility was shown and was analyzed by sensitivity analysis.

6.1 Conclusions

Regarding experimental results, the major effects of reforming reaction on CH_4 conversion were temperature and the $\%CH_4$-to-CO_2 volumetric ratio while the CO_2 conversion depended on only the $\%CH_4$-to-CO_2 volumetric ratio. The H_2O feed flows rate, and $\%CH_4$-to-CO_2 volumetric ratio affected the H_2/CO ratio of the reforming reaction. The temperature and the $\%CH_4$-to-CO_2 volumetric ratio exhibited the synergistic effect on the CH_4 and CO_2 conversions. At the lowest water feed flow rate (0.7 ml/min), the temperature did not affect the H_2/CO ratio. While at the high-water feed flow rate (1.1, 1.5 ml/min), the increasing in temperature led to the decreasing in the H_2/CO ratio. For methanol synthesis reaction, all inputs (temperature, H_2/CO ratio and $\%CO_2$ in feed) affected the CO conversion, the $\%CO_2$ in feed and the temperature affected the methanol yield, and the only temperature affected in the H_2 conversion. The methanol yield was an interaction between the $\%CO_2$ in feed and the temperature while the CO and H_2 conversions were the interaction between the $\%CO_2$ in feed and the H_2/CO ratio.

For the optimal conditions, the outputs of reforming reaction (%CH4 conversion, $\%CO_2$ conversion, and H_2/CO) were balanced to suitable for the next step reaction as methanol synthesis. For the reforming reaction, the optimal condition was 700 $^{\circ}$C, 35%, and 1.5 ml/min of temperature, $\%CH_4$-to-CO_2 volumetric ratio and water feed, respectively. For methanol synthesis, the optimal condition was 5%, 2, and 200 $^{\circ}$C for $\%CO_2$ feed, H_2/CO ratio, and temperature, respectively.

The accuracy of kinetic models showed that the mean absolute errors (MAE) of the CH_4 conversion, the CO_2 conversion and the H_2/CO ratio were 2.65, 2.91 and 0.168, respectively. The standard deviation (SD) was obtained in 1.77 for the CH4 conversion, 1.94 for the CO_2 conversion and 0.11 for the H_2/CO ratio. R^2 values were obtained 0.6494, 0.9009 and 0.8562 of CH_4 conversion, CO_2 conversion and H_2/CO Ratio, respectively. The model was an agreement between experiment and simulation for the preliminary design process that was also confirmed by values of R^2. The mean absolute errors (MAE) of the Methanol yield, the CO Conversion and the H_2 Conversion were 4.44, 6.16 and 3.11, respectively. The standard deviation (SD) was obtained in 2.96 for the methanol yield, 4.11 for the CO conversion and 2.07 for the H_2 conversion. R^2 values indicated 0.9308, 0.7380 and 0.8287 of Methanol yield, CO conversion and H_2 Conversion, respectively, which were acceptable for process simulation.

Concerning the process simulation and economic study, The process simulation was simulated 15,000 kg/day methanol production rate dividing of 3 cases: Case I Recycling residue gas as a raw material for methanol production, Case II Recycling residue gas for substituting for renewable fuel in generator and Case III Recycling residue gas as a raw material for methanol production and added extra biogas for producing electricity. The results showed that the Case I and III consumed the close amount of CO_2 around 3,082 and 825 m^3/day, respectively, and the Case II spent the most amount CO_2 till 3,890 m^3/day. It could be classified in % CO_2 consumption for the case I, II, III as 34.7%, 18.8%, and 6.7% respectively. In an economic study, Case III was most profitable yielded 53.40 MTHB and resulting in a good payback period of 4.72 years. However, the sensitivity study showed that the assumption of electricity price lower than 2 THB/kwh, the Case I had much profit returned comparing with Case III. Therefore, the Case I was suitable when it can be supplied low price of electricity such as power plants. By the way, the Case III was fit for the biogas producer that had large biogas capacity.

6.2 Recommendations

This research focused on the kinetic and simulation of the bio-methanol process and preliminary feasibility study. This research would be useful for other researches in the future for bio-methanol process modification, such as considering the heat exchanger network and combining reforming and methanol synthesis reactors. It can be applied for the optimizing of process, scaling up the processing capacity and evaluate the economic feasibility for a potential investment.

REFERENCES

1. Slesser, M., *THE GLOBAL SYSTEMATIZATION OF RESOURCE DEPLETION IN TERMS OF NON-RENEWABLE FACTORS*, in *Renewable Resources a Systematic Approach*, E. Campos-LÓPez, Editor. 1980, Academic Press. p. 39-47.
2. Da Costa Gomez, C., *1 - Biogas as an energy option: an overview*, in *The Biogas Handbook*, A. Wellinger, J. Murphy, and D. Baxter, Editors. 2013, Woodhead Publishing. p. 1-16.
3. Ghasemzadeh, K., et al., *Chapter 23 - Economic Assessment of Methanol Production*, in *Methanol*, A. Basile and F. Dalena, Editors. 2018, Elsevier. p. 613-632.
4. Wang, X. and M. Economides, *CHAPTER 7 - Gas-To-Liquids (GTL)*, in *Advanced Natural Gas Engineering*, X. Wang and M. Economides, Editors. 2009, Gulf Publishing Company. p. 243-287.
5. Xu, J., et al., *Biogas upgrading*, in *Advances in Bioenergy*. 2020, Elsevier.
6. Dalena, F., et al., *Chapter 1 - Methanol Production and Applications: An Overview*, in *Methanol*, A. Basile and F. Dalena, Editors. 2018, Elsevier. p. 3-28.
7. Lewis, W.K., *The Rate of Drying of Solid Materials.* Journal of Industrial & Engineering Chemistry, 1921. **13**(5): p. 427-432.
8. Ni, G., et al., *Reforming of methane and carbon dioxide by DC water plasma at atmospheric pressure.* International Journal of Hydrogen Energy, 2011. **36**(20): p. 12869-12876.
9. Zhang, C., et al., *Carbon dioxide utilization in a gas-to-methanol process combined with CO2/Steam-mixed reforming: Techno-economic analysis.* Fuel, 2017. **190**: p. 303-311.
10. Zhang, C., et al., *Efficient utilization of carbon dioxide in a gas-to-methanol process composed of CO2/steam–mixed reforming and methanol synthesis.* Journal of CO2 Utilization, 2016. **16**: p. 1-7.
11. Benguerba, Y., et al., *Modelling of methane dry reforming over Ni/Al2O3 catalyst in a fixed-bed catalytic reactor*. Vol. 114. 2014.

12. Snoeck, J.W., G.F. Froment, and M. Fowles, *Kinetic Study of the Carbon Filament Formation by Methane Cracking on a Nickel Catalyst.* Journal of Catalysis, 1997. **169**(1): p. 250-262.
13. Lewis, W.K., E.R. Gilliland, and W.A. Reed, *Reaction of Methane with Copper Oxide in a Fluidized Bed.* Industrial & Engineering Chemistry, 1949. **41**(6): p. 1227-1237.
14. Bodrov, I.M., L.O. Apelba'oom, and M.I. T'Yomkeen, *Kinetics of steam-methane reaction on nickel surface.* Journal of Catalysis, 1965. **4**(3): p. 413.
15. Richardson, J.T. and S.A. Paripatyadar, *Carbon dioxide reforming of methane with supported rhodium.* Applied Catalysis, 1990. **61**(1): p. 293-309.
16. Tsipouriari, V.A., et al., *Reforming of methane with carbon dioxide to synthesis gas over supported Rh catalysts.* Catalysis Today, 1994. **21**(2): p. 579-587.
17. Mark, M.F. and W.F. Maier, *CO2-Reforming of Methane on Supported Rh and Ir Catalysts.* Journal of Catalysis, 1996. **164**(1): p. 122-130.
18. Olsbye, U., T. Wurzel, and L. Mleczko, *Kinetic and Reaction Engineering Studies of Dry Reforming of Methane over a Ni/La/Al2O3 Catalyst.* Industrial & Engineering Chemistry Research, 1997. **36**(12): p. 5180-5188.
19. Osaki, T. and T. Mori, *Kinetic studies of CO2dissociation on supported Ni catalysts.* Reaction Kinetics and Catalysis Letters, 2005. **87**(1): p. 149-156.
20. Kroll, V., G. Tjatjopoulos, and C. Mirodatos, *Kinetics of methane reforming over Ni/SiO 2 catalysts based on a step-wise mechanistic model.* Studies in Surface Science and Catalysis - STUD SURF SCI CATAL, 1998. **119**: p. 753-758.
21. Bradford, M.C.J. and M. Albert Vannice, *The role of metal–support interactions in CO2 reforming of CH4.* Catalysis Today, 1999. **50**(1): p. 87-96.
22. Wang, H.Y. and E. Ruckenstein, *Carbon dioxide reforming of methane to synthesis gas over supported rhodium catalysts: the effect of support.* Applied Catalysis A: General, 2000. **204**(1): p. 143-152.
23. Leonov, V.E., Karavaev, M. M., Tsybina, E. N. and Petrischeva, G. S., *Methanol synthesis kinetic.* Kinetics Katal, 1973. **14**: p. 848.
24. Natta, G., *Direct Catalytic Synthesis of Higher Alcohols from CO and H 2. Catalysis.* P. H. Emmett, Ed. New York: Reinhold, 1955. **349**: p. 131-114.

25. Chen, K., et al., *Simple strategy synthesizing stable CuZnO/SiO2 methanol synthesis catalyst.* Journal of Catalysis, 2019. **372**: p. 163-173.

26. Chinchen, G.C., et al., *Mechanism of methanol synthesis from CO2/CO/H2 mixtures over copper/zinc oxide/alumina catalysts: use of14C-labelled reactants.* Applied Catalysis, 1987. **30**(2): p. 333-338.

27. Takagawa, M. and M. Ohsugi, *Study on reaction rates for methanol synthesis from carbon monoxide, carbon dioxide, and hydrogen.* Journal of Catalysis, 1987. **107**(1): p. 161-172.

28. McNeil, M.A., C.J. Schack, and R.G. Rinker, *Methanol synthesis from hydrogen, carbon monoxide and carbon dioxide over a CuO/ZnO/Al2O3 catalyst: II. Development of a phenomenological rate expression.* Applied Catalysis, 1989. **50**(1): p. 265-285.

29. Rozovskii, A.Y. and G.I. Lin, *Fundamentals of Methanol Synthesis and Decomposition.* Topics in Catalysis, 2003. **22**(3): p. 137-150.

30. Fujitani, T., et al., *Methanol synthesis by hydrogenation of CO2 over a Zn-deposited Cu(111): formate intermediate.* Applied Surface Science, 1997. **121-122**: p. 583-586.

31. Klier, K., et al., *Catalytic synthesis of methanol from COH2: IV. The effects of carbon dioxide.* Journal of Catalysis, 1982. **74**(2): p. 343-360.

32. Liu, G., et al., *The role of CO2 in methanol synthesis on Cu□Zn oxide: An isotope labeling study.* Journal of Catalysis, 1985. **96**(1): p. 251-260.

33. Lim, H.-W., et al., *Modeling of the Kinetics for Methanol Synthesis using Cu/ZnO/Al2O3/ZrO2 Catalyst: Influence of Carbon Dioxide during Hydrogenation.* Industrial & Engineering Chemistry Research, 2009. **48**(23): p. 10448-10455.

34. Villa, P., et al., *Synthesis of alcohols from carbon oxides and hydrogen. 1. Kinetics of the low-pressure methanol synthesis.* Industrial & Engineering Chemistry Process Design and Development, 1985. **24**(1): p. 12-19.

35. Skrzypek, J., M. Lachowska, and H. Moroz, *Kinetics of methanol synthesis over commercial copper/zinc oxide/alumina catalysts.* Chemical Engineering Science, 1991. **46**(11): p. 2809-2813.

36. Graaf, G.H., et al., *Intra-particle diffusion limitations in low-pressure methanol synthesis.* Chemical Engineering Science, 1990. **45**(4): p. 773-783.
37. Askgaard, T.S., et al., *A Kinetic Model of Methanol Synthesis.* Journal of Catalysis, 1995. **156**(2): p. 229-242.
38. Bussche, K.M.V. and G.F. Froment, *A Steady-State Kinetic Model for Methanol Synthesis and the Water Gas Shift Reaction on a Commercial Cu/ZnO/Al2O3Catalyst.* Journal of Catalysis, 1996. **161**(1): p. 1-10.
39. Kubota, T., et al., *Kinetic study of methanol synthesis from carbon dioxide and hydrogen.* Applied Organometallic Chemistry, 2001. **15**(2): p. 121-126.
40. Grabow, L.C. and M. Mavrikakis, *Mechanism of Methanol Synthesis on Cu through CO2 and CO Hydrogenation.* ACS Catalysis, 2011. **1**(4): p. 365-384.
41. Šetinc, M. and J. Levec, *Dynamics of a mixed slurry reactor for the three-phase methanol synthesis.* Chemical Engineering Science, 2001. **56**(21): p. 6081-6087.
42. Waugh, K.C., *Methanol Synthesis.* Catalysis Today, 1992. **15**(1): p. 51-75.
43. Skrzypek, J., et al., *Thermodynamics and kinetics of low pressure methanol synthesis.* The Chemical Engineering Journal and the Biochemical Engineering Journal, 1995. **58**(2): p. 101-108.
44. Kulawska, M. and J. Skrzypek, *Kinetics of the synthesis of higher aliphatic alcohols from syngas over a modified methanol synthesis catalyst.* Chemical Engineering and Processing: Process Intensification, 2001. **40**(1): p. 33-40.
45. Grace, A.N., et al., *Electrochemical reduction of carbon dioxide at low overpotential on a polyaniline/Cu2O nanocomposite based electrode.* Applied Energy, 2014. **120**: p. 85-94.
46. Stempien, J.P., et al., *Production of sustainable methane from renewable energy and captured carbon dioxide with the use of Solid Oxide Electrolyzer: A thermodynamic assessment.* Energy, 2015. **82**: p. 714-721.
47. Fu, X., et al., *Carbon Dioxide Capture by MgO-modified MCM-41 Materials.* Adsorption Science & Technology - ADSORPT SCI TECHNOL, 2009. **27**: p. 593-602.
48. Iaquaniello, G., et al., *Waste-to-methanol: Process and economics assessment.* Bioresource Technology, 2017. **243**: p. 611-619.

49. Specht, M., et al., *Synthesis of methanol from biomass/CO2 resources*. 1999, United Kingdom: Elsevier Science Ltd.

50. Martín, M. and I.E. Grossmann, *Towards zero CO2 emissions in the production of methanol from switchgrass. CO2 to methanol.* Computers & Chemical Engineering, 2017. **105**: p. 308-316.

51. Shamsul, N.S., et al., *An overview on the production of bio-methanol as potential renewable energy.* Renewable and Sustainable Energy Reviews, 2014. **33**: p. 578-588.

52. Jadhav, S.G., et al., *Catalytic carbon dioxide hydrogenation to methanol: A review of recent studies.* Chemical Engineering Research and Design, 2014. **92**(11): p. 2557-2567.

53. Yokota, O., et al., *Hexaaluminate Catalysts of the Novel Process of Syngas Production through Catalytic Oxidation and Steam-CO2 Reforming of Methane*, in *Studies in Surface Science and Catalysis*, S.-E. Park, J.-S. Chang, and K.-W. Lee, Editors. 2004, Elsevier. p. 141-144.

54. Speight, J.G., *Chapter 8 - Hydrocarbons from Synthesis Gas*, in *Handbook of Industrial Hydrocarbon Processes*, J.G. Speight, Editor. 2011, Gulf Professional Publishing: Boston. p. 281-323.

55. Speight, J.G., *Chapter 5 - The Fischer–Tropsch Process*, in *Gasification of Unconventional Feedstocks*, J.G. Speight, Editor. 2014, Gulf Professional Publishing: Boston. p. 118-134.

56. Salameh, Z., *Chapter 4 - Energy Storage*, in *Renewable Energy System Design*, Z. Salameh, Editor. 2014, Academic Press: Boston. p. 201-298.

57. de Klerk, A., *Chapter 12 - Transport Fuel: Biomass-, Coal-, Gas- and Waste-to-Liquids Processes*, in *Future Energy (Second Edition)*, T.M. Letcher, Editor. 2014, Elsevier: Boston. p. 245-270.

58. Petrov, L.A., et al., *Role of Chemical Kinetics in the Heterogeneous Catalysis Studies.* Chinese Journal of Catalysis, 2011. **32**(6): p. 1085-1112.

59. Li, X. and Z. Huang, *An inverted classroom approach to educate MATLAB in chemical process control.* Education for Chemical Engineers, 2017. **19**: p. 1-12.

60. Bzik, T., *Statistical Methods for Engineers and Scientists.* Technometrics, 2012.

39.

61. Al-Muharrami, S., *Economic Feasibility Study: Preparation and Analysis*. 2019.
62. K.K., R.J. *The effect of contaminated gases in syngas to biomethanol production. PACCON*. in *PACCON.(2018)*. 2018.
63. K.K., R.J. *Reforming of residue gas from CBG process to synthetic gas for bio-methanol production.* . in *PACCON.(2018)*. 2018.
64. Hill, C., *An Introduction to Chemical Engineering Kinetics & Reactor Design.* SERBIULA (sistema Librum 2.0), 1977.
65. Abbas, S.Z., V. Dupont, and T. Mahmud, *Kinetics study and modelling of steam methane reforming process over a NiO/Al2O3 catalyst in an adiabatic packed bed reactor.* International Journal of Hydrogen Energy, 2017. **42**(5): p. 2889-2903.
66. Graaf, G.H., E.J. Stamhuis, and A.A.C.M. Beenackers, *Kinetics of low-pressure methanol synthesis.* Chemical Engineering Science, 1988. **43**(12): p. 3185-3195.
67. Froment, G.F., *Catalytic Kinetics: Modeling.* Catalysis: Science and Technology, 1981. **2**: p. 97-170.
68. Jiménez, N., J. Bassama, and P. Bohuon, *Estimation of the kinetic parameters of anthocyanins degradation at different water activities during treatments at high temperature (100–140 °C) using an unsteady-state 3D model.* Journal of Food Engineering, 2020. **279**: p. 109951.
69. Abd Ghani, N.A., et al., *Dry reforming of methane for syngas production over Ni–Co-supported Al2O3–MgO catalysts.* Applied Petrochemical Research, 2018. **8**(4): p. 263-270.
70. Łącki, K.M., J. Joseph, and K.O. Eriksson, *Chapter 32 - Downstream Process Design, Scale-Up Principles, and Process Modeling**, in *Biopharmaceutical Processing*, G. Jagschies, et al., Editors. 2018, Elsevier. p. 637-674.
71. Reubroycharoen, P., et al., *Continuous Low-Temperature Methanol Synthesis from Syngas Using Alcohol Promoters.* Energy & Fuels, 2003. **17**(4): p. 817-821.

Appendix

Appendix A

Biogas potential from agricultural and food processing industries

A-1 The potential of biogas production from industrial wastewater

Table A-1.1 The potential of biogas production from industrial wastewater in Thailand

Factory type	Number of factories	Biogas potential (Mm^3/year)
Starch	77	377
Liquor and beer	13	110
Food	108	100
Palm	44	25.3
Paper	23	29
Rubber	87	84
Ethanol	24	218.4
	Total biogas production rate	943.7

Appendix B

Raw data form the laboratory of methanol production from biogas

B-1 The results of the response variables for methane reforming reaction

Table B-1.1 Reaction condition: 600-700 °C of Temperatures, 15-35% Methane feeds ratio, 0.7 – 1 ml/min of H2O feed flows rate under atmospheric pressure

#RUN	Temp. (°C)	CH_4 ratio (%)	H_2O (ml/min)	CH_4 Conversion (%)	CO_2 Conversion (%)	H_2/CO ratio	Flow Out/IN
1	600	15%	0.7	92.57	39.07	1.05	1.33
2	650	15%	0.7	96.52	38.70	1.11	1.41
3	700	15%	0.7	97.81	37.55	1.48	1.19
4	600	35%	0.7	93.78	57.01	2.14	1.84
5	650	35%	0.7	97.19	58.21	2.05	1.88
6	700	35%	0.7	98.13	57.92	2.21	2.20
7	600	55%	0.7	87.43	61.85	2.70	2.11
8	650	55%	0.7	95.44	68.07	2.24	2.01
9	700	55%	0.7	97.72	65.29	2.68	2.29
10	600	15%	1.1	90.35	37.66	1.11	1.03
11	650	15%	1.1	97.66	39.59	1.74	1.09
12	700	15%	1.1	97.75	38.61	2.39	1.08
13	600	35%	1.1	90.68	38.71	2.10	1.25
14	650	35%	1.1	98.37	38.62	2.05	1.05
15	700	35%	1.1	97.77	54.49	2.94	1.28
16	600	55%	1.1	86.54	40.30	1.54	1.13
17	650	55%	1.1	97.73	58.76	2.03	1.22
18	700	55%	1.1	96.47	61.66	2.07	1.30
19	600	15%	1.5	90.75	37.61	2.39	1.08
20	650	15%	1.5	98.68	38.71	2.10	1.25
21	700	15%	1.5	97.37	38.62	2.05	1.05
22	600	35%	1.5	89.77	54.49	2.94	1.28

23	650	35%	1.5	98.73	40.30	1.54	1.13
24	700	35%	1.5	98.54	58.76	2.03	1.22
25	600	55%	1.5	87.47	61.66	2.07	1.30
26	650	55%	1.5	97.75	67.82	1.55	1.22
27	700	55%	1.5	97.09	57.72	2.59	1.27

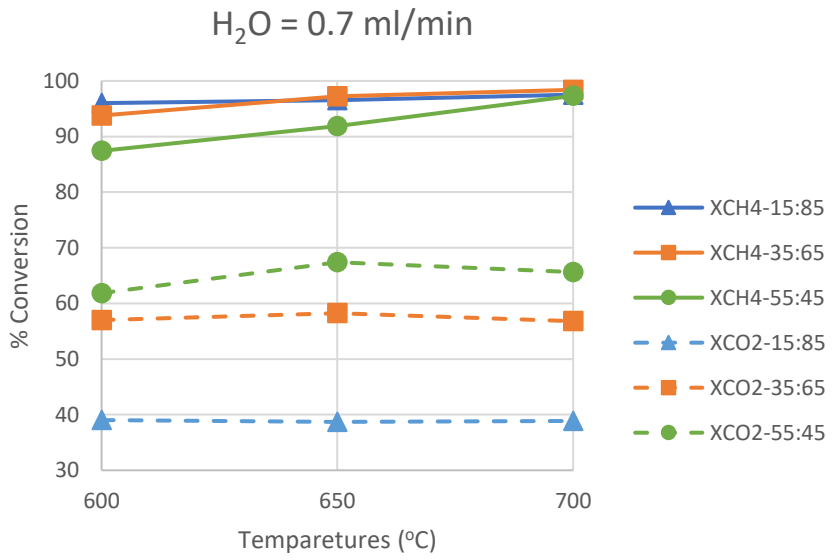

Figure B-1.1 The experimental results of 0.7 ml/min water feed flow rate varying 600 – 700 °C of temperature vs 15:85, 35:65 and 55:45 of CH_4: CO_2 feed ratio on CH_4 conversion and CO_2 conversion

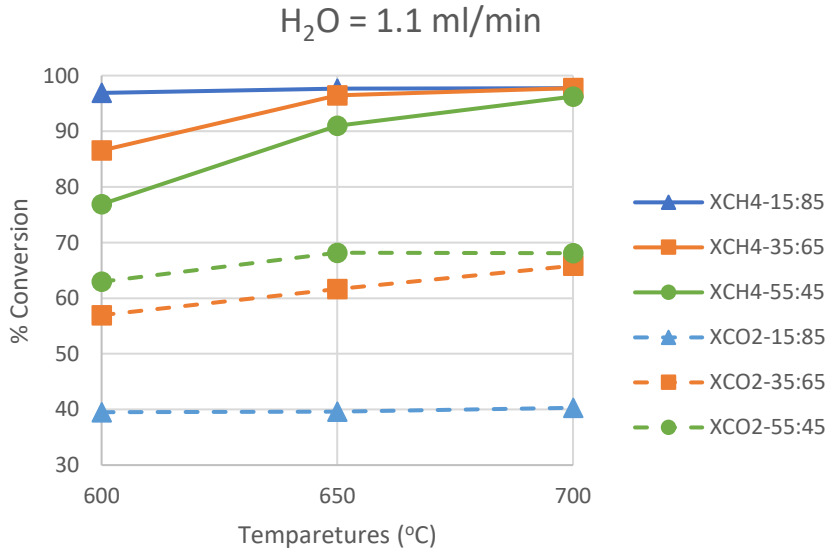

Figure B-1.2 The experimental results of 1.1 ml/min water feed flow rate varying 600 – 700 °C of temperature vs 15:85, 35:65 and 55:45 of CH_4: CO2 feed ratio on CH_4 conversion and CO_2 conversion

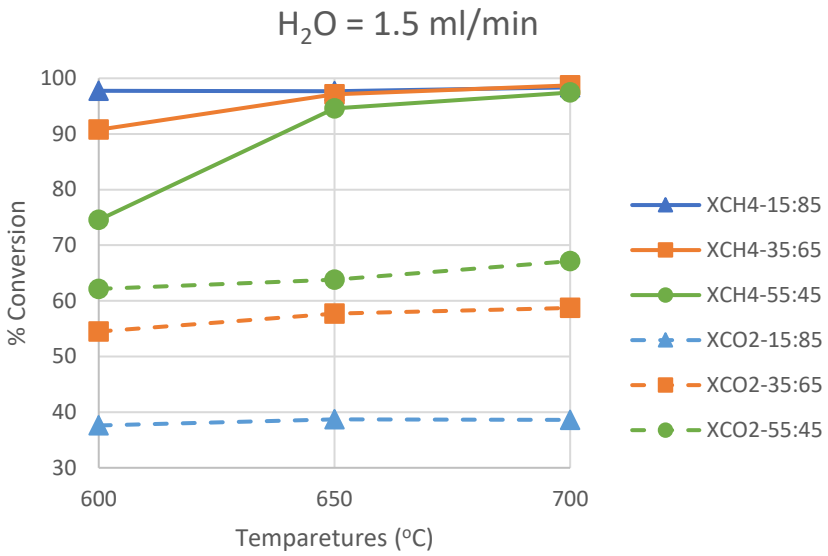

Figure B-1.3 The experimental results of 1.5 ml/min water feed flow rate varying 600 – 700 °C of temperature vs 15:85, 35:65 and 55:45 of CH_4: CO_2 feed ratio on CH_4 conversion and CO_2 conversion

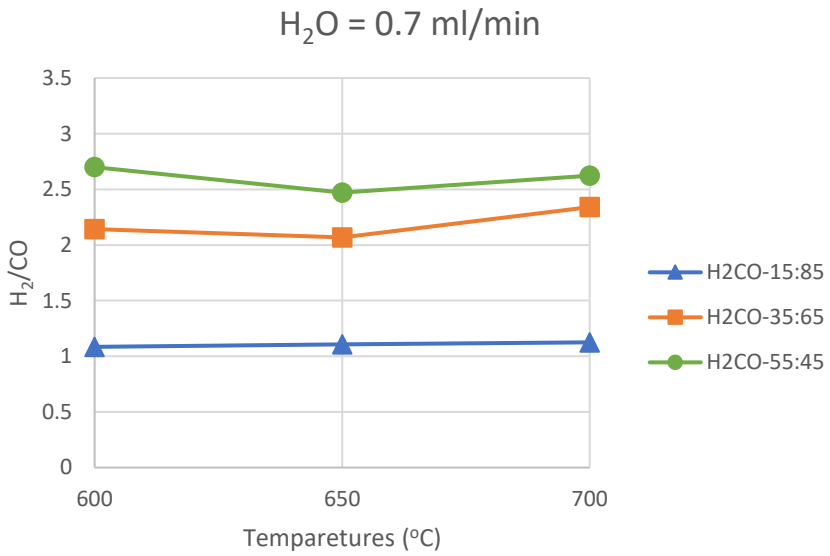

Figure B-1.4 The experimental results of 0.7 ml/min water feed flow rate varying 600 – 700 °C of temperature vs 15:85, 35:65 and 55:45 of CH_4: CO_2 feed ratio on H_2/CO ratio

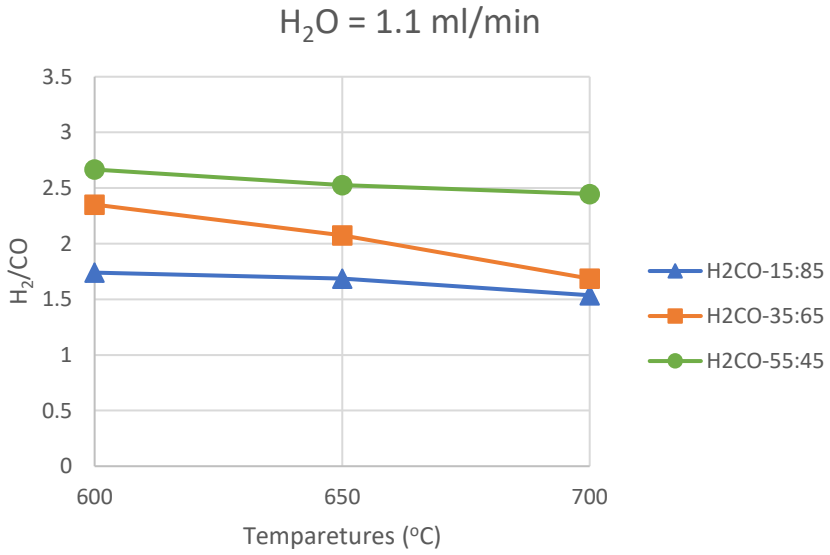

Figure B-1.5 The experimental results of 1.1 ml/min water feed flow rate varying 600 – 700 °C of temperature vs 15:85, 35:65 and 55:45 of CH_4: CO_2 feed ratio on H_2/CO ratio

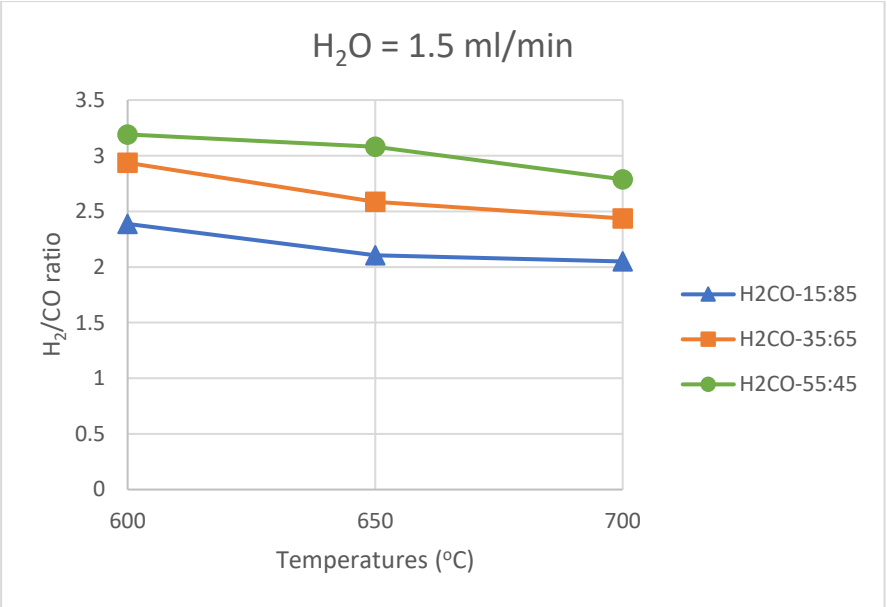

Figure B-1.6 The experimental results of 1.5 ml/min water feed flow rate varying 600 – 700 °C of temperature vs 15:85, 35:65 and 55:45 of CH_4: CO_2 feed ratio on H_2/CO ratio

B-2 The results of the response variables for the methanol synthesis reaction

Table B-2.1 Reaction condition: 170-230 °C of Temperatures, 1.2-2.8 of H_2/CO feeds ratio, 5 - 45 of $\%CO_2$ feed under constant pressure at 40 bar

#RUN	Temp. (°C)	H_2/CO ratio	$\%CO_2$	CO Conversion (%)	H_2 Conversion (%)	MeOH Yield (%)
1	230	1.2	5	50.35	63.34	79.01
2	200	1.2	5	45.67	66.20	83.80
3	170	1.2	5	35.16	44.58	70.15
4	170	2	5	44.43	48.23	59.22
5	200	2	5	75.60	76.47	92.44
6	230	2	5	73.22	61.61	89.36
7	230	2.8	5	79.78	57.67	91.18
8	200	2.8	5	88.43	68.67	89.45
9	170	2.8	5	87.78	61.20	67.30
10	170	2.8	25	47.65	40.46	23.02
11	200	2.8	25	64.29	53.72	69.52
12	230	2.8	25	62.96	53.28	65.21
13	230	2	25	63.12	53.14	62.16
14	200	2	25	61.17	60.21	68.58
15	170	2	25	42.04	38.84	26.87
16	170	1.2	25	36.71	37.87	32.97
17	200	1.2	25	47.64	64.31	70.40
18	230	1.2	25	46.32	60.96	67.34
19	230	1.2	45	44.08	57.02	41.36
20	200	1.2	45	49.15	61.68	54.93
21	170	1.2	45	36.25	43.42	29.45
22	170	2	45	34.69	46.45	25.48
23	200	2	45	55.51	58.58	54.27
24	230	2	45	48.62	54.16	49.50
25	230	2.8	45	47.91	51.28	50.03

26	200	2.8	45	55.51	54.09	50.32
27	170	2.8	45	36.33	37.84	34.78

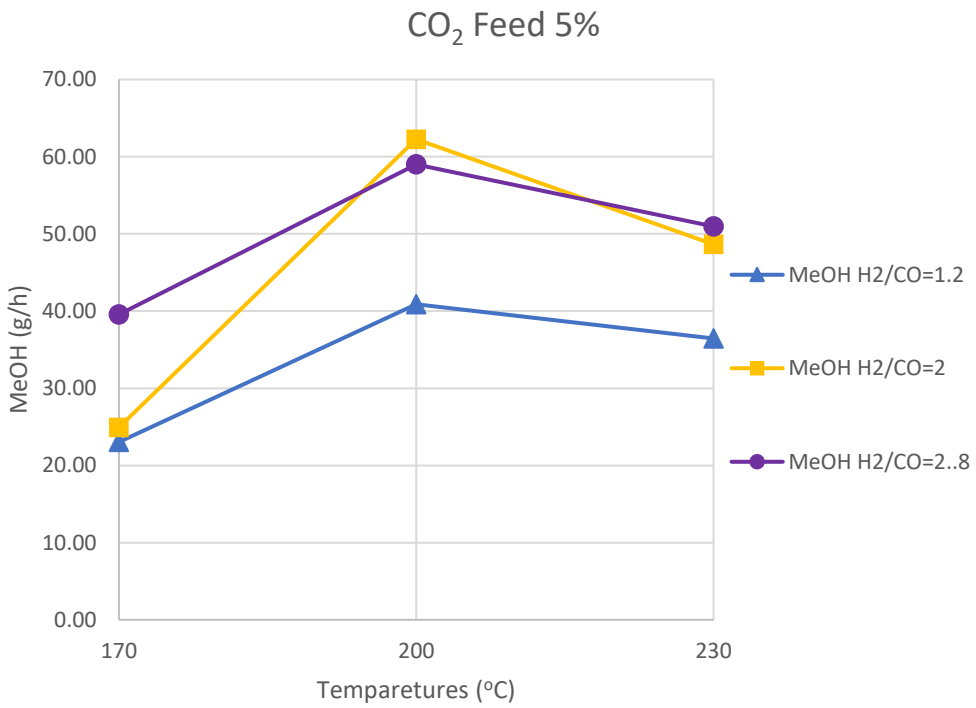

Figure B-2.1 The experimental results of 5% CO_2 feed varying 170 –230 °C of temperatures vs 1.2 - 2 of H_2/CO feed ratio on Methanol production rates

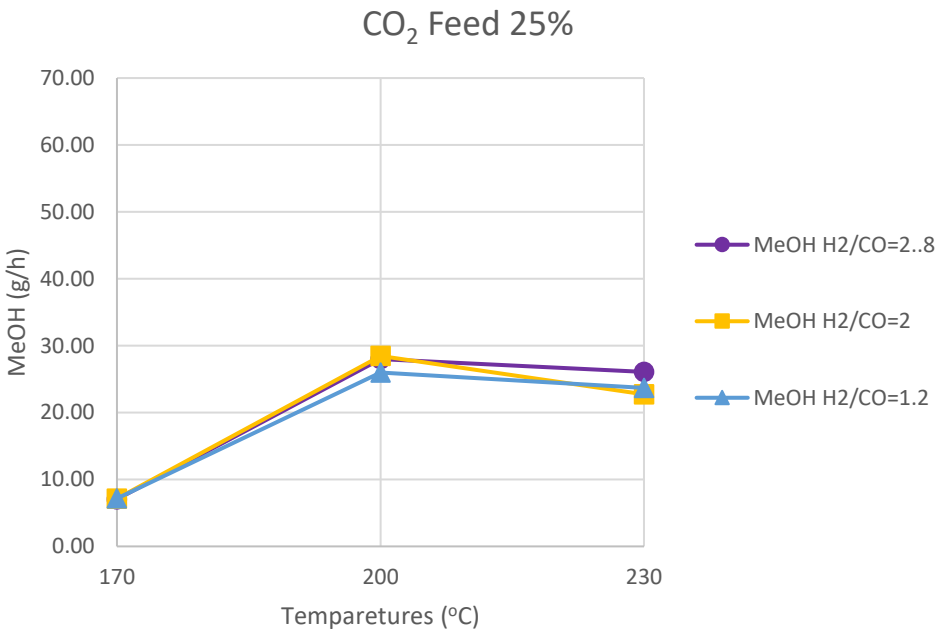

Figure B-2.2 The experimental results of 25% CO_2 feed varying 170 –230 °C of temperatures vs 1.2 - 2 of H_2/CO feed ratio on Methanol production rates

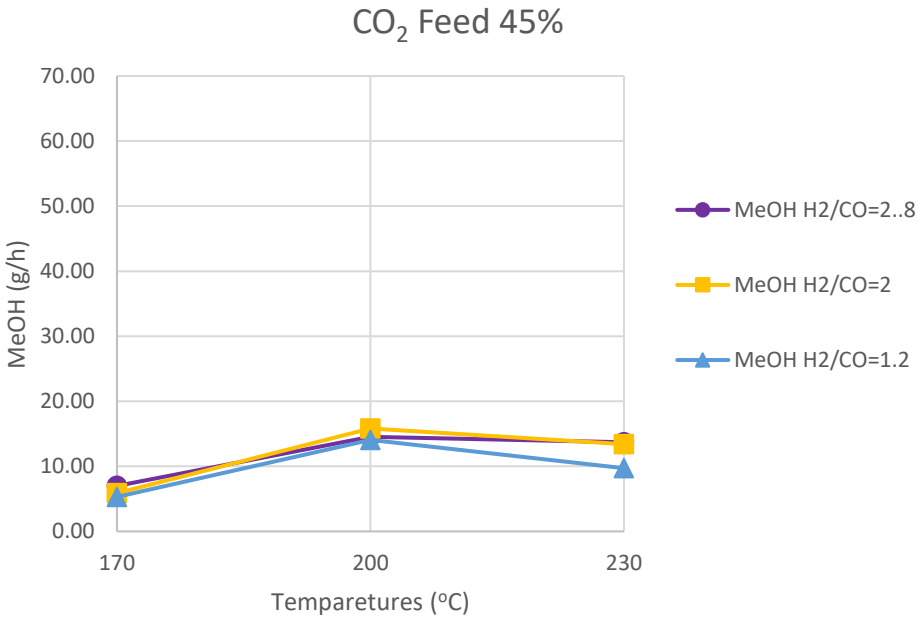

Figure B-2.3 The experimental results of 45% CO_2 feed varying 170 –230 °C of temperatures vs 1.2 - 2 of H_2/CO feed ratio on Methanol production rates

Appendix C

Programing for kinetic modelling by using MATLAB software

Appendix C-1 Source Code in MATLAB software for modelling methane reforming reaction

The kinetic models were investigated by using experimental data in excel format. The MATLAB software was used for performing the estimation of kinetic parameters. The source codes were divided into three parts: 1) main function 2) reactor model function and 3) kinetic model function, as shown in Figure B-1.1, B-1.2 and B-1.3, respectively. The sub-function was used for calculating unit conversion, as shown in Figure B-1.4.

```
clc,clear
% Import the data
[~, ~, raw] = xlsread('EXP.xlsx','R1','A2:H28');

% Create output variable
expR1 = reshape([raw[71]],size(raw));
data = expR1;

% Allocate imported array to column variable names
RUN = data(:,1);
Temp = data(:,2);
pCH4f = data(:,3);
H2O = data(:,4);
XCH4 = data(:,5);
XCO2 = data(:,6);
H2CO = data(:,7);
Flow = data(:,8);
n = length(RUN);
% Clear temporary variables
clearvars data raw;
RUN = reshape(RUN,[1,n]);
Temp = reshape(Temp,[1,n]);
pCH4f = reshape(pCH4f,[1,n]);
H2O = reshape(H2O,[1,n]);
XCH4 = reshape(XCH4,[1,n]);
XCO2 = reshape(XCO2,[1,n]);
H2CO = reshape(H2CO,[1,n]);
Flow = reshape(Flow,[1,n]);


%Data

%Plot
figure(1)
plot(RUN,XCH4,'bo')
grid on
hold on
```

```
plot(RUN,XCO2,'ro')
hold off
xlabel('%RUN')
ylabel('%Conversion [%]')
legend('Model','EXP')

figure(2)
plot(RUN,H2CO,'yo')
xlabel('%RUN')
ylabel('Ratio')
legend('H2/CO')


%Data processing
Exp_input = RUN;
Exp_output = [XCH4;XCO2;H2CO];

%Starting point for lsqcurvefit
k1 = 1.29e6;
KCO21 = 2.61e-2;
KCH41 = 2.61e-2;
Kp1 = 6.78e14;
k2 = 0.35e6;
KCO22 = 0.5771;
KH22 = 1.494;
Kp2 = 56.4971;
%k0 = [k1 k2 KCO21 KCH41 Kp1 KCO22 KH22 Kp2];
k0 = [0 0 0 0 0 0 0 0 0 0 0 0 0 0 0];
%Lsqcurvefit
xdata = Exp_input;
ydata = Exp_output;

fun = @(x,xdata)fnReactionrate(x,xdata,Temp,pCH4f,H2O);

k = lsqcurvefit(fun,k0,xdata,ydata);

FitData = fnReactionrate(k,xdata,Temp,pCH4f,H2O);
XCH4SIM = FitData(1,:);
XCO2SIM = FitData(2,:);
H2COSIM = FitData(3,:);


% %Plot
figure(3)
plot(RUN,XCH4,'bo')
grid on
hold on
plot(RUN,XCO2,'ro')
grid on
hold on
plot(RUN,XCH4SIM,'bx')
plot(RUN,XCO2SIM,'rx')
hold off
xlabel('RUN')
ylabel('Conversion [%]')
legend('CH4','CO2')

figure(4)
plot(RUN,H2CO,'bo')
grid on
hold on
plot(RUN,H2COSIM,'bx')
```

```
100.        hold off
101.        xlabel('%RUN')
102.        ylabel('Ratio')
103.        legend('H2/CO')
104.
105.
106.         SStotC1 = sum((XCH4 - mean(XCH4)).^2);
107.         SSresC1 = sum((XCH4 - XCH4SIM).^2);
108.         R2XCH4 = 1 - SSresC1/SStotC1
109.
110.         SStotC2 = sum((XCO2 - mean(XCO2)).^2);
111.         SSresC2 = sum((XCO2 - XCO2SIM).^2);
112.         R2XCO2 = 1 - SSresC2/SStotC2
113.
114.         SStotC3 = sum((H2CO - mean(H2CO)).^2);
115.         SSresC3 = sum((H2CO - H2COSIM).^2);
116.         R2H2CO = 1 - SSresC3/SStotC3
```

Figure B-1.1 Main function of kinetic modelling for methane reforming reaction

Appendix D

Equipment sizing and costing

Appendix D-1 Equipment sizing for the methanol production process

The specification of equipment was determined for 15,000 kg/day methanol capacity by based on 1 litre/day production of the bio-methanol semi-pilot plant by TISTR. The equipment sizing was determined by using basic principles of scale-up via scale-up factors such as Reynolds number, residence time and retention time [70] as shown in **Table D-1.1.**

Table D-1.1 The specification of equipment 15,000 kg/day methanol production process

Code	Equipment	Specification
MX-1	Biogas Mixer 1	Re: 11,493 ID: 60 cm x L 300 cm
MX-2	Biogas Mixer 2	Re: 31,665 ID: 60 cm x L 300 cm
HX-1	Biogas preheater	Shell ID: 80 cm, Tube OD 1in x L 600 cm Number of tubes: 300 tubes
HX-2	Syngas preheater	Shell ID: 60 cm, Tube OD 1in x L 600 cm Number of tubes: 100 tubes
HX-3	Methanol cooler	Shell ID: 80 cm, Tube OD 1in x L 600 cm Number of tubes: 300 tubes
HX-4	Methanol cooler by CW	Shell ID: 80 cm, Tube OD 1in x L 600 cm Number of tubes: 300 tubes
HX-5	Methanol cooler by CH	Shell ID: 80 cm, Tube OD 1in x L 400 cm Number of tubes: 300 tubes
SP-4	Water trap vessel	V= 1.5 Nm^3, Horizontal Cylinder tank
SP-5	Methanol trap vessel	V= 1.5 Nm^3, Horizontal Cylinder tank
R-1	Reforming reactor	74 modules: 1 module = 8 tube, Tube size = ID: 0.2m x Length: 2 m, WHSV: 1.38, 25% Excess,

		Cat: 23 ton
R-2	Methanol synthesis reactor	56 modules: 1 module = 8 tube, Tube size = ID: 0.2m x Length: 3 m, ID: 0.2m x Length: 2 m, WHSV: 1.39, 25% Excess, Cat: 26 ton
AB-1	Water absorber	Re 384-500 (laminar flow), packed silica gel and filter x4.
F-1	Furnace	Output Heating: 608 kW, Auto Ignite Burner

Appendix D-2 Equipment cost estimation

The equipment costs were evaluated from the local vendor and real industries cost based on the basic design of 15,000 kg/day methanol production rates. The equipment costs showed price in Bath (THB) per unit in Table D-2.1.

Table D-2.1 Equipment cost estimation

Code	Equipment	Price (THB/unit)	References
RT-1,2	Biogas root blower 1,2	175,000	Henan Yuanju Machinery Co., Ltd.
RT-3	CO_2 root blower	175,000	Henan Yuanju Machinery Co., Ltd.
MX-1	Biogas Mixer 1	200,000	PAKCO INTERNATIONAL CO., LTD.
MX-2	Biogas Mixer 2	200,000	PAKCO INTERNATIONAL CO., LTD.
HX-1	Biogas preheater	1,000,000	Jiangsu Xiabang Refrigeration Equipment Co., Ltd.
HX-2	Syngas cooler	1,000,000	Jiangsu Xiabang Refrigeration Equipment Co., Ltd.
HX-3	Methanol cooler	1,000,000	Jiangsu Xiabang Refrigeration Equipment Co., Ltd.
HX-4	Methanol cooler by CW	1,000,000	Jiangsu Xiabang Refrigeration Equipment Co., Ltd.
HX-5	Methanol cooler by CH	1,000,000	Jiangsu Xiabang Refrigeration Equipment Co., Ltd.
CP-1	Biogas compressor	350,000	Sichuan New Tianyuan Co., Ltd.

CP-2	Methane compressor 1	350,000	Sichuan New Tianyuan Co., Ltd.
CP-3	Syngas compressor	350,000	Sichuan New Tianyuan Co., Ltd.
SP-4	Water trap vessel	1,000,000	TISTR & Cryotech Asia Co., Ltd.
SP-5	Methanol trap vessel	1,000,000	TISTR & Cryotech Asia Co., Ltd.
R-1	Reforming reactor	3,000,000	TISTR & Cryotech Asia Co., Ltd.
R-2	Methanol synthesis reactor	2,000,000	TISTR & Cryotech Asia Co., Ltd.
AB-1	Water absorber	1,000,000	Hangzhou Shanli Purify Co., Ltd.
P-1	Water tank pump	19,000	TISTR & Cryotech Asia Co., Ltd.
F-1	Furnace	5,000,000	TISTR & Cryotech Asia Co., Ltd.
CW	Cooling tower	1,050,000	Xinxiang Jiahui FRP Environmental Equipment Co., Ltd.
CH	Chiller	1,575,000	Senova Biotech (Shanghai) Co., Ltd.
	Electric generator	20,000,000	Shandong Lvhuan Power Equipment Co., Ltd.
	Piping & valve	2,000,000	TISTR & Cryotech Asia Co., Ltd.

VITA

NAME	Rujiroj Tamnitra
DATE OF BIRTH	22 January 1994
PLACE OF BIRTH	Bangkok
INSTITUTIONS ATTENDED	Bachelor's degree of chemical engineering, Silpakorn University
HOME ADDRESS	666/85 Prayasuren Rd., bang Chan, Khlong Sam Wa, Bangkok, 10510